



The Abdus Salam
International Centre for Theoretical Physics



2157-14

Workshop on Principles and Design of Strongly Correlated Electronic Systems

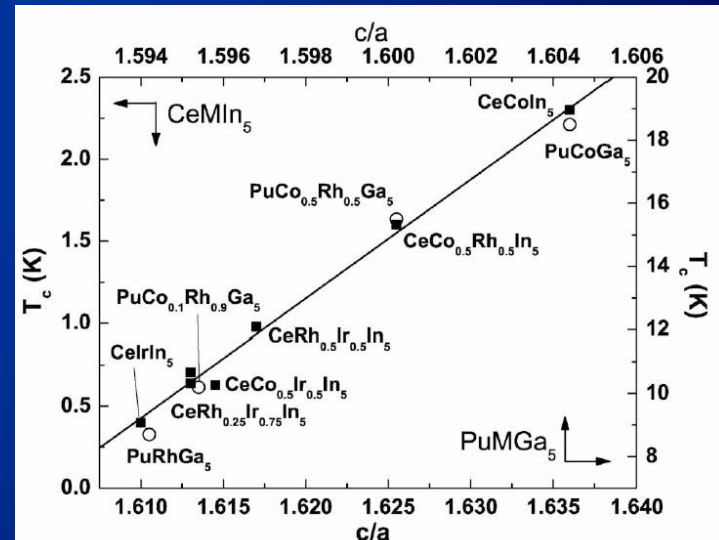
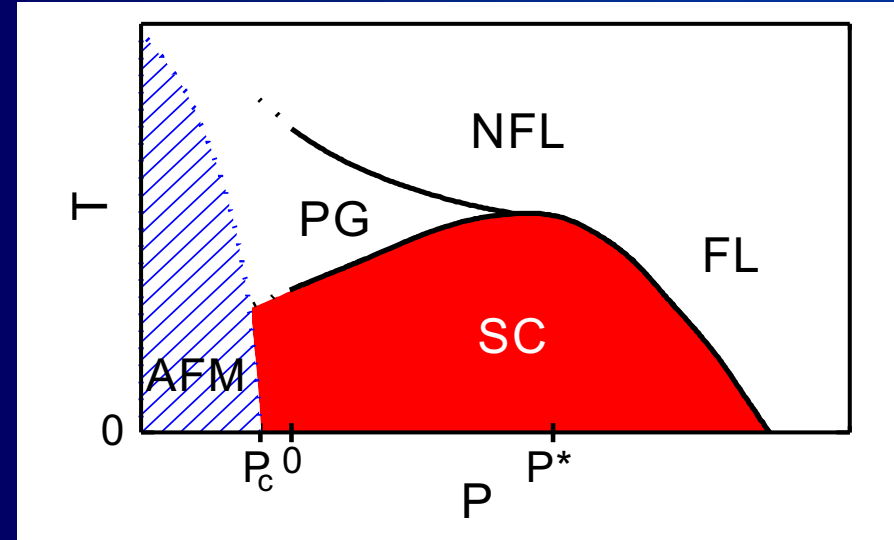
2 - 13 August 2010

**Low symmetry structures and hybridization:
Key ingredients for finding new superconductors**

Pascoal G. PAGLIUSO
*GPOMS, Instituto de Fisica "Gleb Wataghin"
UNICAMP, Campinas, SP
Brazil*

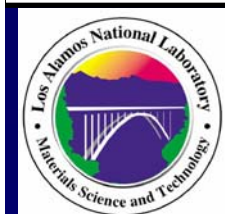
Workshop on Principles and Design of Strongly Correlated Electronic Systems – Trieste - 08/10

Low symmetry structures and hybridization: key ingredients for finding new superconductors



Pascoal G. Pagliuso

Grupo de Propriedades Ópticas e Magnéticas dos Sólidos (GPOMS)
Instituto de Física ``Gleb Wataghin'', UNICAMP – Campinas -SP



UC - Irvine



CBPF



NIST
National Institute of
Standards and Technology



LNLS



ESRF





Campinas City 1.5 million inhabitants



Universidade Estadual de Campinas “UNICAMP”

~ 4 km² - 35,000 Students (40 years old)

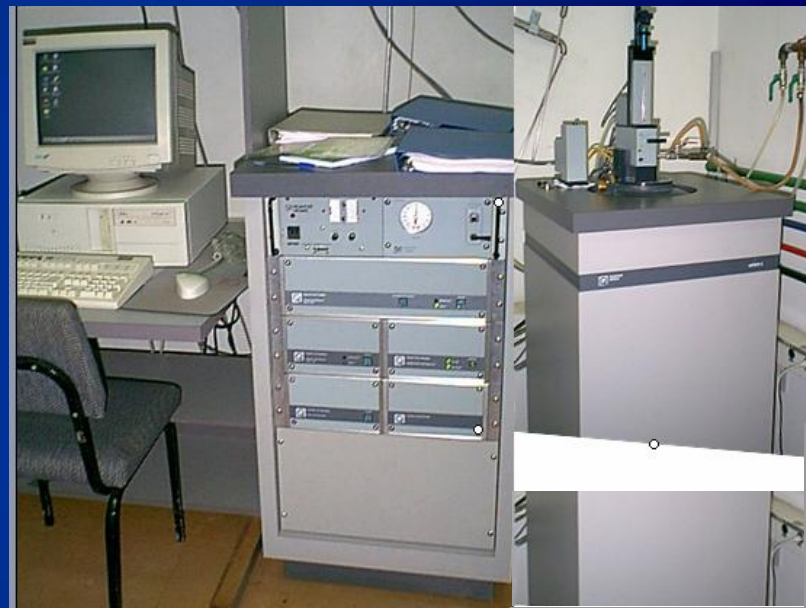


Magnetic and Optics Facilities GPOMS



PPMS-QD 9T, 0.3 K
14 T 50 mK

$C_p(T,H)$
 $M(T,H)$
 $\rho(T,H)$ e R_H
 $\kappa(T,H)$
 $0 < P < 25$ kbar.



MPMS
SQUID-QD 7T
 $1.8 < T < 800$ K
 $0 < P < 12$ kbar.



RAMAN Lab
 $1.6 < T < 800$ K
 $0 < H < 7$ T.

10 K
-
1000 °C



V S M



X - R A Y



300 K

F U R N A C E S



ESR Spectrometers

L (1.4 GHz); S (4.0 GHz); X (9.4 GHz) Q; (34.4 GHz)
(400 G) (1.200 G) (3.200 G) (12.000 G)



Bruker-ELEXSYS E-500

VARIAN

CAMPINAS SYNCHROTRON NATIONAL
LABORATORY
EXAFS-XANES-XDR (structural and magnetic)

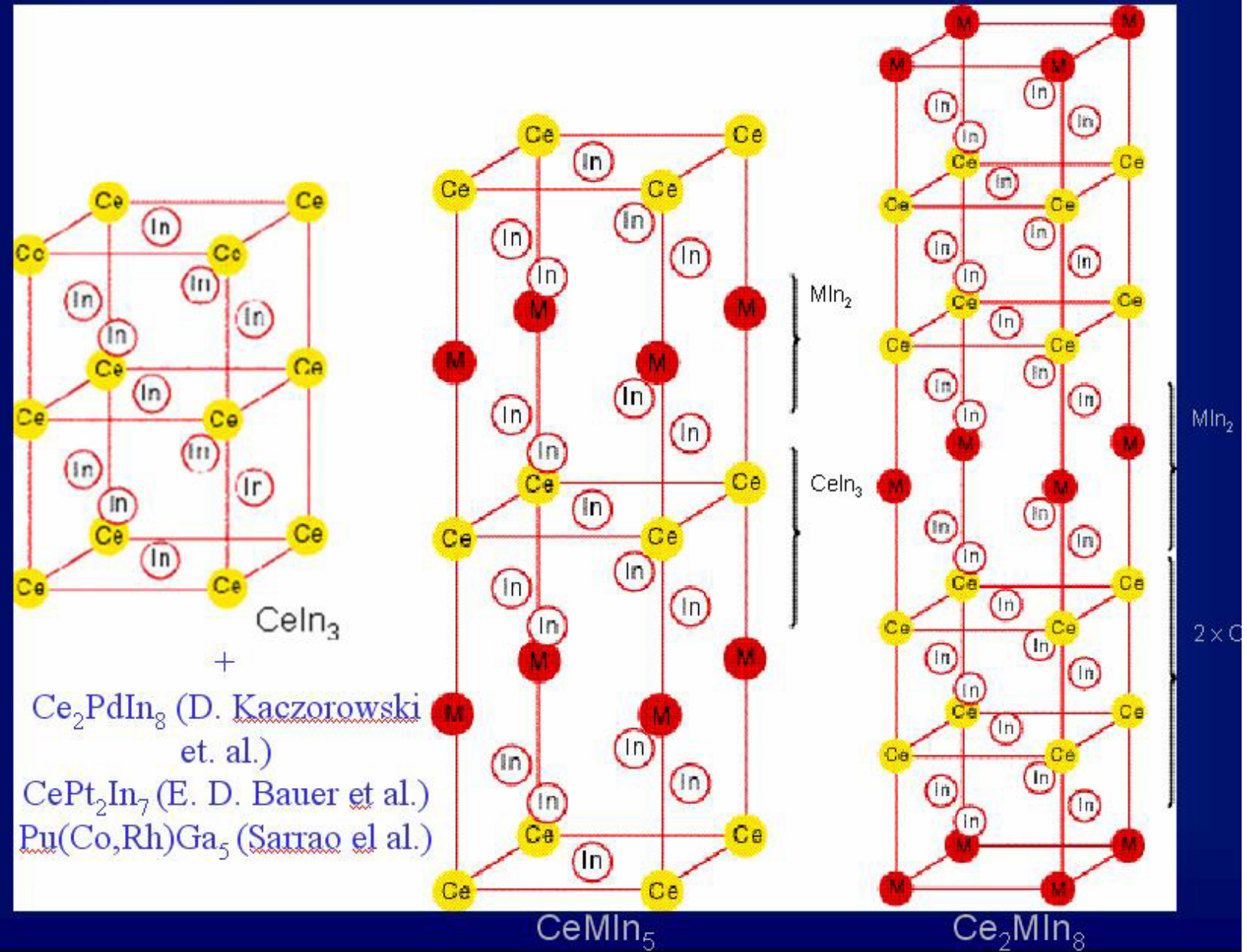


$\sim 10^{11}$ fótons/s @ 200 mA @ E = 8keV ($\ddot{e} \sim 1.5^-$); D ~30 m

Outline

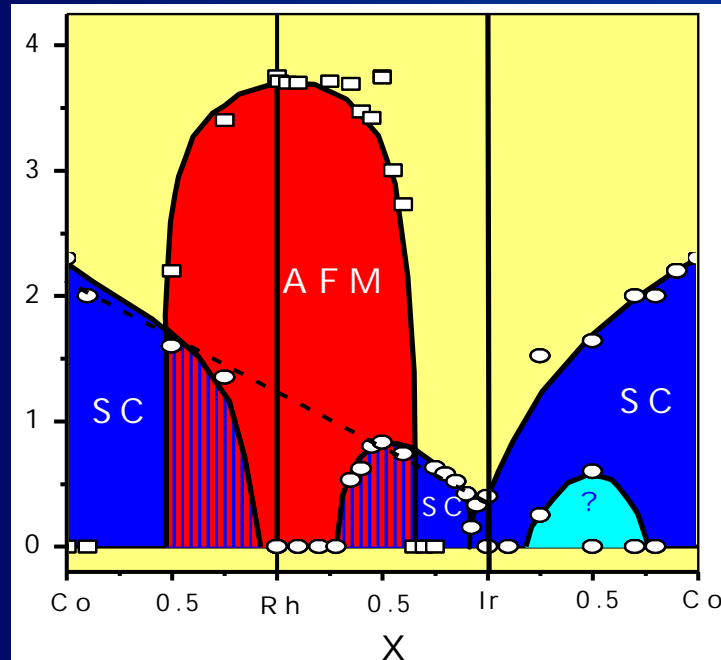
- I. Review of structurally related physical properties of HFS families $\text{Ce}_m\text{M}_n\text{In}_{3m+2}$ – the role of CEF tetragonal symmetry – layered structural
- II. CeRhIn_5 doped with La and Sn
- III. Cd-doped $\text{Ce}_2(\text{Rh},\text{Ir})\text{In}_8$
- IV. Possible relationship to FeAs-based, Yb-based HFS
- V. Implications in new materials search

6 HFS – What is special about these structures?

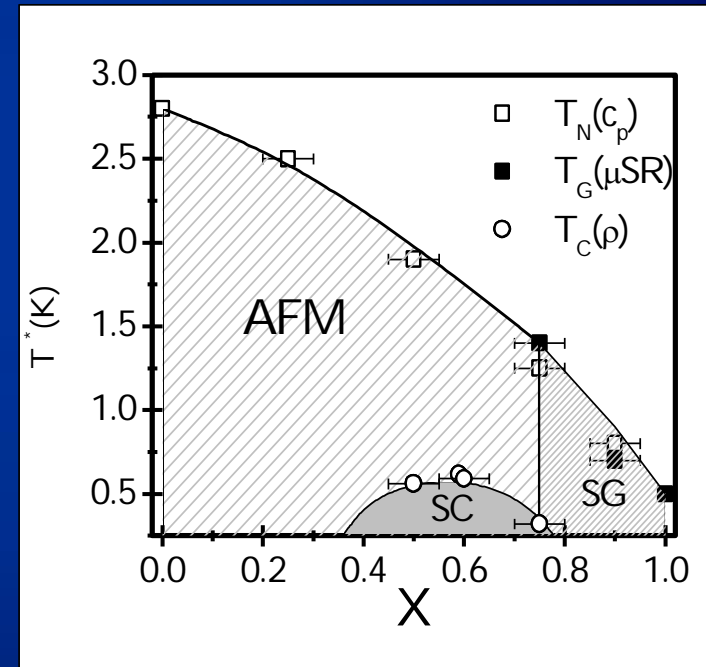


$Ce_mM_nIn_{3m+2n}$

$CeRh_{1-x}(Ir,Co)_xIn_5$ [1,2]



$Ce_2Rh_{1-x}Ir_xIn_8$ [3,4,5]



- Ce_2CoIn_8

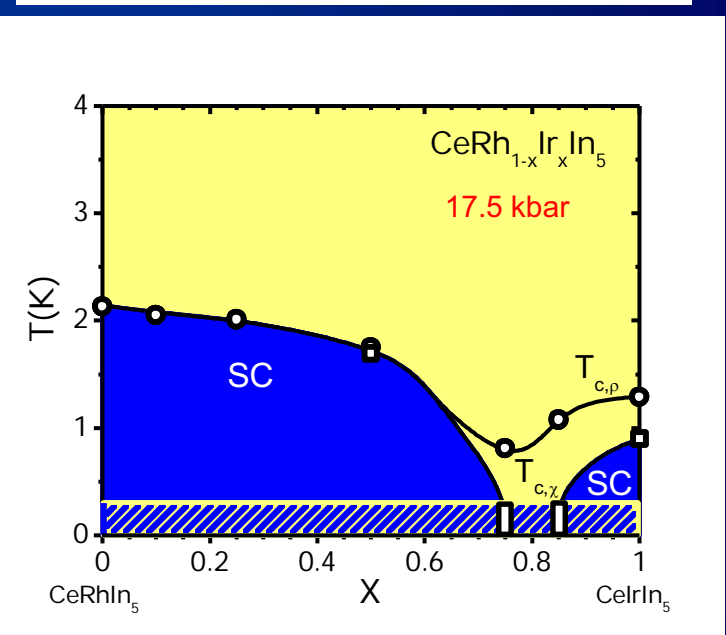
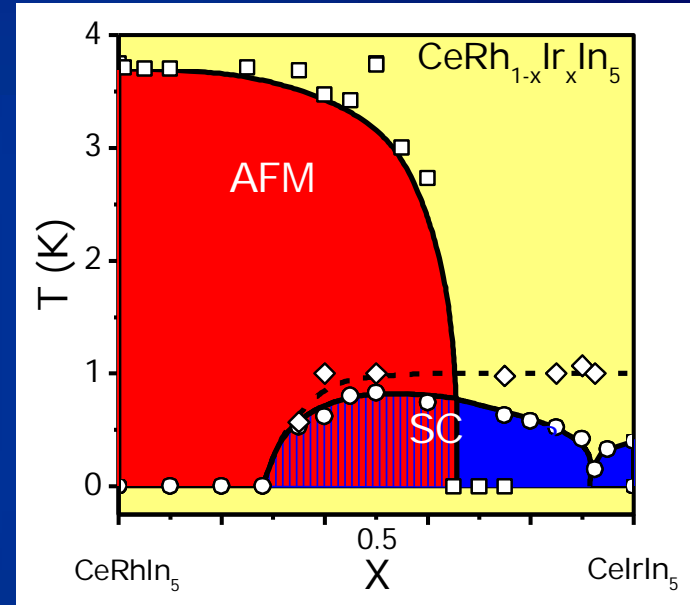
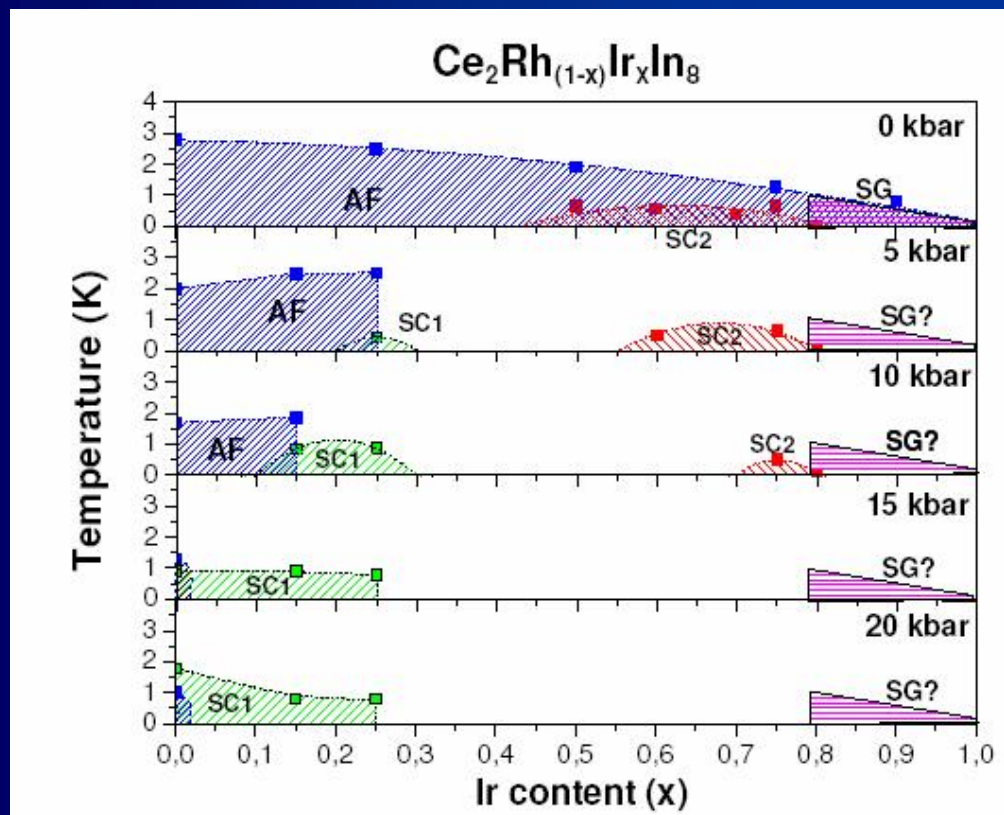
$T_C \approx 1.0$ K

$\gamma \geq 600$ mJ/K² mole Ce

- [1] Pagliuso et al, Physica B, 312, 129 (2002).
- [2] Pagliuso et al, Phys. Rev B, 64, 100503(R) (2001).

- [3] E.N. Hering et al Physica B, 378, 423 (2006).
- [4] E.N. Hering, Physica B, 403, 780 (2008);
- [5] E. N. Hering, C. Adriano, et al, submitted to PRB (2010).

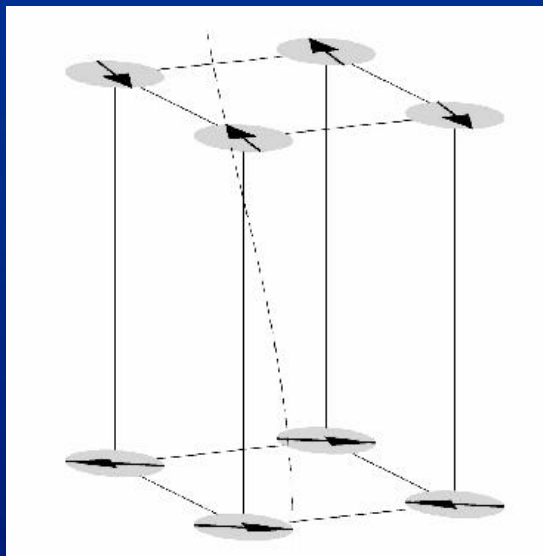
$\text{Ce}_2(\text{Rh},\text{Ir})_{1-x}\text{Co}_x\text{In}_8$ – Phase Diagrams



E. N Hering, et al
M. Nicklas et al.

Magnetic Structure

CeRhIn₅



$T_N = 3.8 \text{ K}$

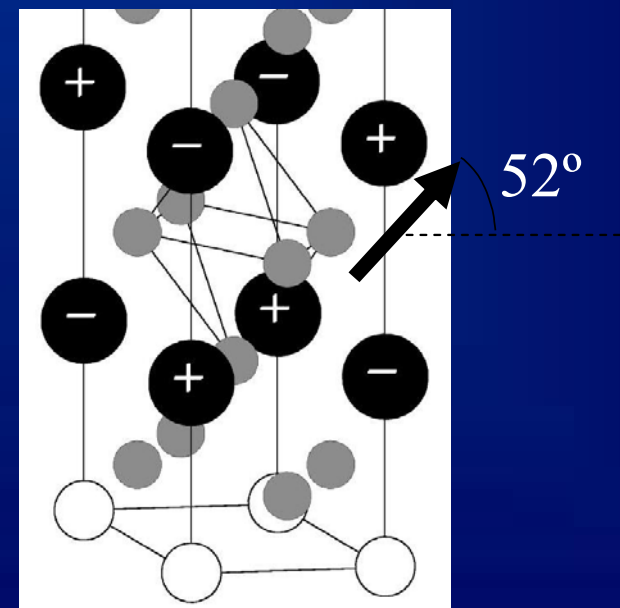
$\mu_{\text{ord}} = 0.7 \mu_B$ (in plane)

107° spiral layer-to-layer

Curro et al., PRB 62, R6100 (2000)
Bao et al., PRB 62, R14621 (2000)

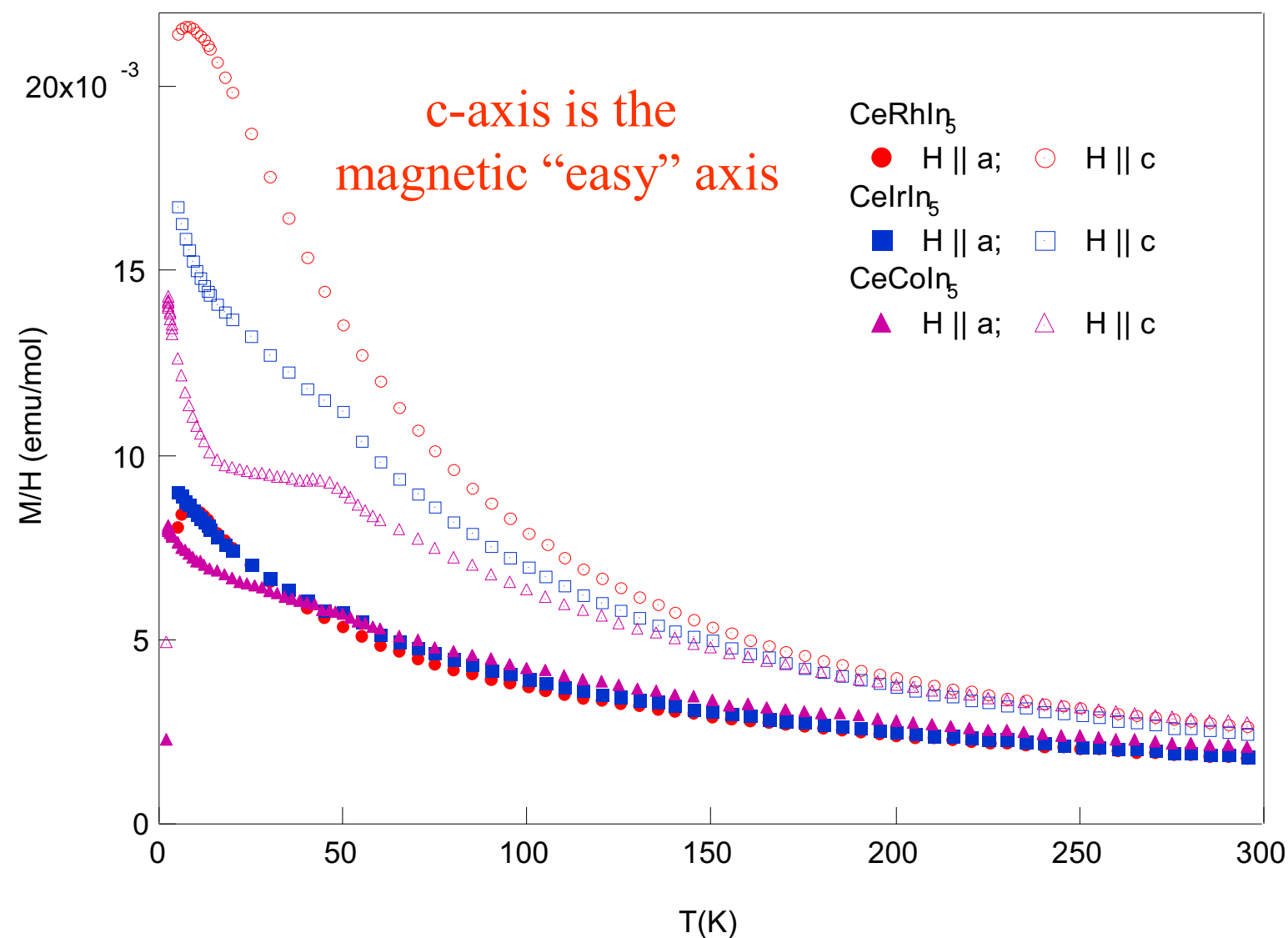
Ce₂RhIn₈

- AFM with $T_N = 2.8 \text{ K}$
- $\varepsilon = (1/2, 1/2, 0)$ and $\eta = 52^\circ$
- $\mu_{\text{eff}} = 0.55 \mu_B$

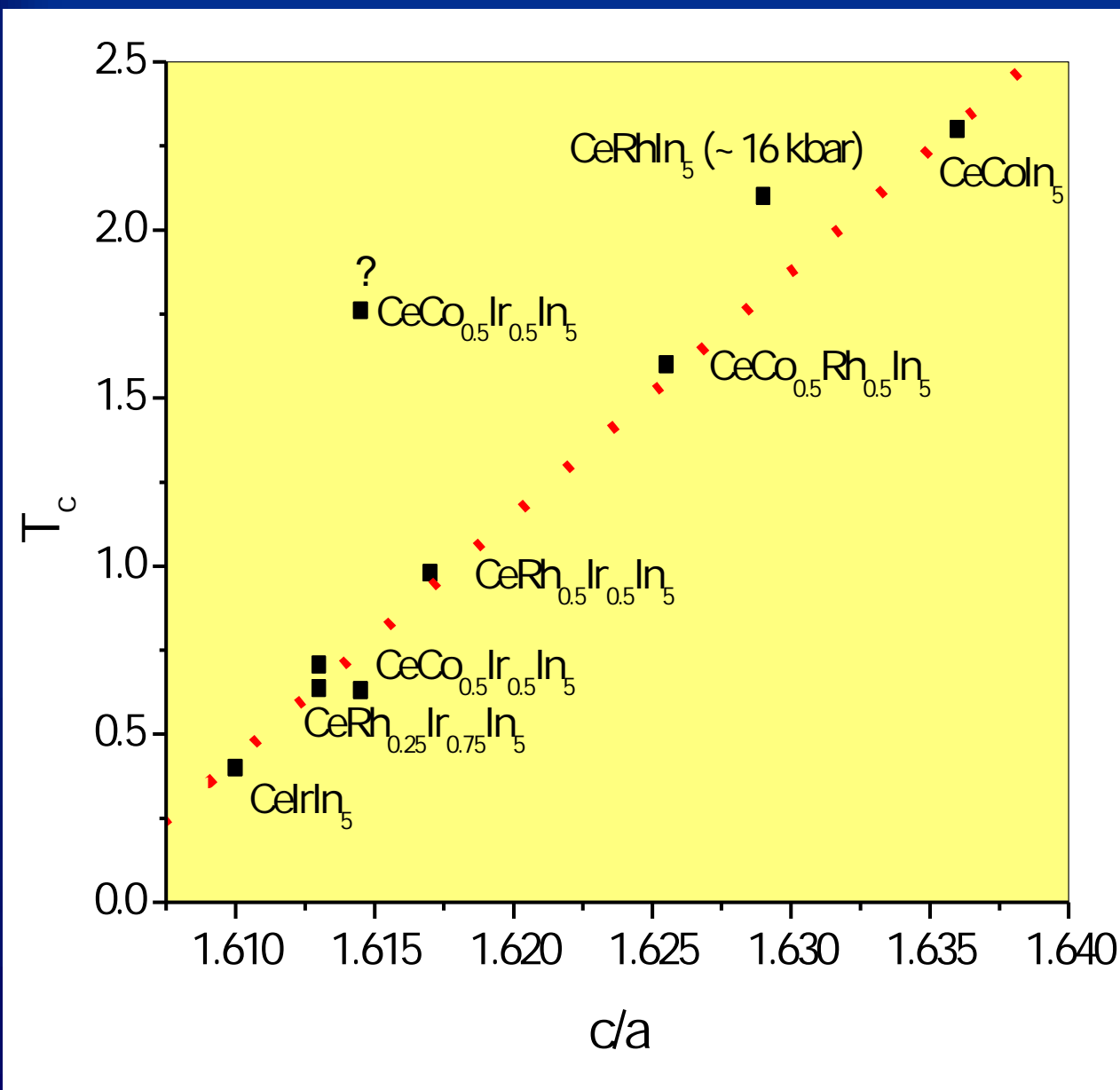


W. Bao et al Phys. Rev. B, 64 020401R (2001)

CeMIn₅ - $\chi(T)$ summary



c/a as control parameter for T_c



Is there an intrinsic parameter in this plot, which depends on c/a and determines T_c ?

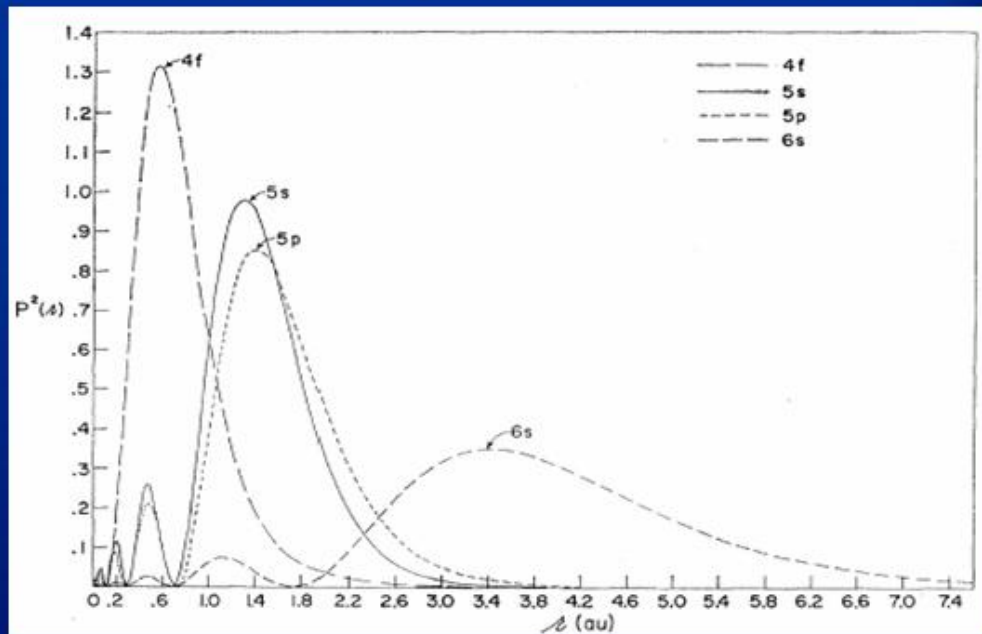
Tuning:
- J_{RKKY}
- T_K
- CEF

The rare-earth ions

Electronic configuration:

	Z	R
La	57	[Xe]5d ¹ 6s ²
Ce	58	[Xe]4f ¹ 5d ¹ 6s ²
Pr	59	[Xe]4f ³ 6s ²
Nd	60	[Xe]4f ⁴ 6s ²
Pm	61	[Xe]4f ⁵ 6s ²
Sm	62	[Xe]4f ⁶ 6s ²
Eu	63	[Xe]4f ⁷ 6s ²
Gd	64	[Xe]4f ⁷ 5d ¹ 6s ²
Tb	65	[Xe]4f ⁹ 6s ²
Dy	66	[Xe]4f ¹⁰ 6s ²
Ho	67	[Xe]4f ¹¹ 6s ²
Er	68	[Xe]4f ¹² 6s ²
Tm	69	[Xe]4f ¹³ 6s ²
Yb	70	[Xe]4f ¹⁴ 6s ²
Lu	71	[Xe]4f ¹⁴ 5d ¹ 6s ²

- Incomplete 4f shells
- Chemically alike – valence 3+.



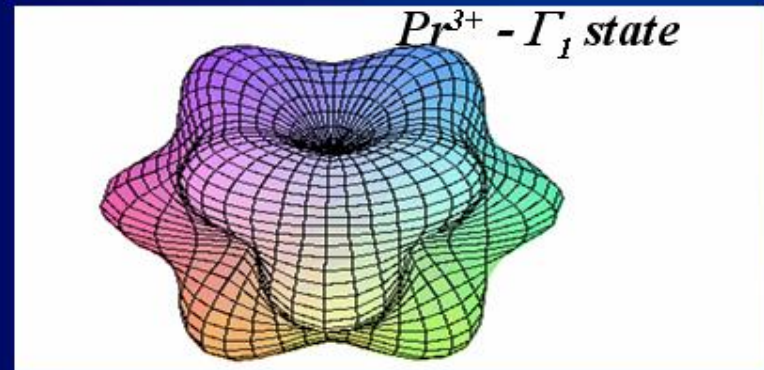
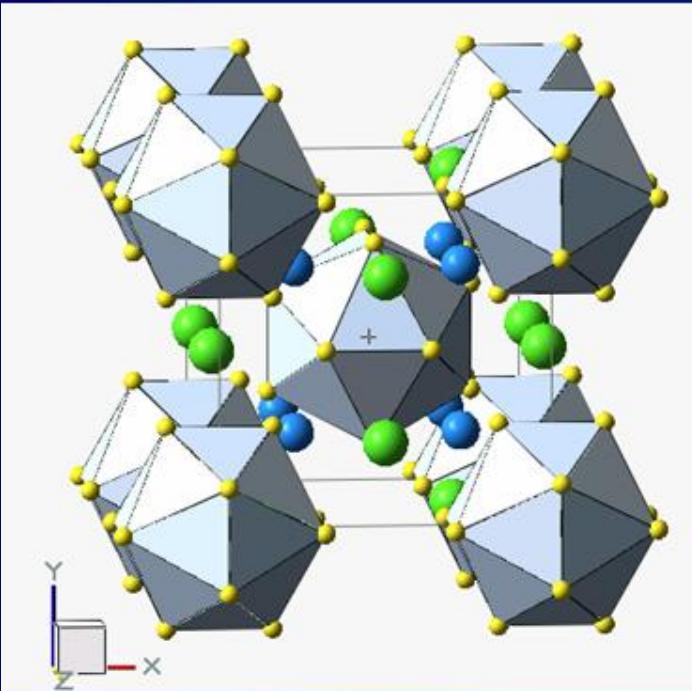
- 4f shells are partially shielded by external orbitals.
- Spin-orbital coupling stronger than crystal field effects

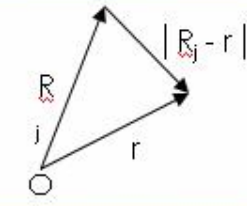
The rare-earth ions

<i>f</i> -shell ($l = 3$)								
n	$l_z = 3, -2, -1, 0, -1, -2, -3$		S	$L = \Sigma l_z $	J			
1	\downarrow	Ce ³⁺	1/2	3	5/2	$J = L - S $	$^2F_{5/2}$	
2	$\downarrow \downarrow$	Pr ³⁺	1	5	4		3H_4	
3	$\downarrow \downarrow \downarrow$	Nd ³⁺	3/2	6	9/2		$^4I_{9/2}$	
4	$\downarrow \downarrow \downarrow \downarrow$		2	6	4		5I_4	
5	$\downarrow \downarrow \downarrow \downarrow \downarrow$		5/2	5	5/2		$^6H_{5/2}$	
6	$\downarrow \downarrow \downarrow \downarrow \downarrow \downarrow$		3	3	0		7F_0	
7	$\downarrow \downarrow \downarrow \downarrow \downarrow \downarrow \downarrow$	Gd ³⁺	7/2	0	7/2		$^8S_{7/2}$	
8	$\uparrow \uparrow \uparrow \uparrow \uparrow \uparrow \uparrow$		3	3	6		7F_6	
9	$\uparrow \uparrow \uparrow \uparrow \uparrow \uparrow \uparrow$		5/2	5	15/2		$^6H_{15/2}$	
10	$\uparrow \uparrow \uparrow \uparrow \uparrow \uparrow \uparrow$		2	6	8	$J = L + S$	5I_8	
11	$\uparrow \uparrow \uparrow \uparrow \uparrow \uparrow \uparrow$		3/2	6	15/2		$^4I_{15/2}$	
12	$\uparrow \uparrow \uparrow \uparrow \uparrow \uparrow \uparrow$		1	5	6		3H_6	
13	$\uparrow \uparrow \uparrow \uparrow \uparrow \uparrow \uparrow$	Yb ³⁺	1/2	3	7/2		$^2F_{7/2}$	
14	$\uparrow \uparrow \uparrow \uparrow \uparrow \uparrow \uparrow$		0	0	0		1S_0	

^a \uparrow = spin $\frac{1}{2}$; \downarrow = spin $-\frac{1}{2}$.

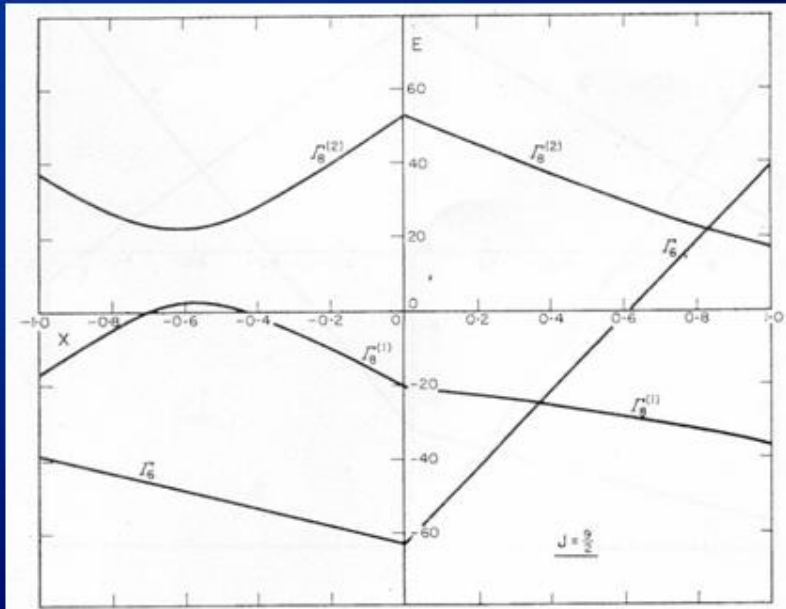
The rare-earth ions in solids



$$V(r, \theta, \phi) = \sum_j \frac{q_j}{|(\mathbf{R}_j - \mathbf{r})|}$$


$$H_{CEF} = B_4(O_4^0 + 5 \cdot O_4^4) + B_6(O_6^0 - 21 \cdot O_6^4)$$

(cubic CEF)



CEF defines single ion spin-anisotropy

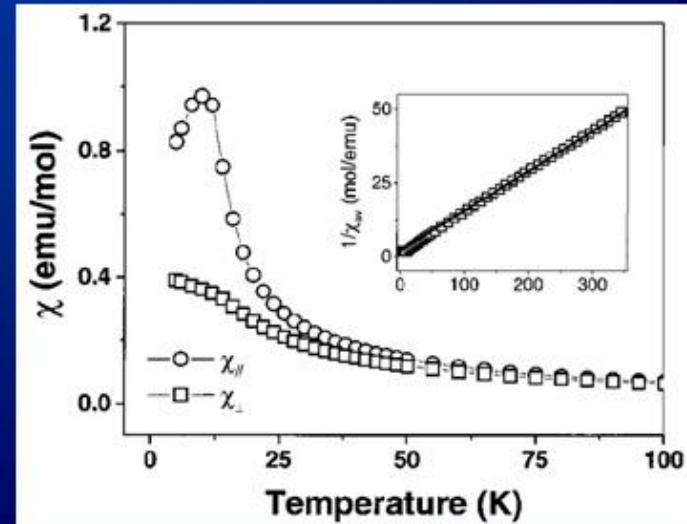
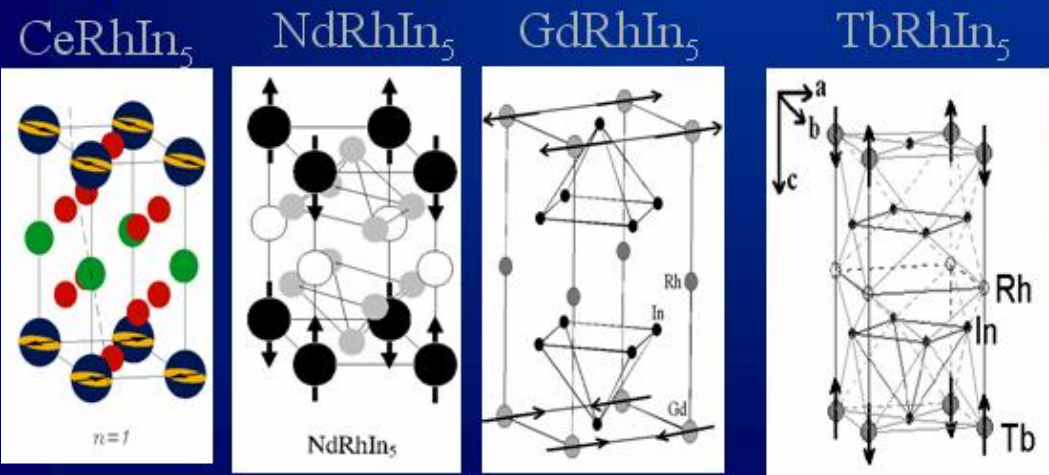
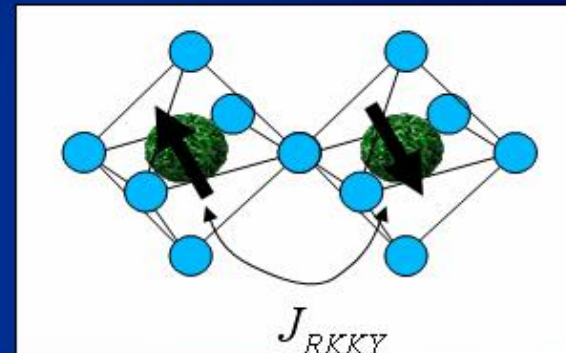
Local f-electrons: Magnetic properties

f-shell ($l = 3$)						
n	$l_z = 3, -2, -1, 0, -1, -2, -3$	S	$L = \Sigma l_z $	J		
1	↓	1/2	3	5/2		$^2F_{5/2}$
2	↓ ↓	1	5	4		3H_4
3	↓ ↓ ↓	3/2	6	9/2	$J = L - S $	$^4I_{9/2}$
4	↓ ↓ ↓ ↓	2	6	4		5I_4
5	↓ ↓ ↓ ↓ ↓	5/2	5	5/2		$^6H_{5/2}$
6	↓ ↓ ↓ ↓ ↓ ↓	3	3	0		7F_0
7	↓ ↓ ↓ ↓ ↓ ↓ ↓	7/2	0	7/2		$^8S_{7/2}$
8	↑ ↑ ↑ ↑ ↑ ↑ ↑	3	3	6		7F_6
9	↑ ↑ ↑ ↑ ↑ ↑ ↑	5/2	5	15/2	$J = L + S$	$^6H_{15/2}$
10	↑ ↑ ↑ ↑ ↑ ↑ ↑	2	6	8		5I_8
11	↑ ↑ ↑ ↑ ↑ ↑ ↑	3/2	6	15/2		$^4I_{15/2}$
12	↑ ↑ ↑ ↑ ↑ ↑ ↑	1	5	6		3H_6
13	↑ ↑ ↑ ↑ ↑ ↑ ↑	1/2	3	7/2		$^2F_{7/2}$
14	↑ ↑ ↑ ↑ ↑ ↑ ↑	0	0	0		1S_0

*↑ = spin $\frac{1}{2}$; ↓ = spin $-\frac{1}{2}$.

Magnetic susceptibility:

$$\chi = \frac{C}{T - \theta_{CW}} \therefore C \propto p^2 = g_j \sqrt{J(J(J+1))} \mu_B^2$$



Why are Ce and Yb specials?

$\text{Ce}^{3+} - 4f^1$

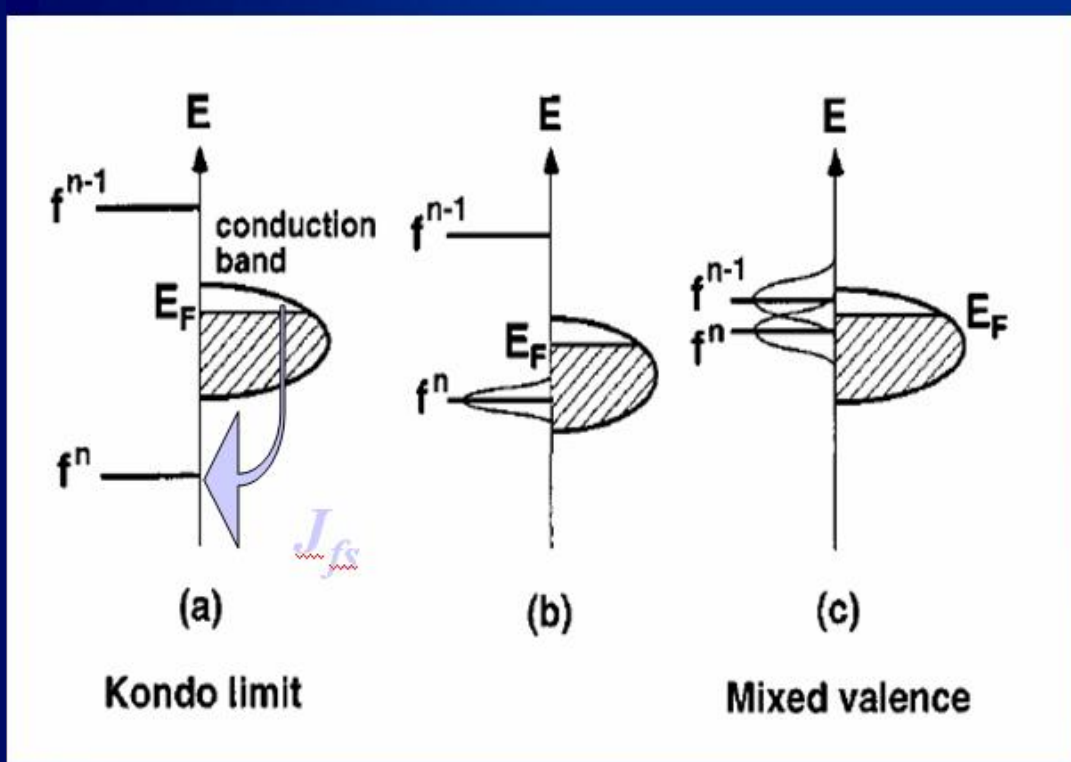
I	-3	-2	-1	0	+1	+2	+3
	↑						

$\text{Yb}^{3+} - 4f^{13}$

I	-3	-2	-1	0	+1	+2	+3
	↓	↓	↑	↑	↑	↑	↑

spin/valence instability
due to desire
to fill/empty shell

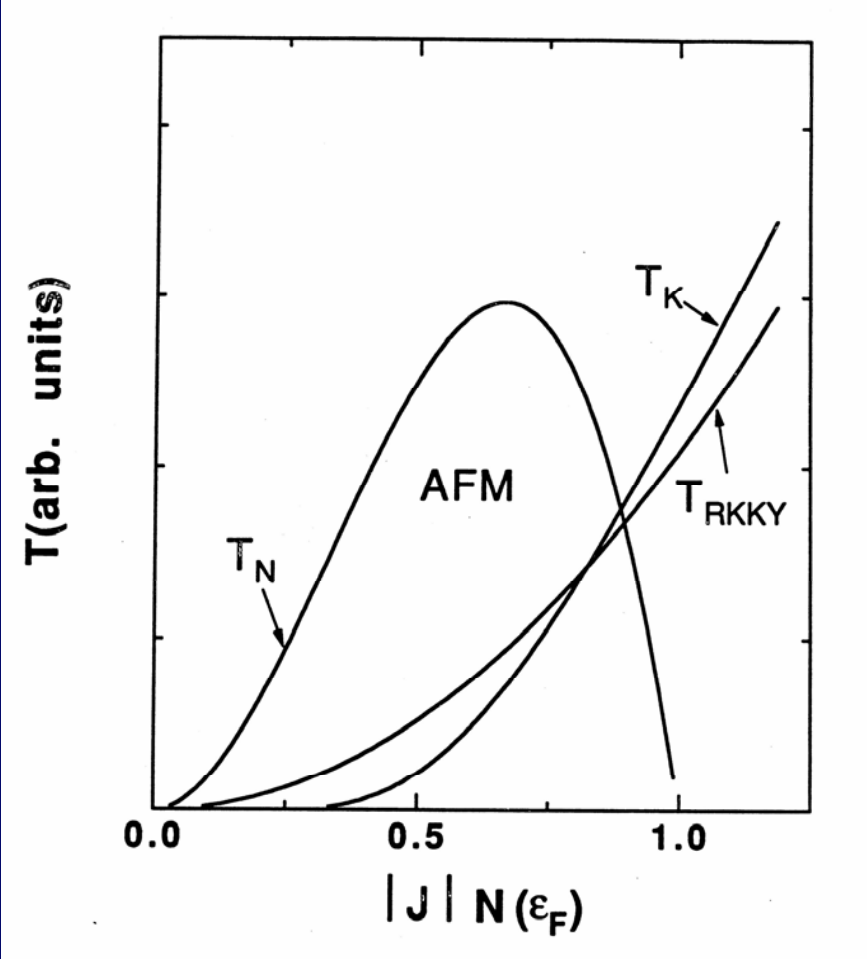
$\text{Ce}^{4+} - 4f^0$ and $\text{Yb}^{2+} - 4f^{14}$
Non-magnetic ions
Pressure effects



J_{fs} is strong and
antiferromagnetic

f - s hybridization
takes place

Ground state competition



Competition between
Kondo screening and
magnetic order

- Tune J with doping or pressure
- Often find superconductivity where $T_N \rightarrow 0$: quantum critical point.

S. Doniach, in Valence Instabilities and Related Narrow Band Phenomena,
ed. R.D. Parks (Plenum, New York, 1977) p. 169.

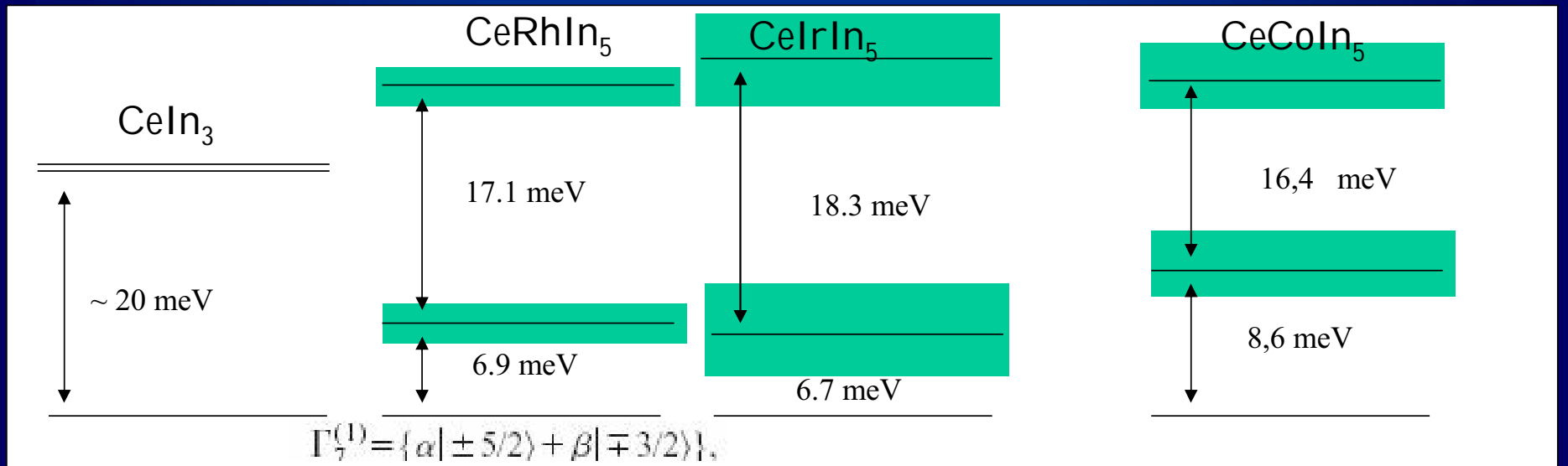
CEF effects on T_K

CEF effects in Ce-M-In₅:

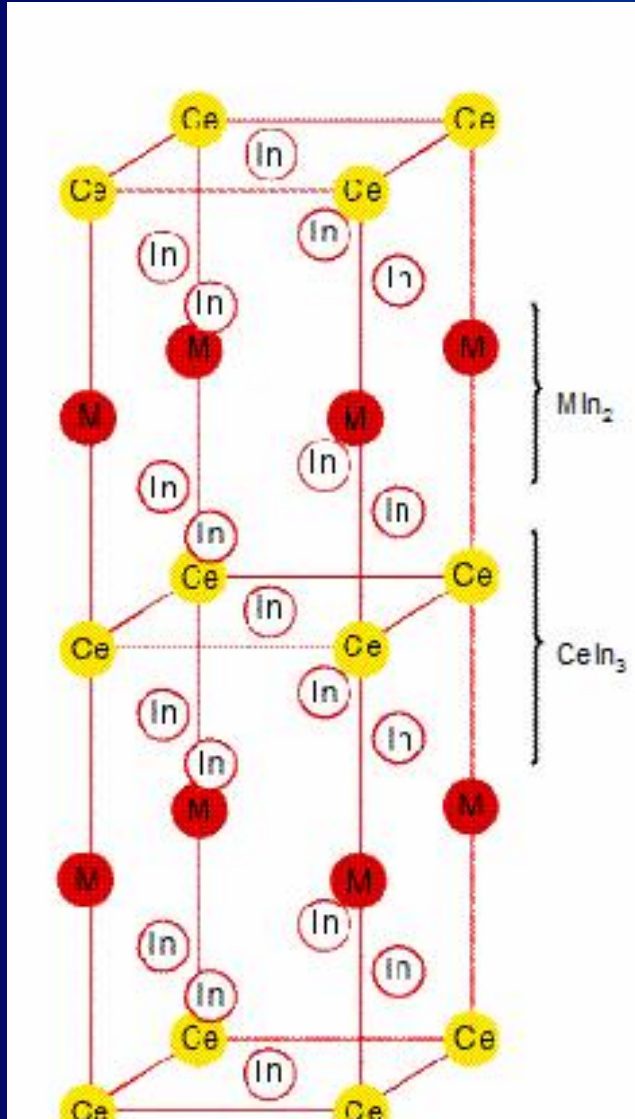
Effective T_K in the presence of CEF:

$$T_K^{\text{eff}} = T_K^{J=5/2} / \Delta_{\text{CEF}}^2$$

	CeRhIn ₅	CeCoIn ₅	CeIrIn ₅
χ^2	0.69	0.52	0.83
B_2^0	-1.03	-.81	-1.2
B_4^0	0.044	0.058	0.06
B_4^4	0.122	0.139	0.12
β [NCA]	0.60 [0.6]	0.86 [0.95]	0.70 [0.71]
Γ_{ie}	2.3	6.6(4)	8.7
$E(\Gamma_7^2)$ [NCA]	6.9 [7]	8.6 [6.45]	6.7 [2]
$E(\Gamma_6)$ [NCA]	24 [25]	25 [21.44]	29 [22.56]
V	456	469	470
λ	35	40	70



CeMIn₅ (M = Rh, Ir, Co) Family

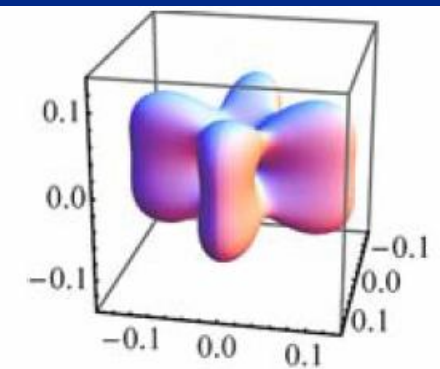


$$H_{\text{CEF}}^{\text{tetrag}} = B_2^0 O_2^0 + B_4^0 O_4^0 + B_6^0 O_6^0 + B_4^4 O_4^4 + B_6^4 O_6^4$$

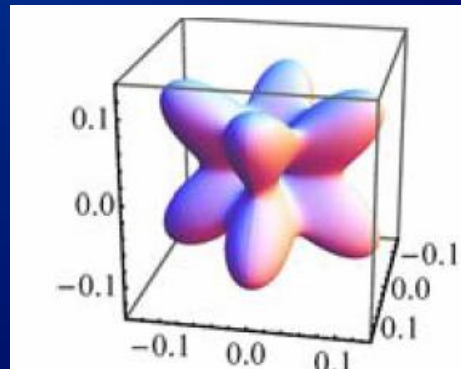
$$|2\rangle = \Gamma_6 = |\pm 1/2\rangle,$$

$$|1\rangle = \Gamma_7^1 = \beta |\pm 5/2\rangle - \alpha |\mp 3/2\rangle,$$

$$|0\rangle = \Gamma_7^2 = \alpha |\pm 5/2\rangle + \beta |\mp 3/2\rangle$$

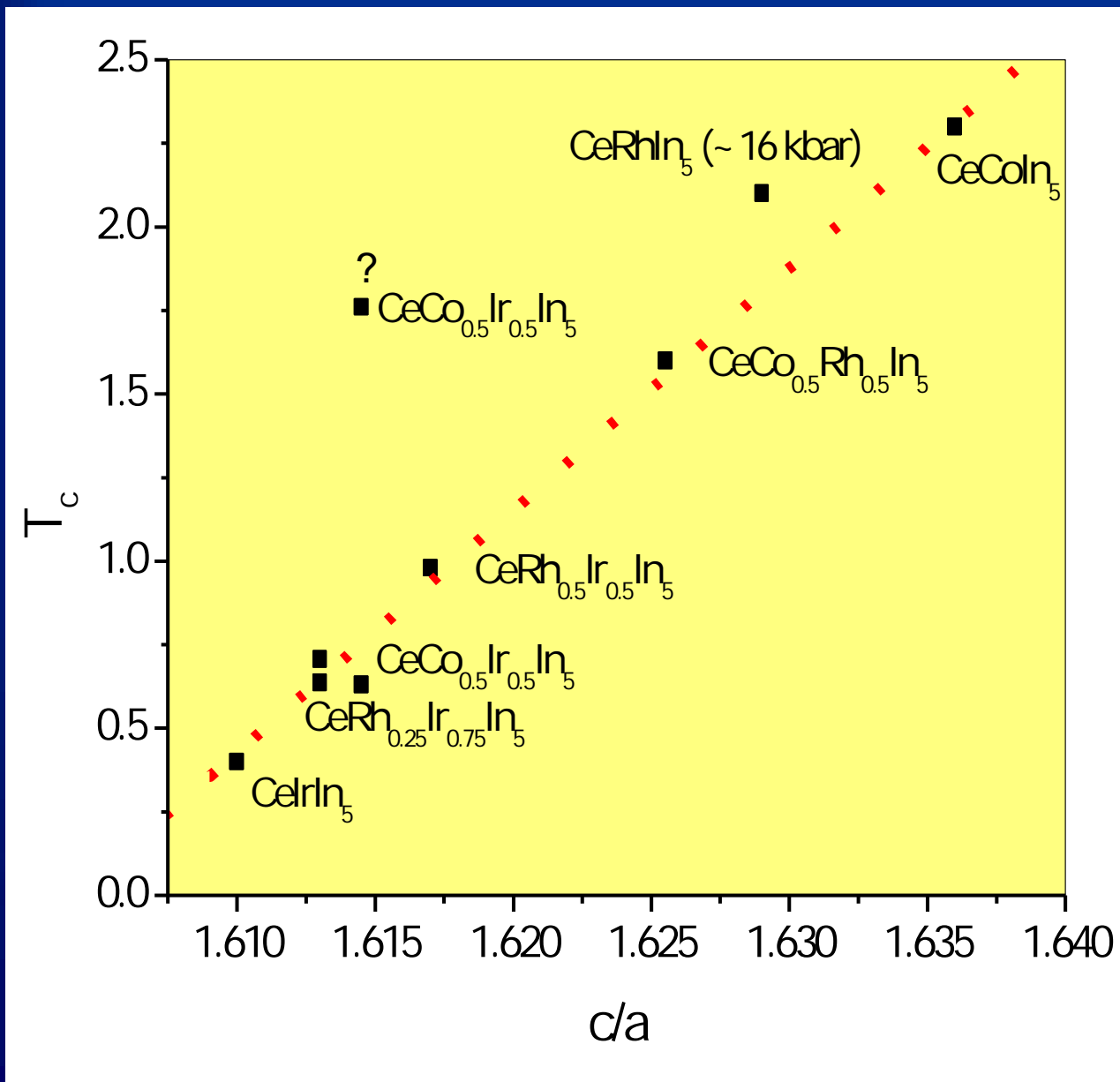


$\alpha=0.62$



$\alpha=0.36$

c/a as control parameter for T_c

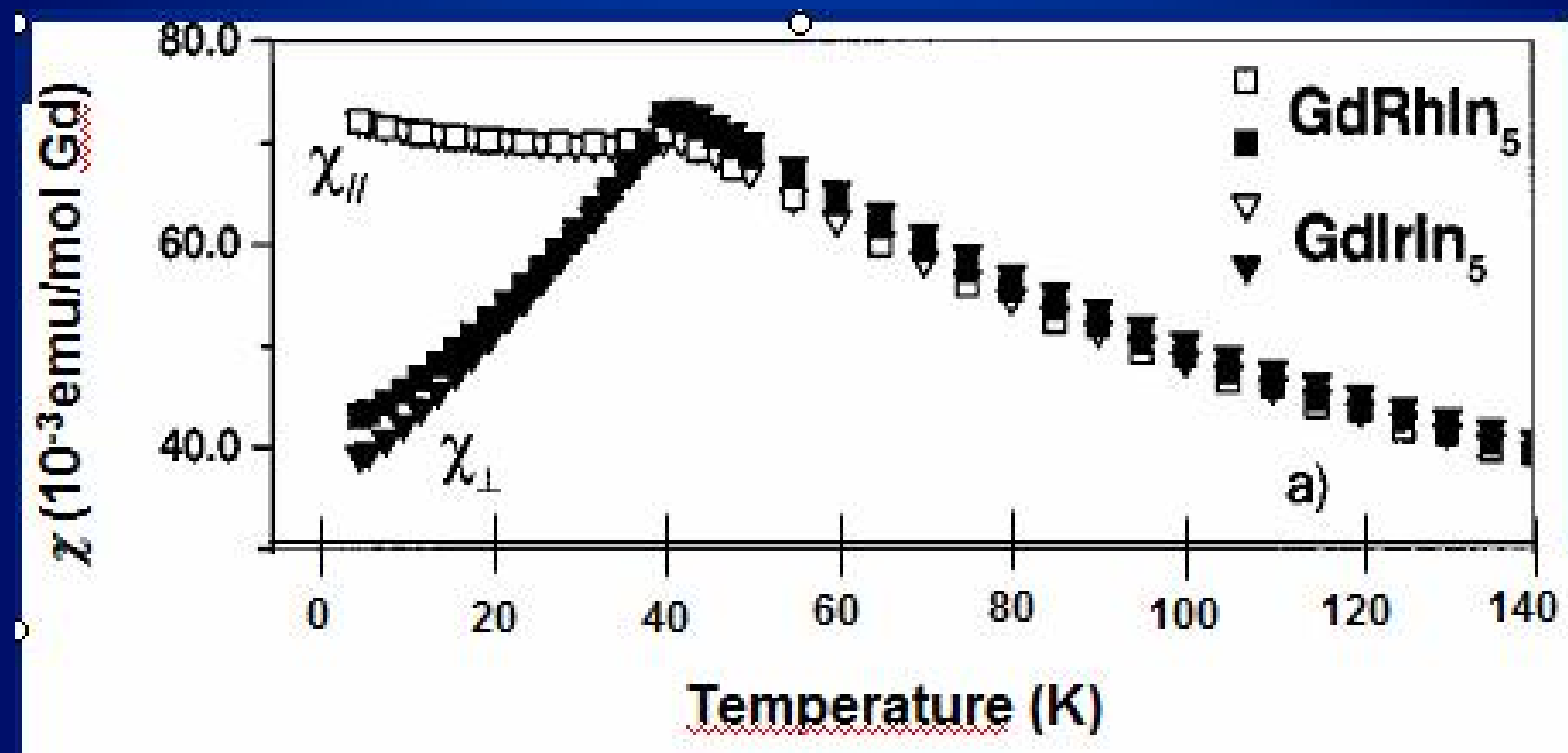


Is there an intrinsic parameter in this plot, which depends on c/a and determines T_c ?

Tuning:
- J_{RKKY}
- T_K
- CEF

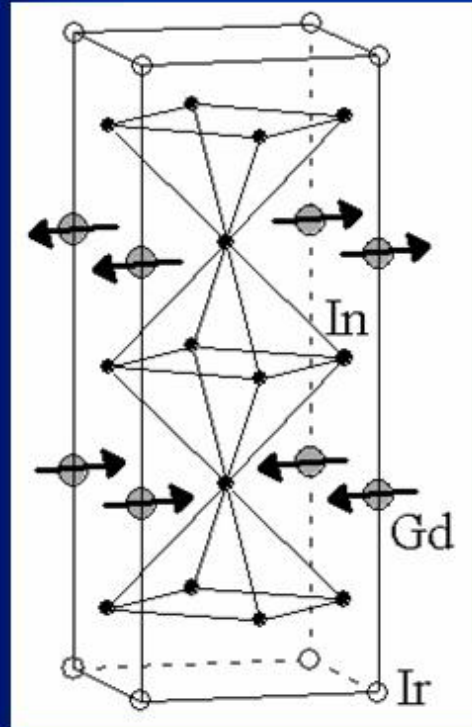
Tuning of J_{RKKY} ?

Gd 4f $^7 \rightarrow S=7/2, L=0$

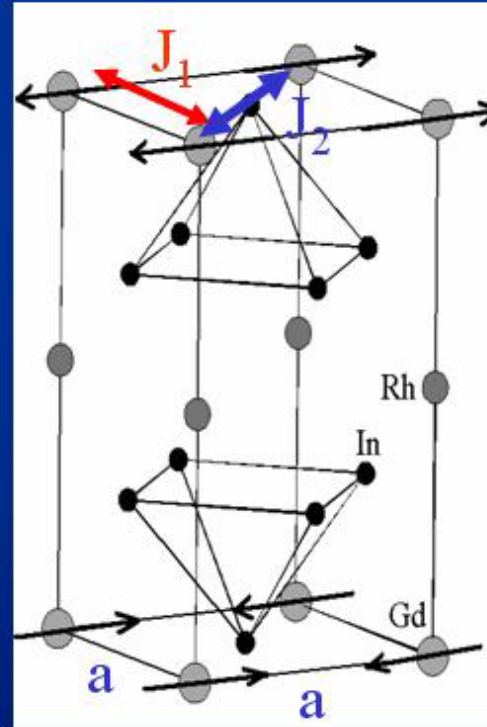


Pagliuso et al. PRB. 62, 12266 (2000); PRB (2001).

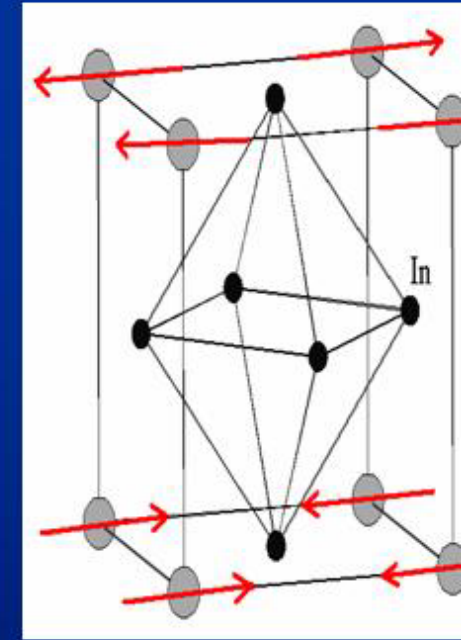
Tuning of J_{RKKY} ?



2-1-8



1-1-5



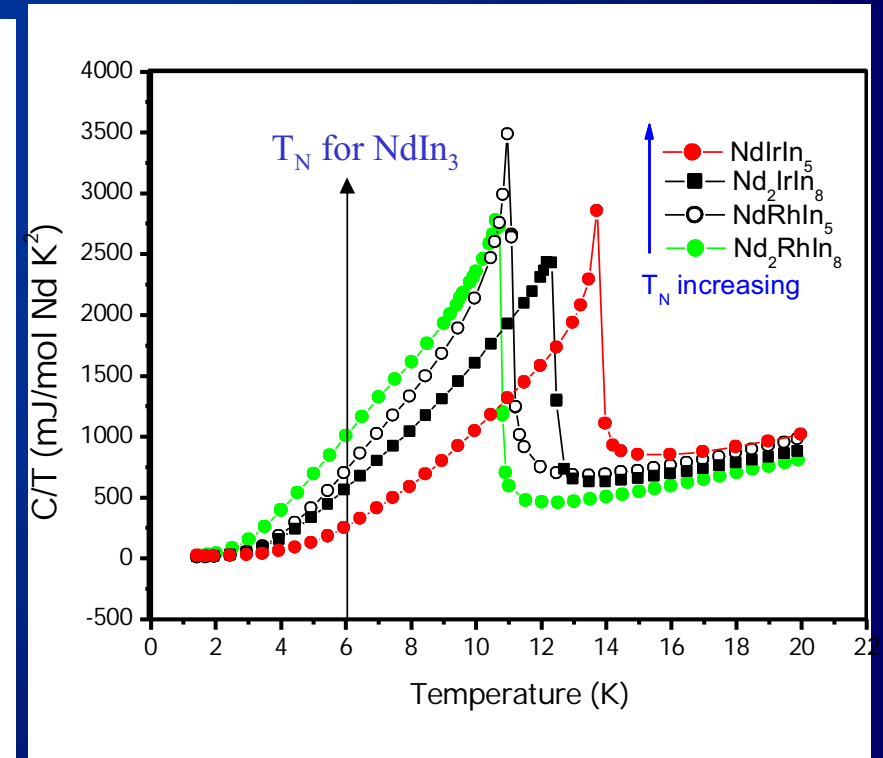
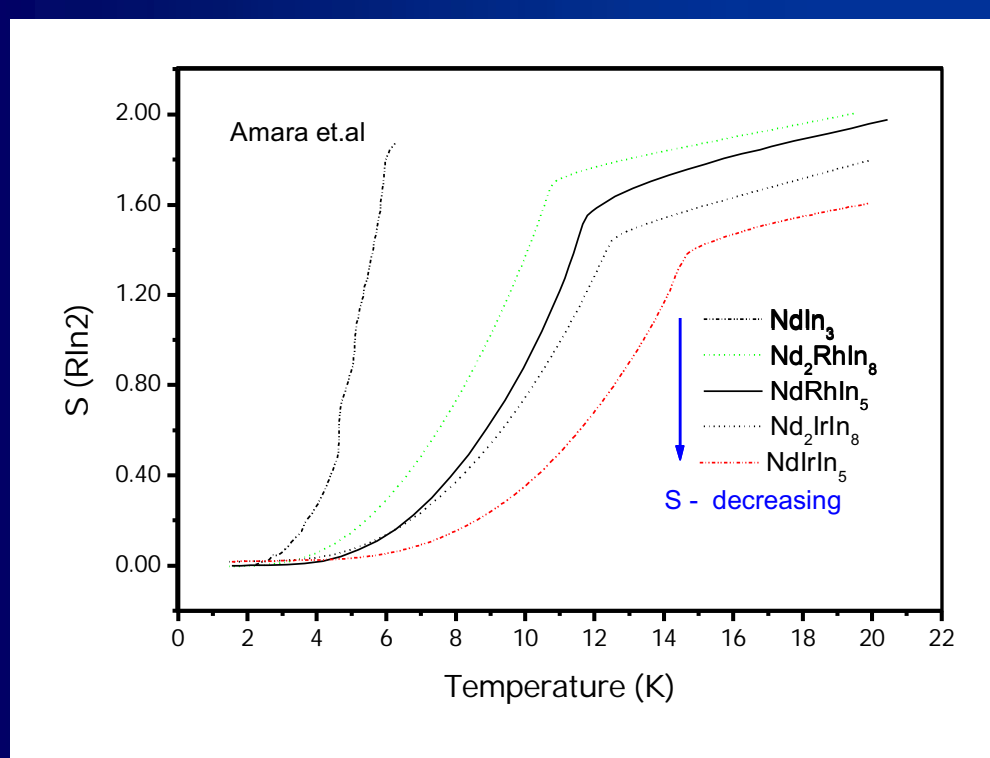
1-0-3

Same T_N and Magnetic Structures ($\epsilon = (1/2, 0, 1/2)$) \rightarrow same J_{RKKY}

$\theta_{\text{CW}} = 70 \text{ K}$ and $T_N = 40 \text{ K}$ - $J_2 > J_1$
- frustrated first neighbor interaction

E. Granado, R. Lora Serri
PRB (2004) - PRB (2006)

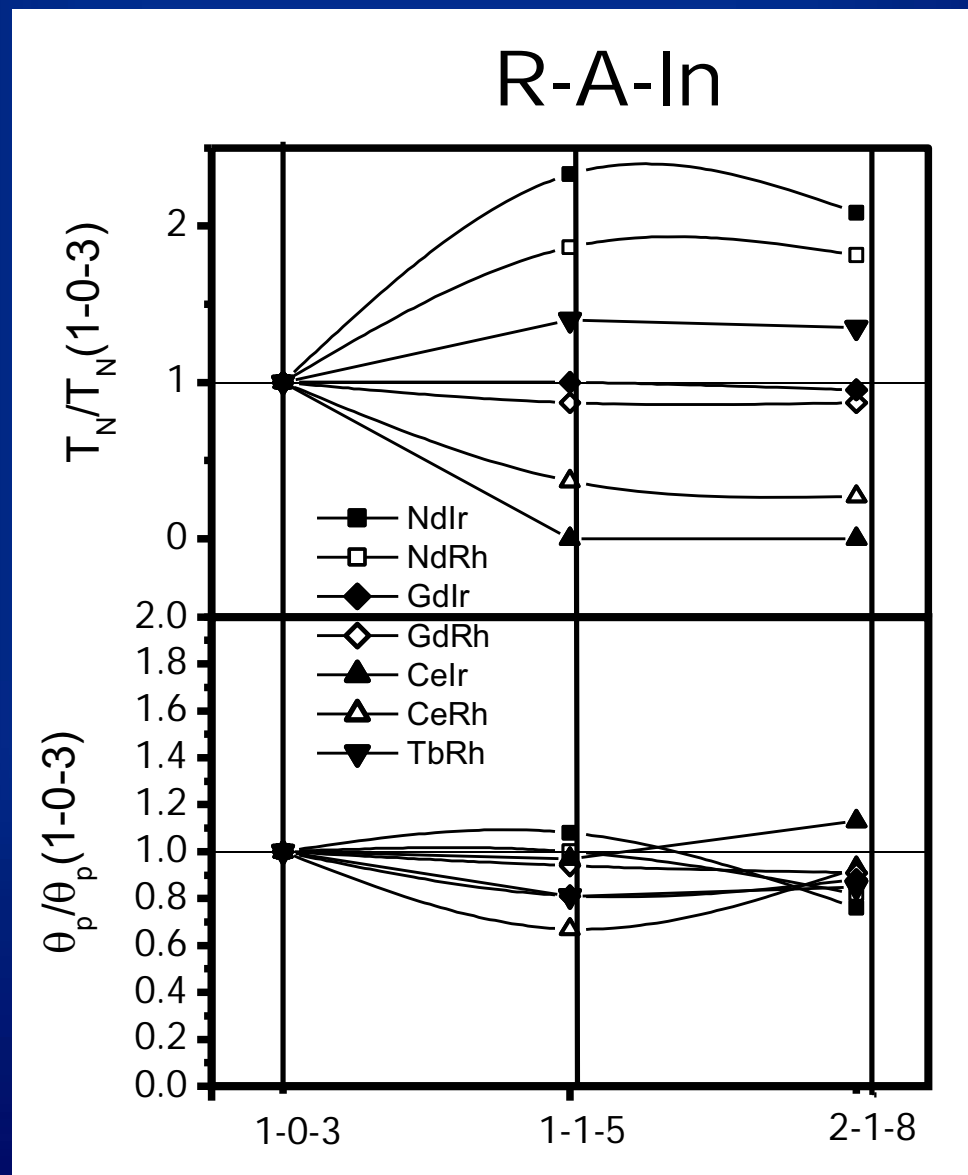
Tuning the CEF? $C_p(T)$ and $S(T)$ for Nd-based compounds



The larger Γ_8 CEF Splitting \Rightarrow larger T_N

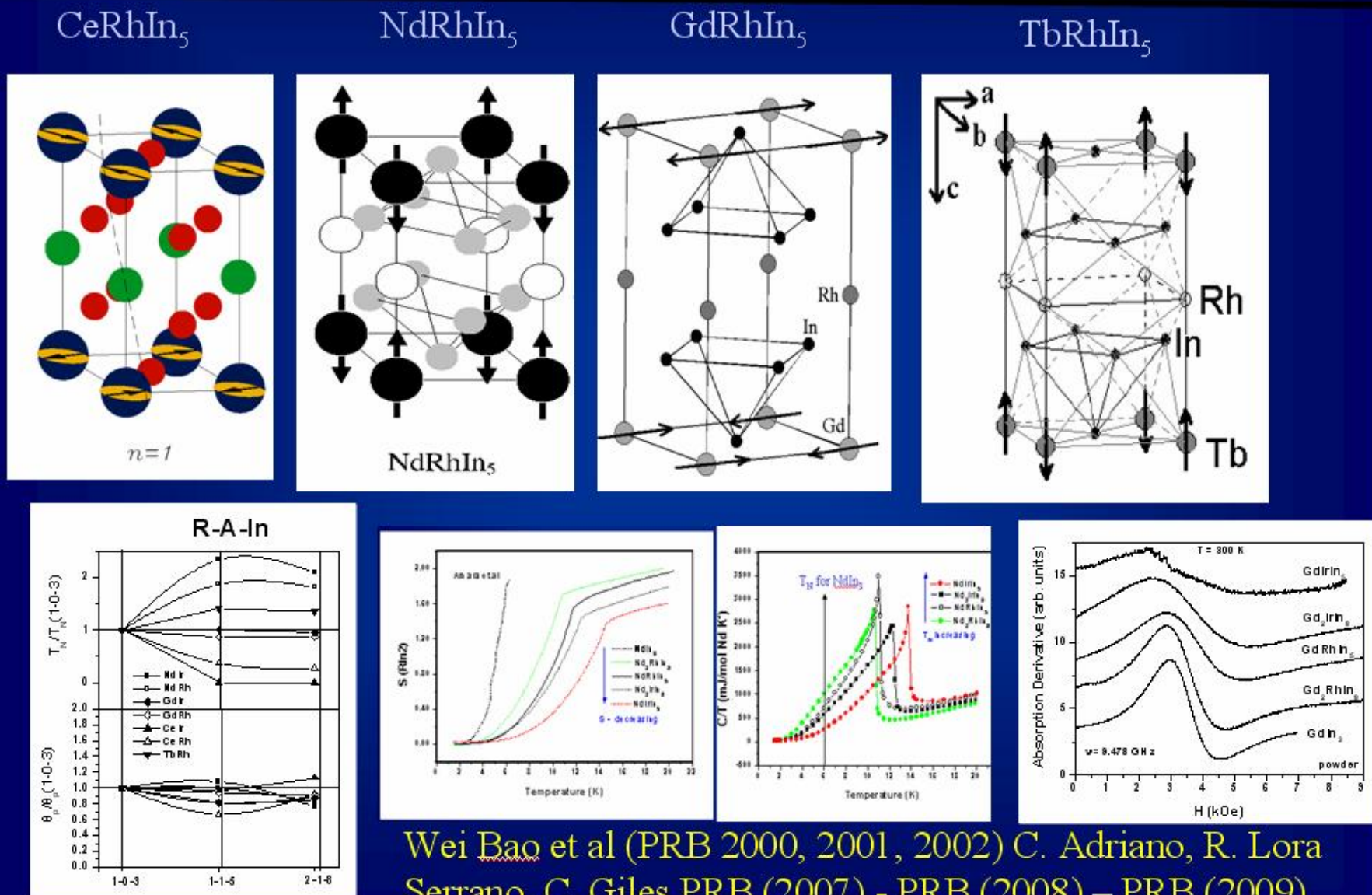
P.G. Pagliuso et al. Physical Review B. 62, 12266 (2000).

T_N evolution for $R_m A_n In_{3m+2n}$ ($m = 1, 2$; $n = 0, 1$) ($R = Nd, Tb, Gd, Sm$)



Pagliuso et al. PRB. 62, 12266 (2000); PRB (2001).

Summary of Experiments Facts

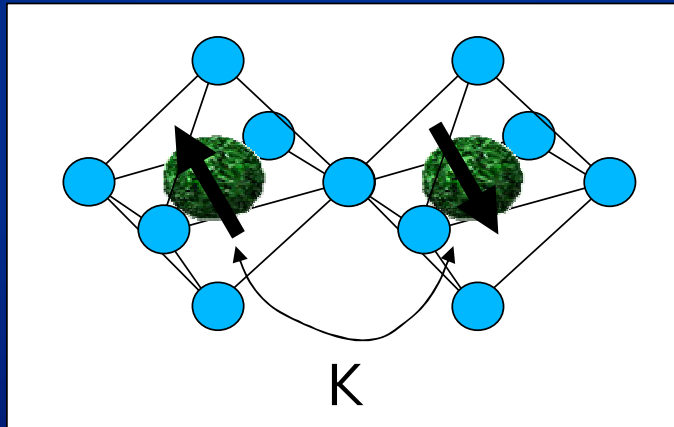


The model: Magnetic Interactions and Crystal Field Effects-

Simplest Magnetic Interaction:
(mimics RKKY interaction)

$$K \vec{J}_i \cdot \vec{J}_j$$

Crystal Field (CFE) Interaction:



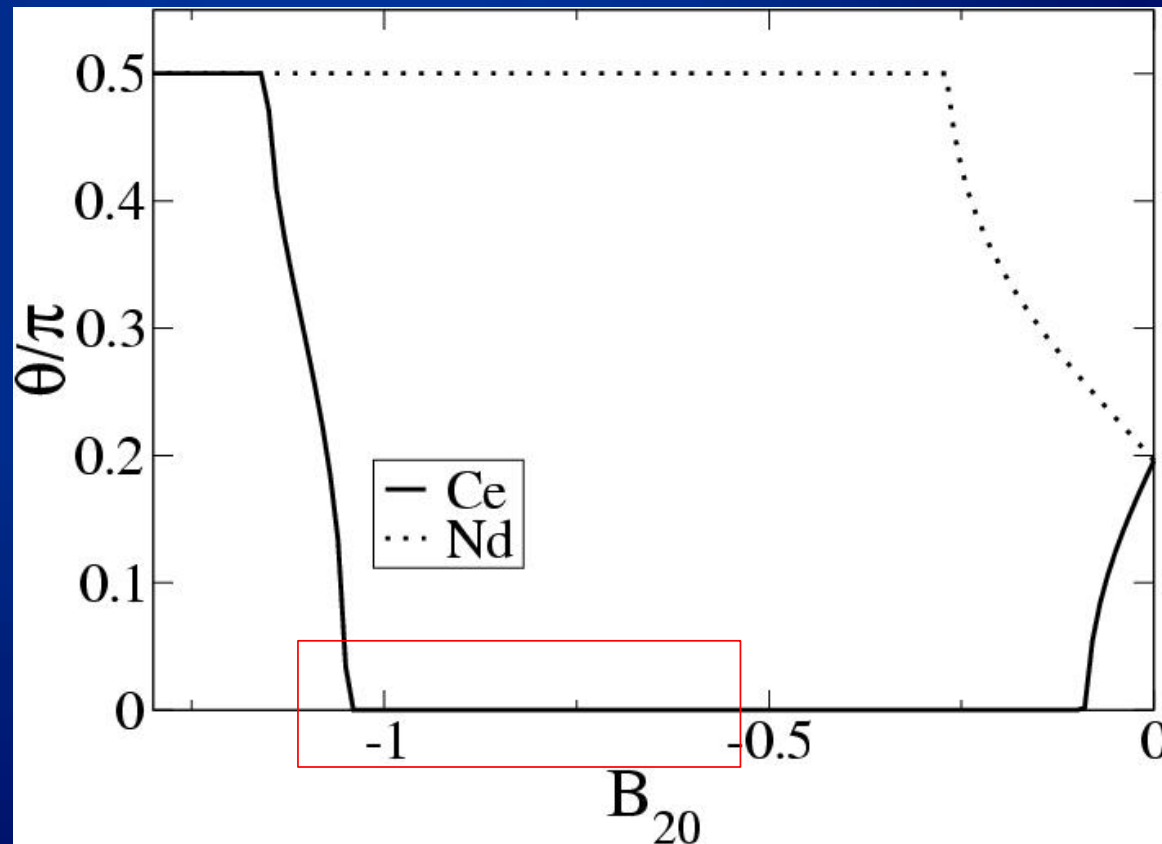
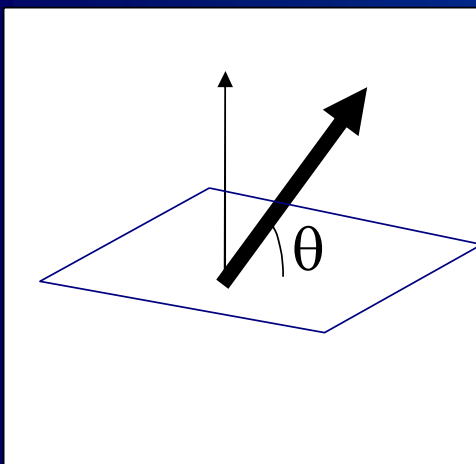
Can this simple model account for change in direction of the order moment along the series and for the T_N behavior?

D. Garcia, E. Miranda, et al. JAP (2006)

Cristal Field Effects:



Results for
 $(B_{44}=5B_{40}=0.25\text{meV})$

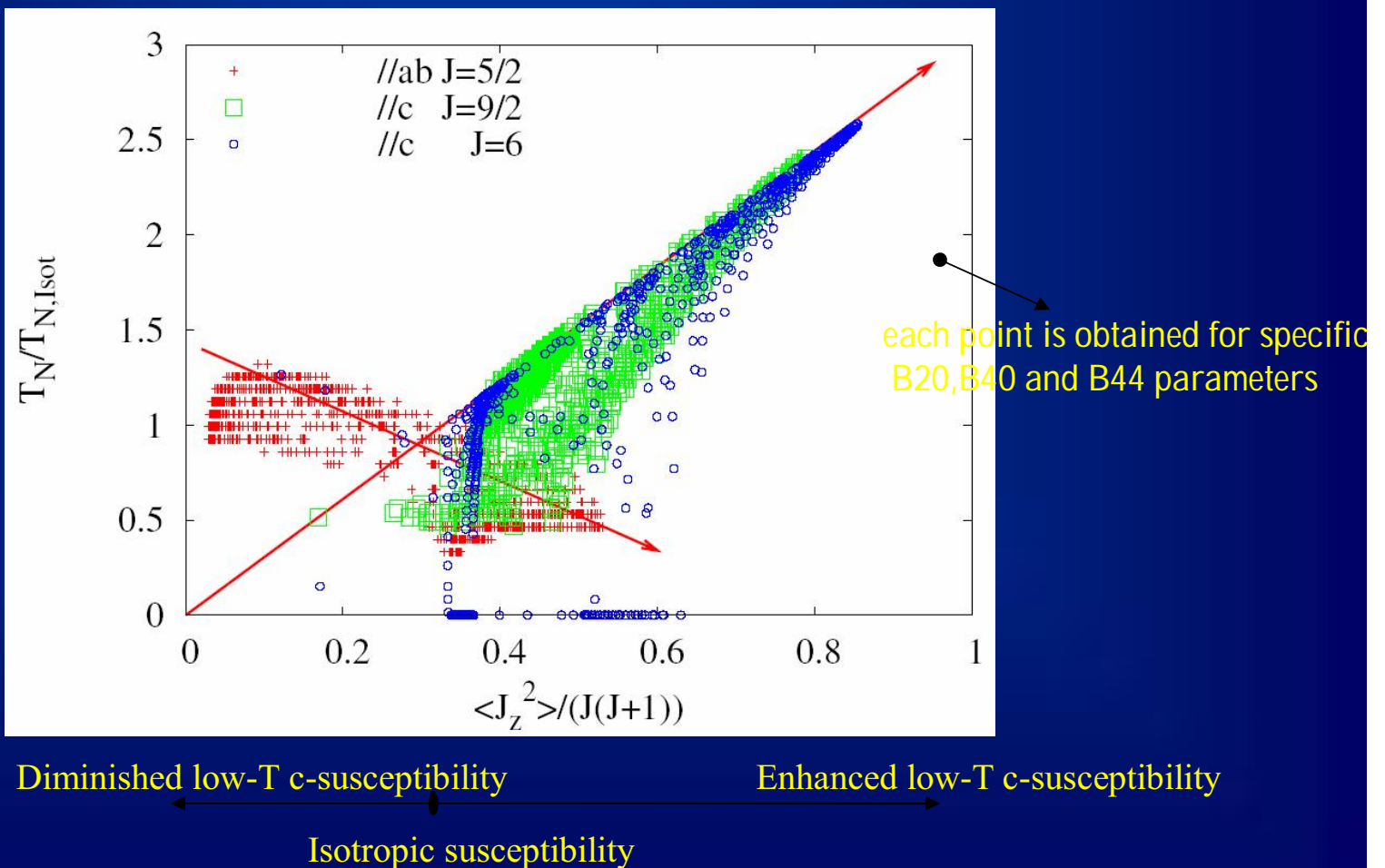


Interaction Effects on the order temperature T_N

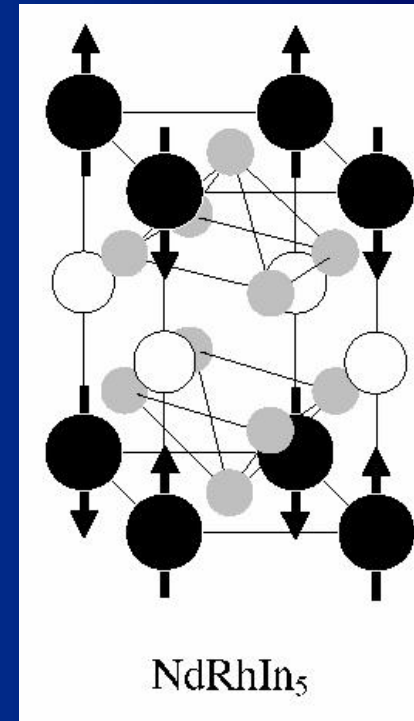
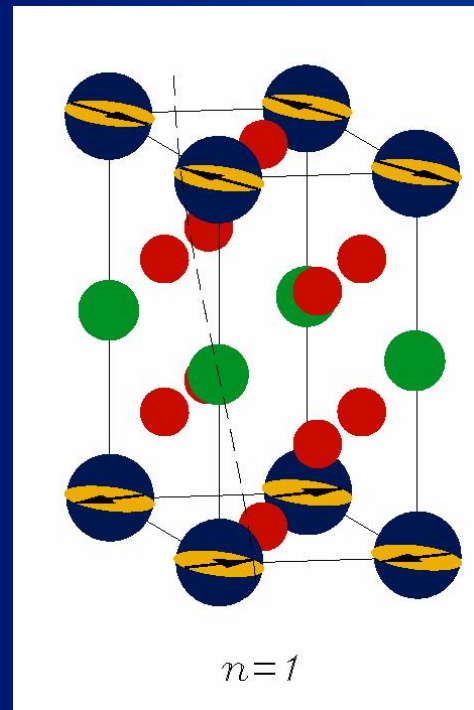
Without CF: isotropic K

CEF
enhanced
order

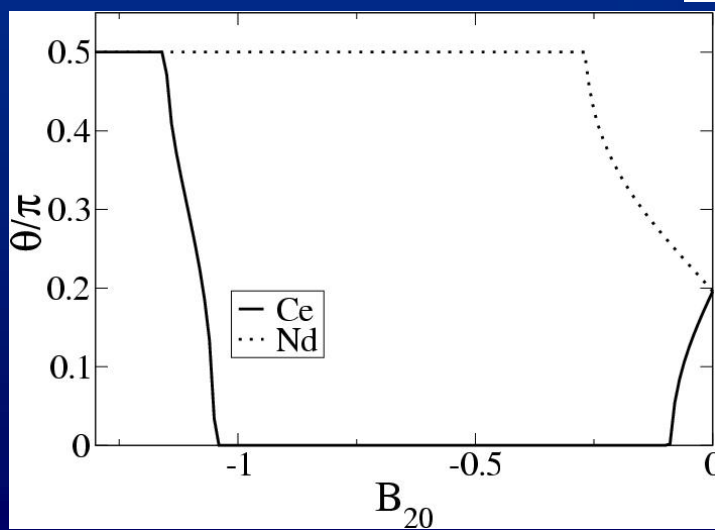
CEF
frustrated
order



R_nMIn_{3n+2} Magnetic Structures

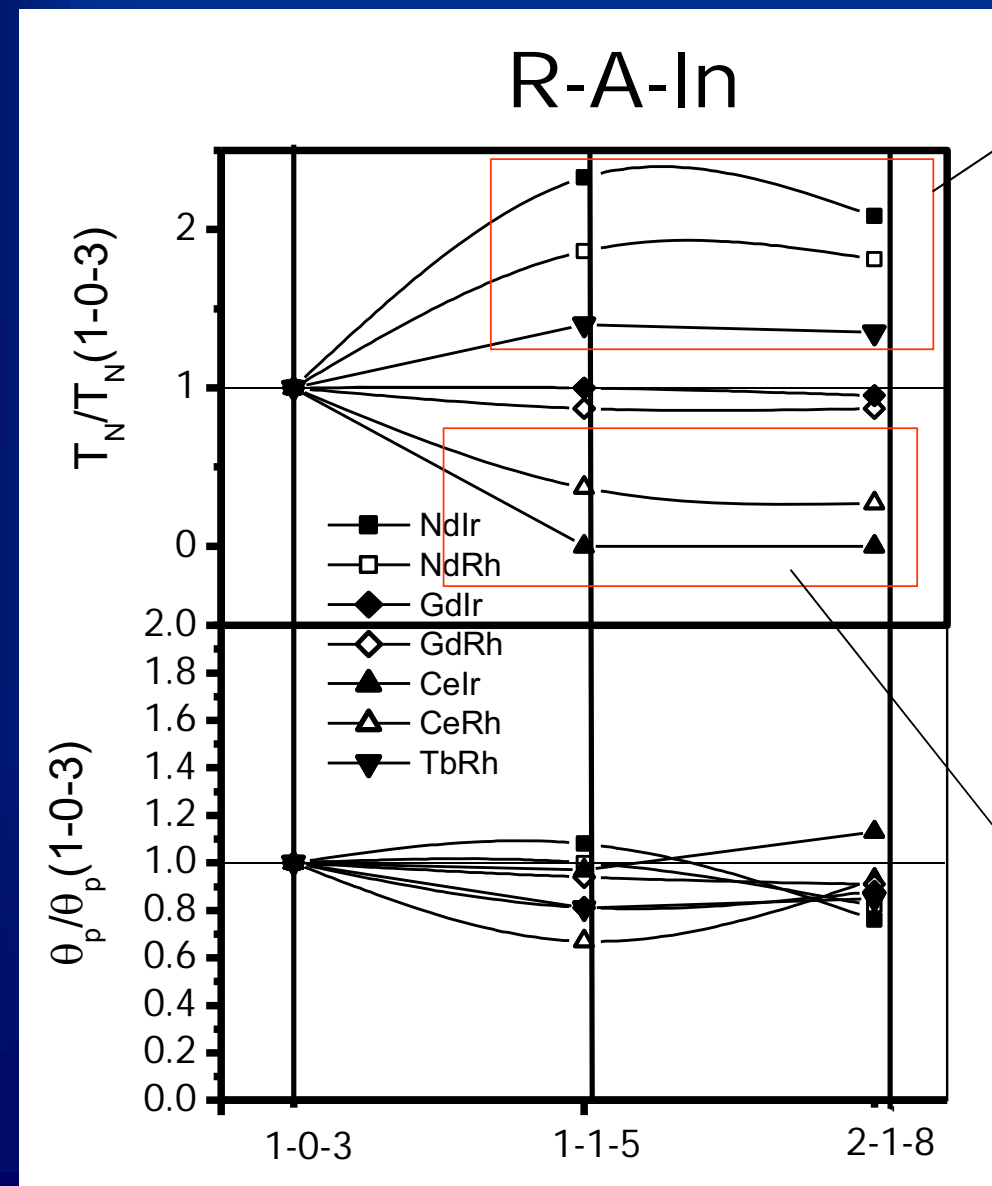


CeRhIn₅

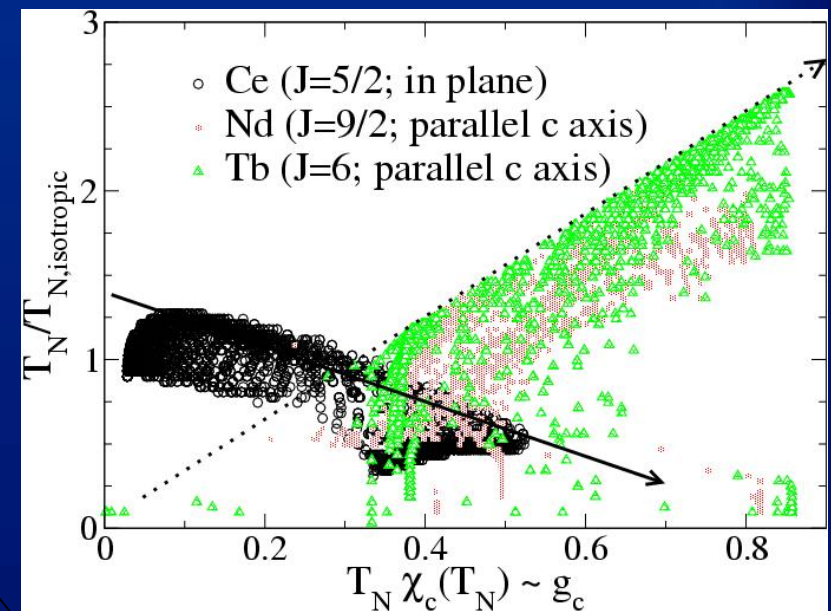


NdRhIn₅

T_N evolution for $R_mA_nIn_{3m+2n}$ ($m = 1,2$; $n = 0,1$)

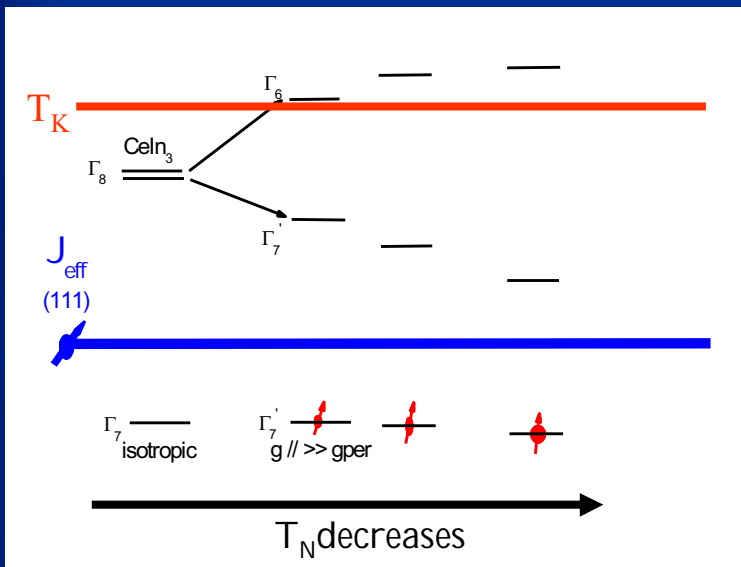


RE moments ordered along c-axis.

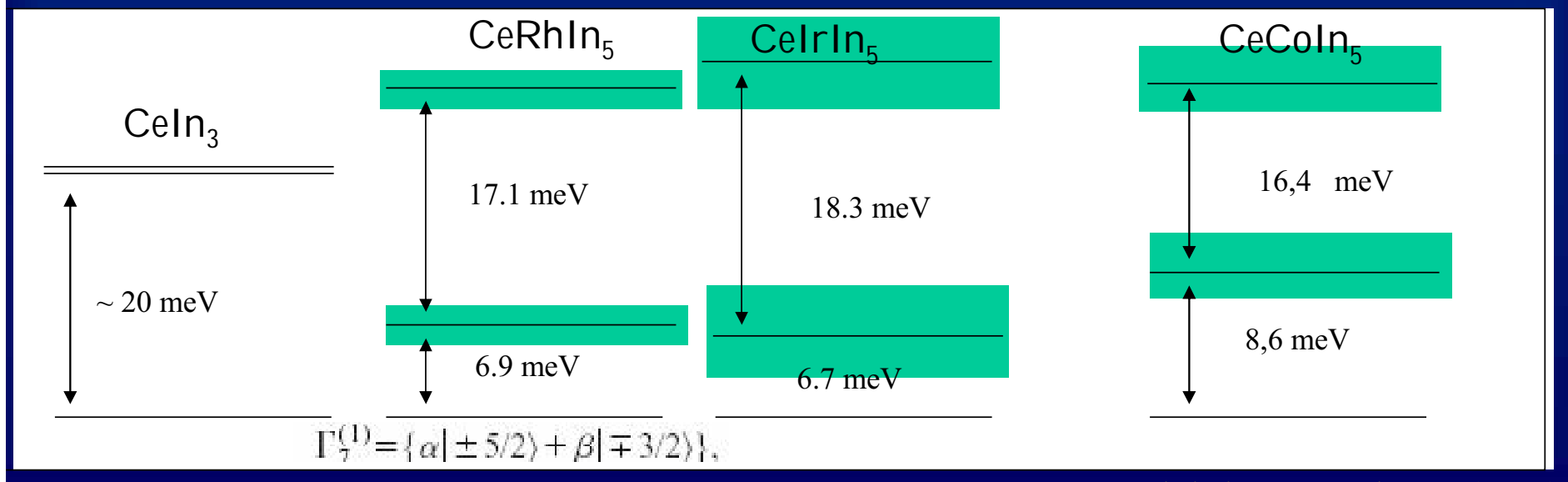


RE moments in the ab-plane.

Extrapolation of CEF trend to Ce-M-In



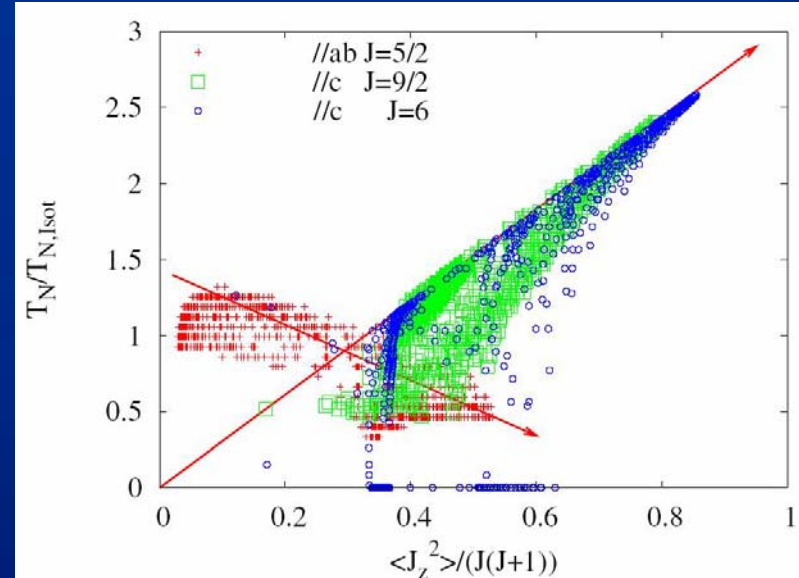
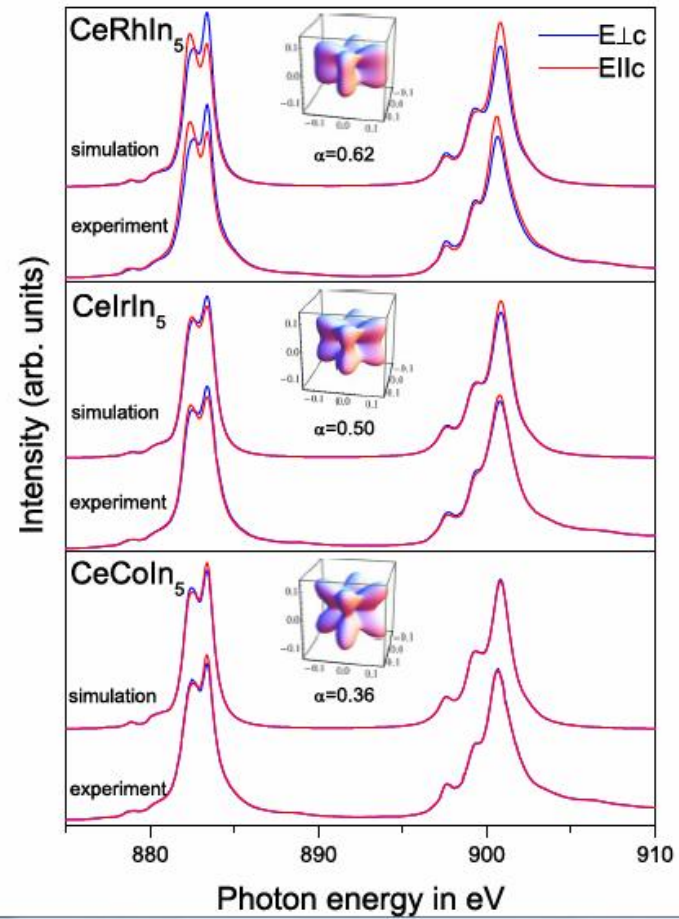
	CeRhIn ₅	CeCoIn ₅	CeIrIn ₅
χ^2	0.69	0.52	0.83
B_2^0	-1.03	-0.81	-1.2
B_4^0	0.044	0.058	0.06
B_4^4	0.122	0.139	0.12
β [NCA]	0.60 [0.6]	0.86 [0.95]	0.70 [0.71]
Γ_{ie}	2.3	6.6(4)	8.7
$E(\Gamma_7^2)$ [NCA]	6.9 [7]	8.6 [6.45]	6.7 [2]
$E(\Gamma_6)$ [NCA]	24 [25]	25 [21.44]	29 [22.56]
V	456	469	470
λ	35	40	70



A.D. Christianson et al PRB (2004).

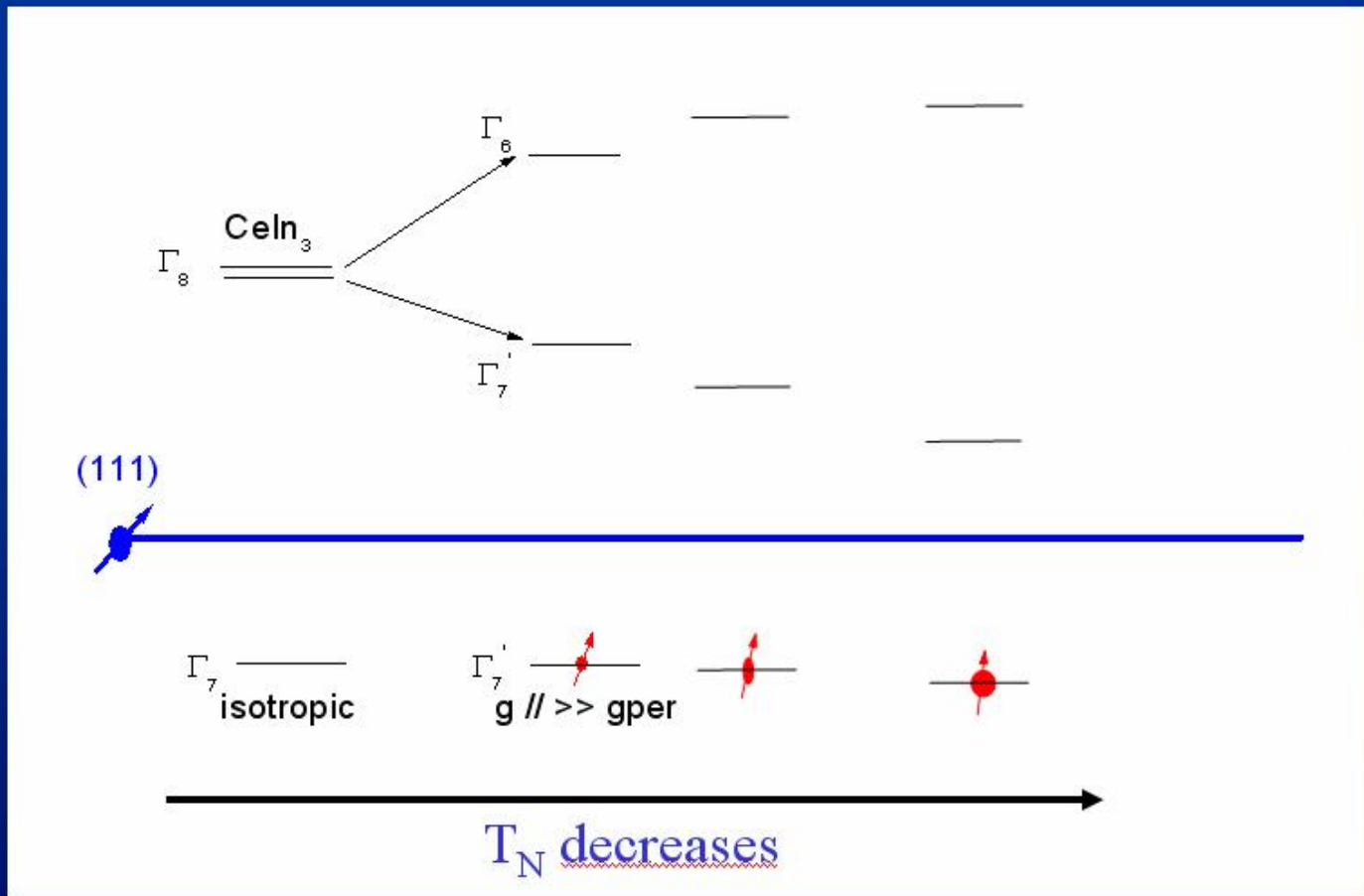
INS and XAS CEF study in Ce-M-In

T. Willers et al. PHYSICAL REVIEW B 81, 195114 (2010)

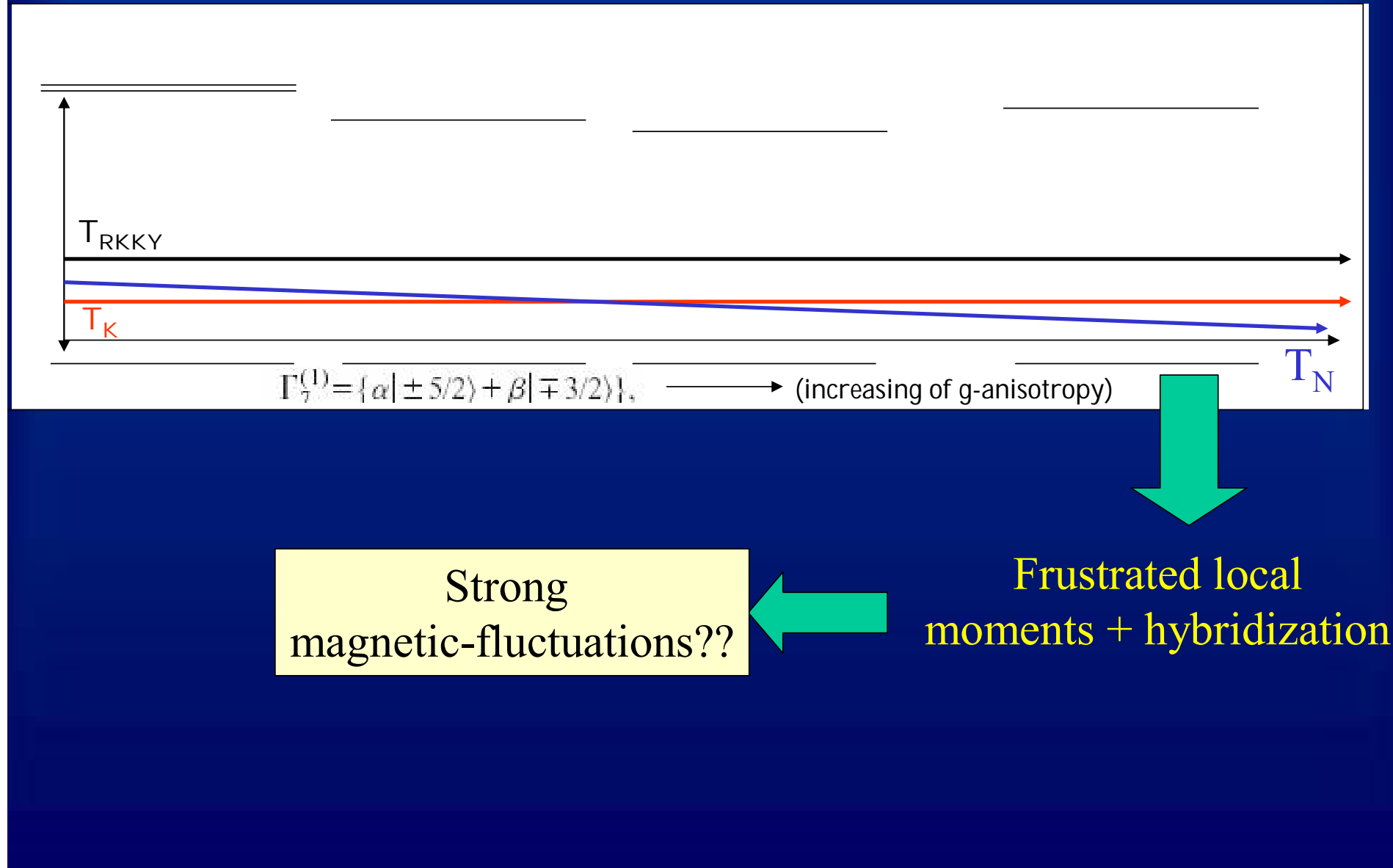


(meV)	CeRhIn ₅	CeIrIn ₅	CeCoIn ₅	Instrument (meV)	CeAu ₂ Si ₂ (Refs. 15 and 36)
$\Gamma_{qu}/2 @ 8\text{ K}$	1.2 ± 0.2			IN6 3.1	0.13
$\Gamma_{qu}/2 @ 75\text{ K}$	1.7 ± 0.2	2.7 ± 0.5	3.9 ± 0.5	IN6 3.1	0.43
F_1	7.0 ± 0.5	5.2 ± 1.0	6.8 ± 1.0	HET 20	16.5
E_2	24.7 ± 1.0	29.4 ± 1.5	25.0 ± 1.5	HET 60	21.0
$\Gamma_{in}^1/2 @ 5\text{ K}$	1.6 ± 0.5	3.0 ± 0.5	4.8 ± 0.8	HET 20/60	
$\Gamma_{in}^2/2 @ 5\text{ K}$	1.8 ± 0.5	3.4 ± 0.8	4.7 ± 0.8	HET 60	
$\Gamma_{in}^1/2 @ 75\text{ K}$	2.5 ± 0.5	3.7 ± 0.5	4.4 ± 0.8	IN6 3.1	
B_{20}	-0.928	-1.197	-0.856		
B_{40}	0.052	0.069	0.063		
$ B_{44} $	0.128	0.088	0.089		

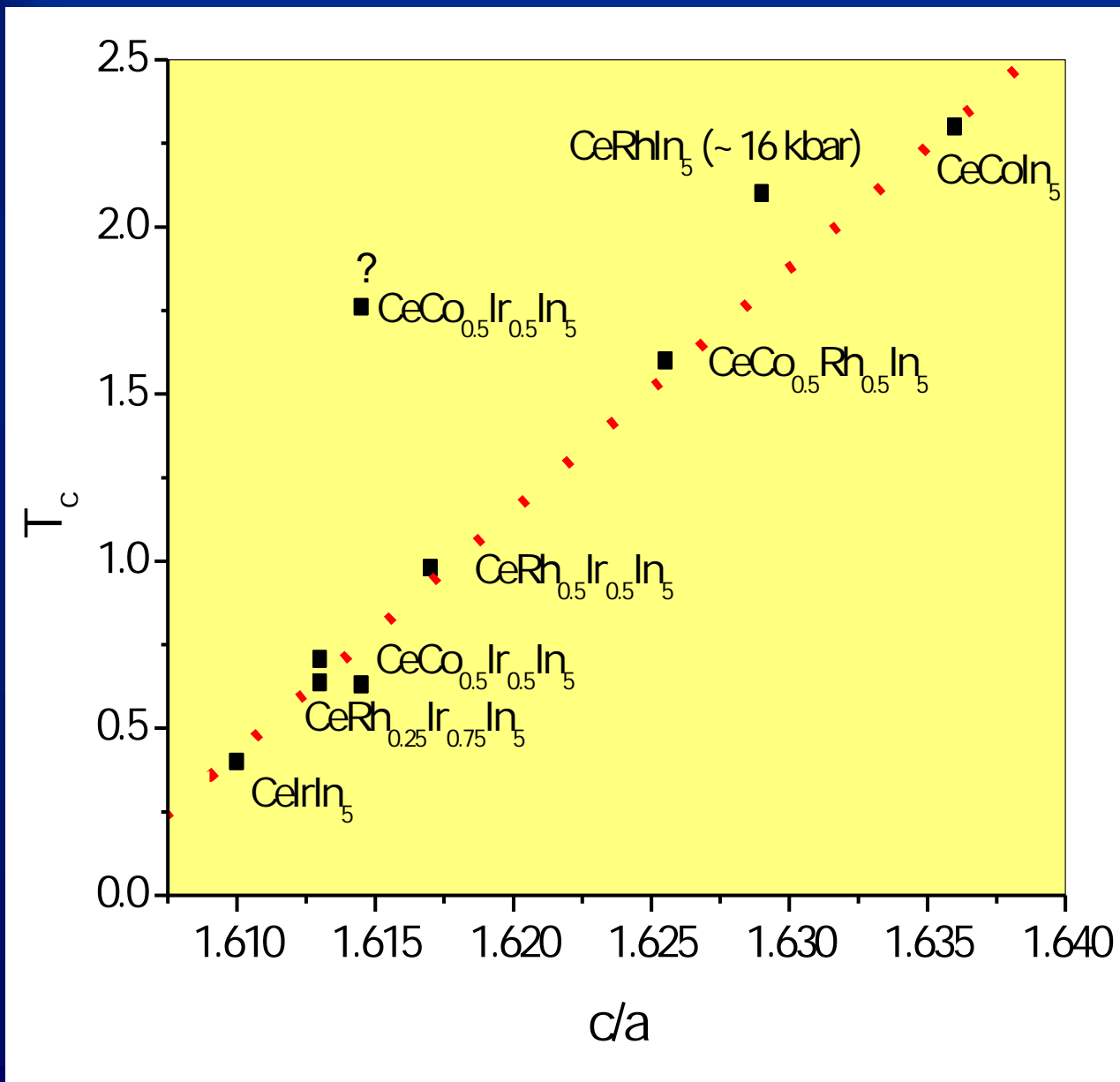
Extrapolation of CEF trend to Ce-M-In



Extrapolation of CEF trend to Ce-based materials



c/a as control parameter for T_c

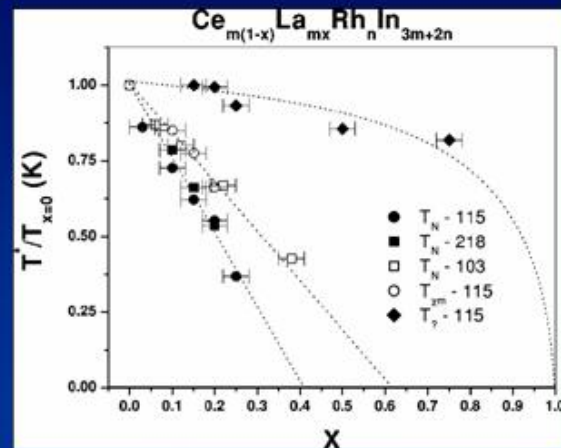
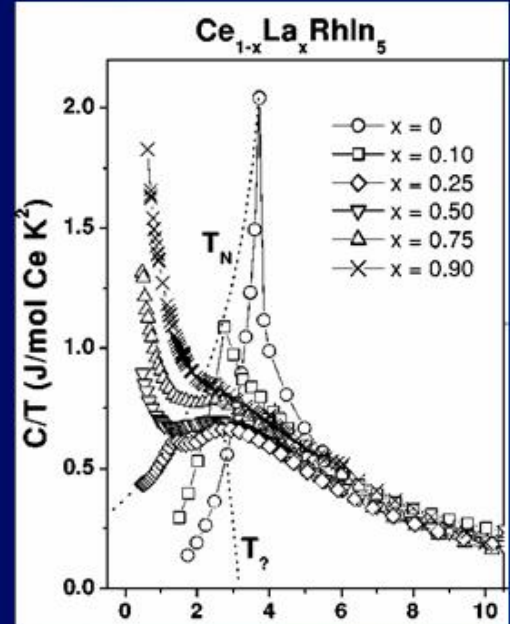


Is there an intrinsic parameter in this plot, which depends on c/a and determines T_c ?

Tuning:
- J_{RKKY}
- T_K
- CEF

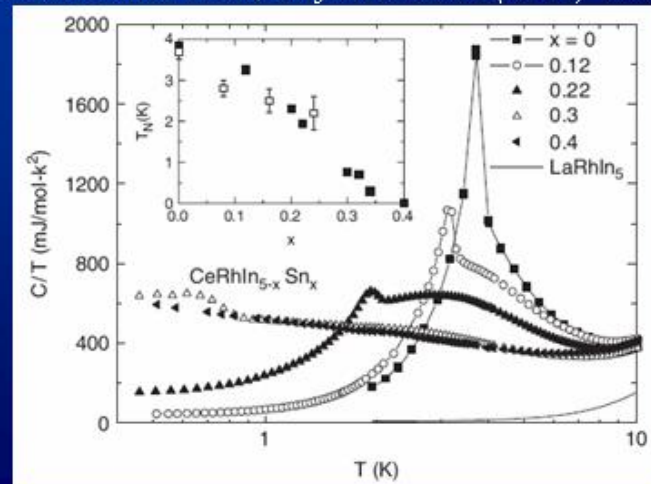
La- and Sn-doped CeRhIn₅

P. G. Pagliuso et al., Phys. Rev. B (2002) 054433.



- AFM is smoothly suppressed by La-doping;
- $T_N \rightarrow 0$ at $x_c \approx 0.40$;
- No SC is found around $x_c \approx 0.40$.

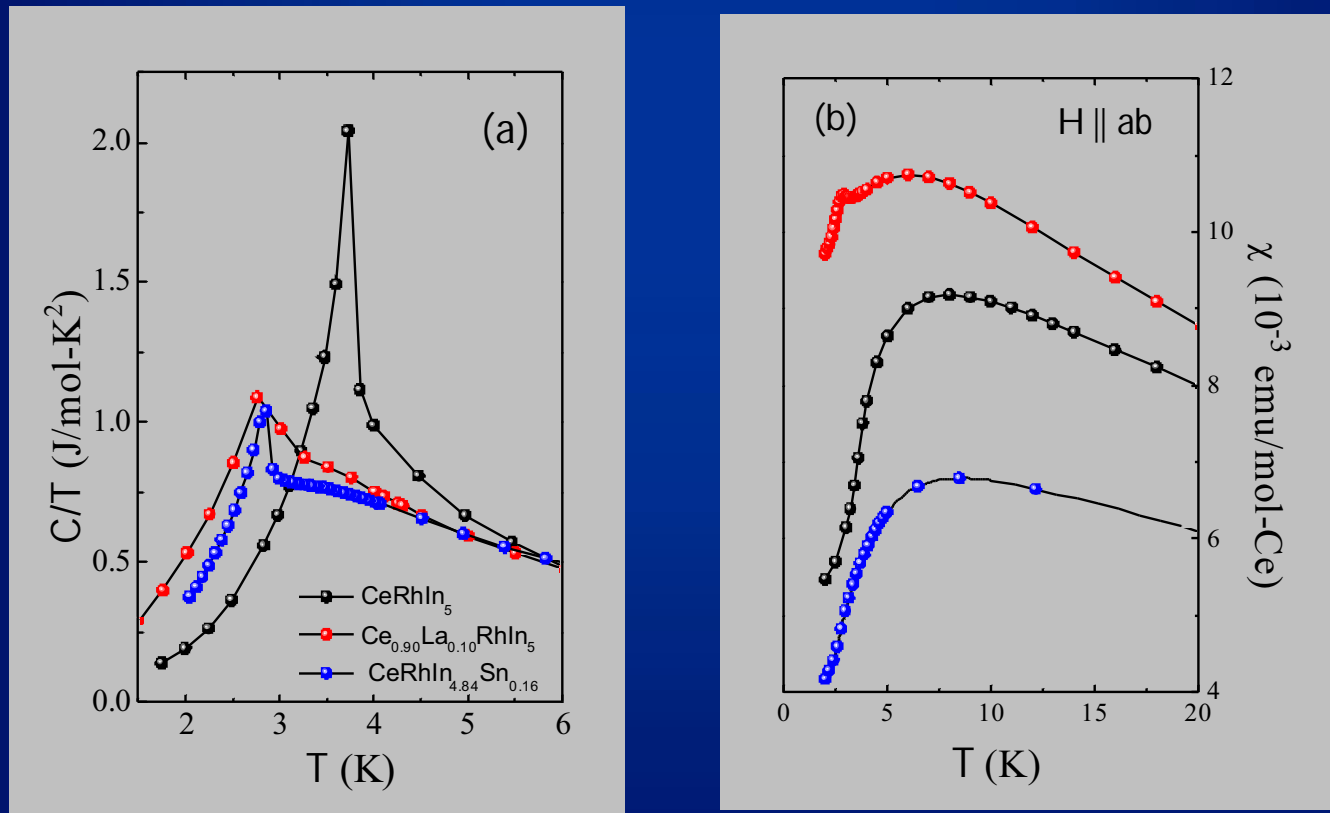
E. D. Bauer et al., Physica B 378 (2006) 142



- AFM is suppressed by Sn-doping;
- $T_N \rightarrow 0$ at $x_c \approx 0.35$;
- No SC is found around $x_c \approx 0.35 < (10\%)$

La- and Sn-doped CeRhIn₅

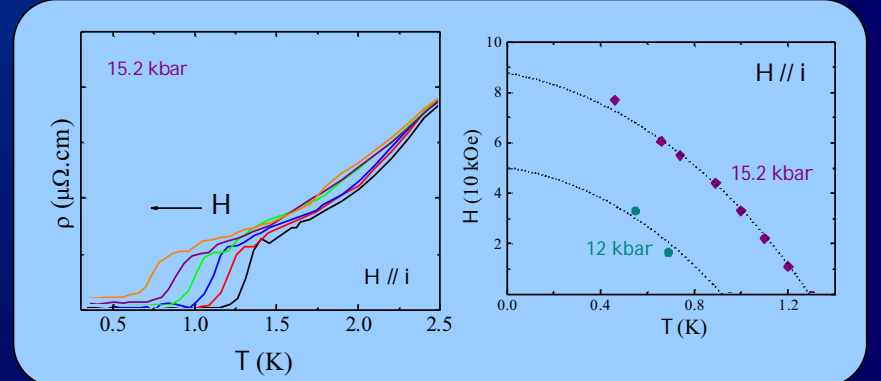
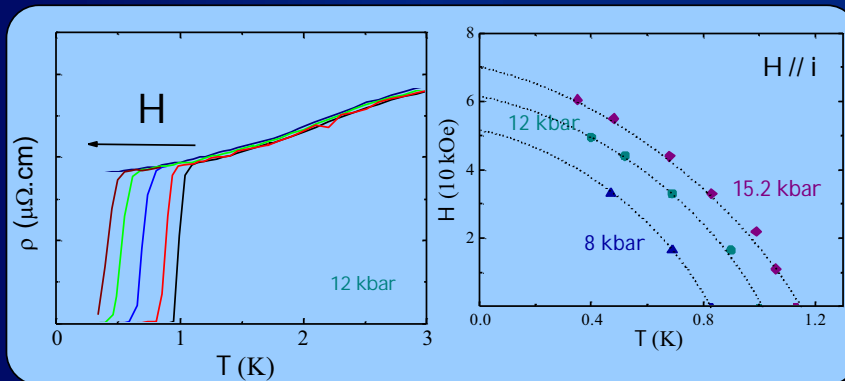
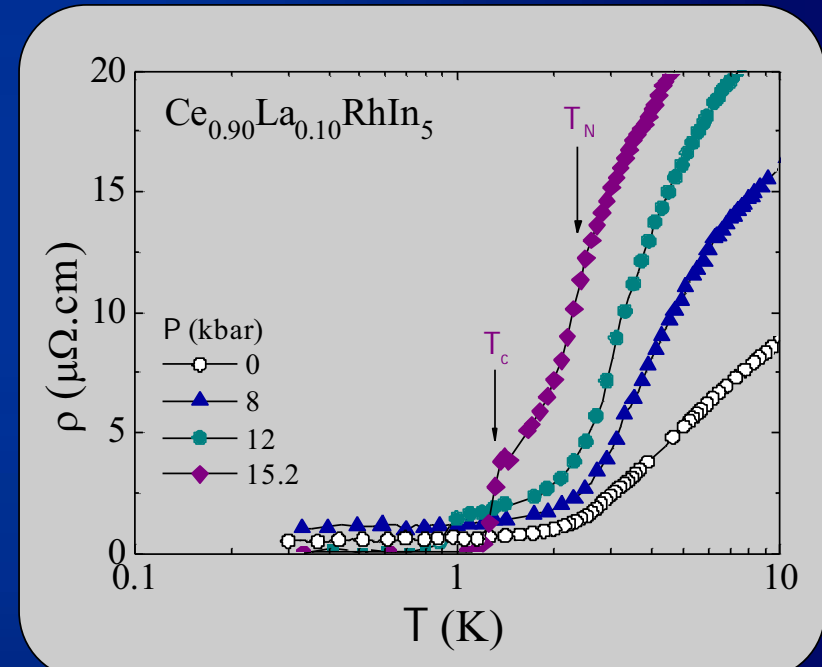
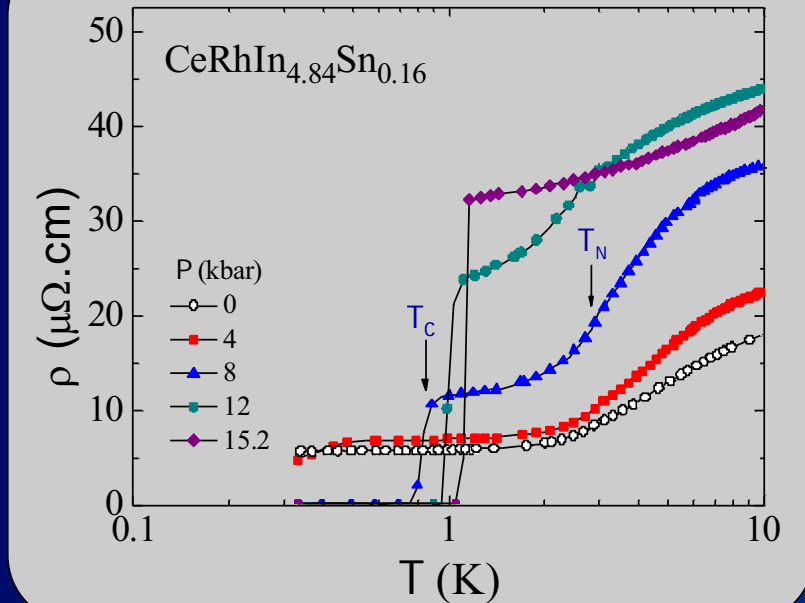
- We have carefully chosen two specific compositions, Ce_{0.90}La_{0.10}RhIn₅ and CeRhIn_{4.84}Sn_{0.16}.



The ordering temperature $T_N = 3.8$ K of undoped CeRhIn₅ was suppressed to the same $T_N \approx 2.8$ K for both La and Sn doping in the studied concentrations.

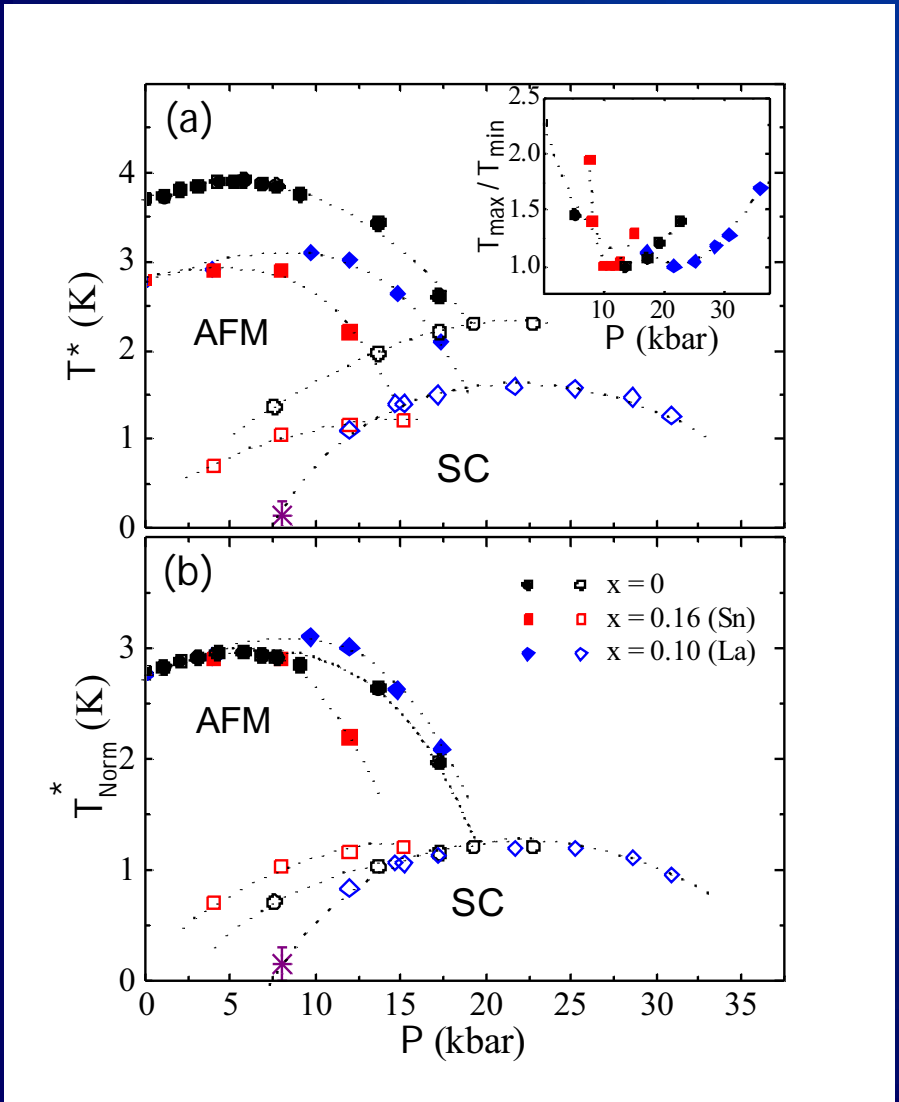
La- and Sn-doped CeRhIn₅

AC electrical resistivity under pressure



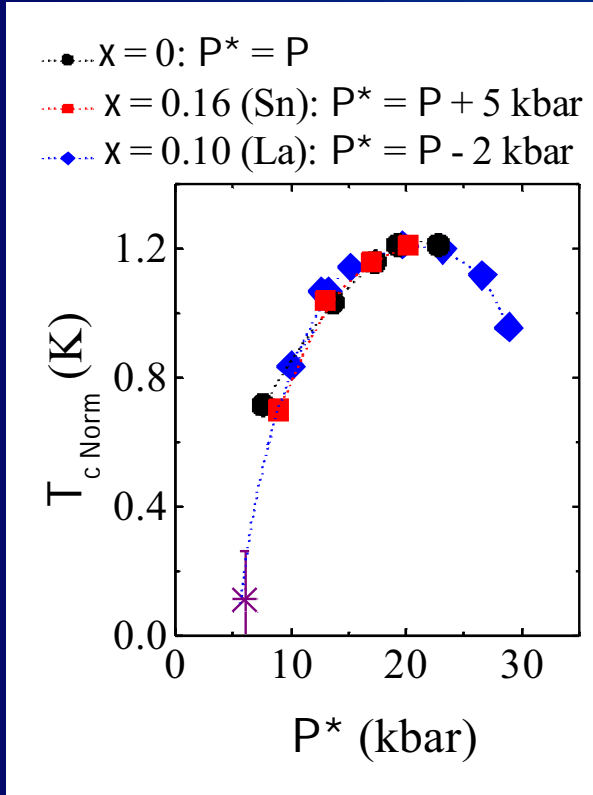
La- and Sn-doped CeRhIn₅

P – T phase diagram



For the two doped samples, T_{\max} , T_N and T_c follow the same qualitative evolution as a function of pressure found for pure CeRhIn₅.

However, by comparing the P – T phase diagram of the three samples, one sees that the La-doping shifts the P – T phase diagram of CeRhIn₅ to higher pressure while the Sn-doping does exactly the opposite.



As the two doped samples have the same T_N at ambient pressure and similar strength of the Ce-Ce inter-site magnetic coupling, it is the strength of the intra-site Kondo-coupling which mainly determines the pressure evolution of the CeRhIn_5 ground state.

The suppression of the magnetism has to be associated with an increasing of T_K and a consequent crossover between localized and itinerant behavior of the Ce 4f.

If a given control parameter tunes T_N to zero by a local mechanism, such as dilution or magnetic frustration which are not necessarily associated with an increase of the Kondo-coupling, this tuning might in fact inhibit SC:

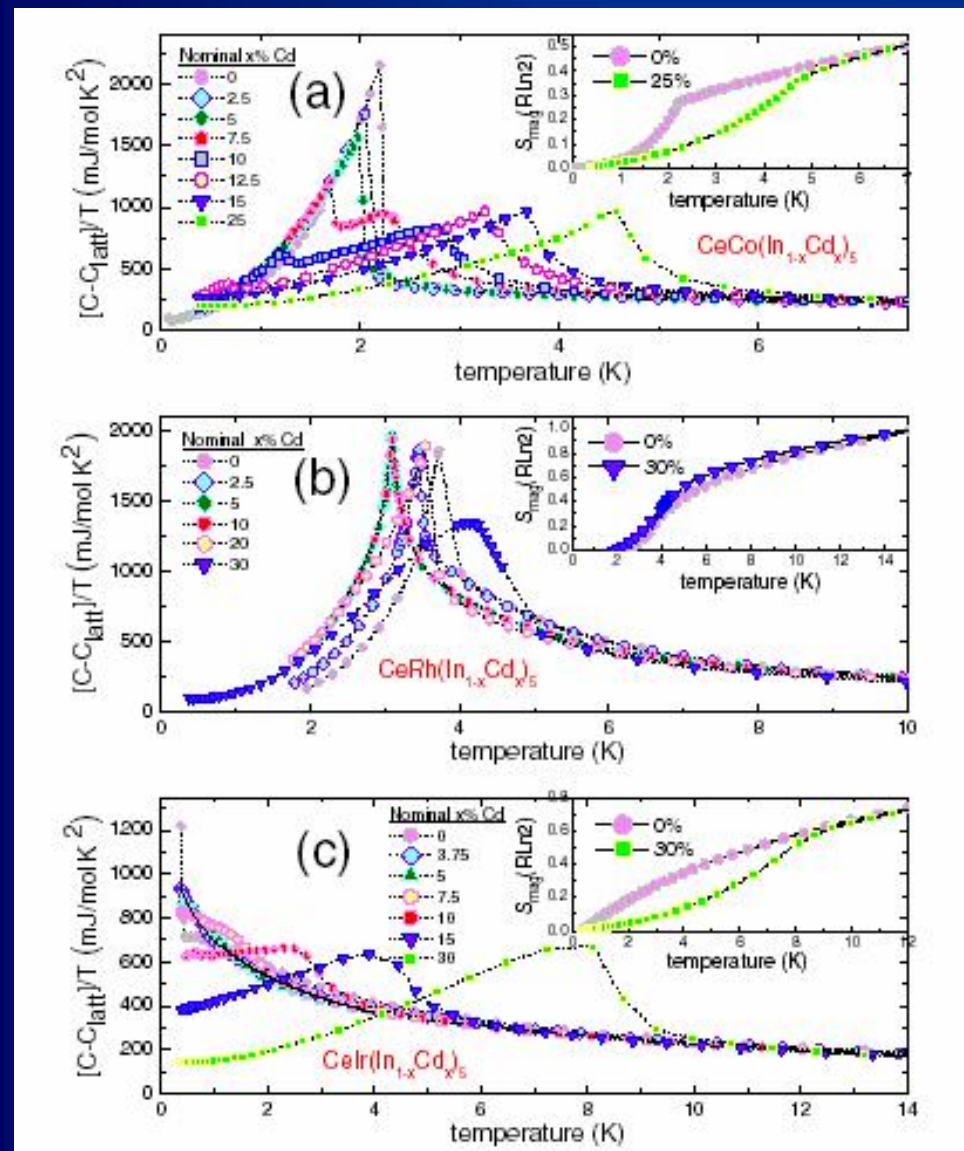
SC would not be expected at ambient pressure in $\text{Ce}_{1-x}\text{La}_x\text{RhIn}_5$, only at much higher P .

However, SC was not found at ambient pressure for $\text{CeRhIn}_5_x\text{Sn}_x$.

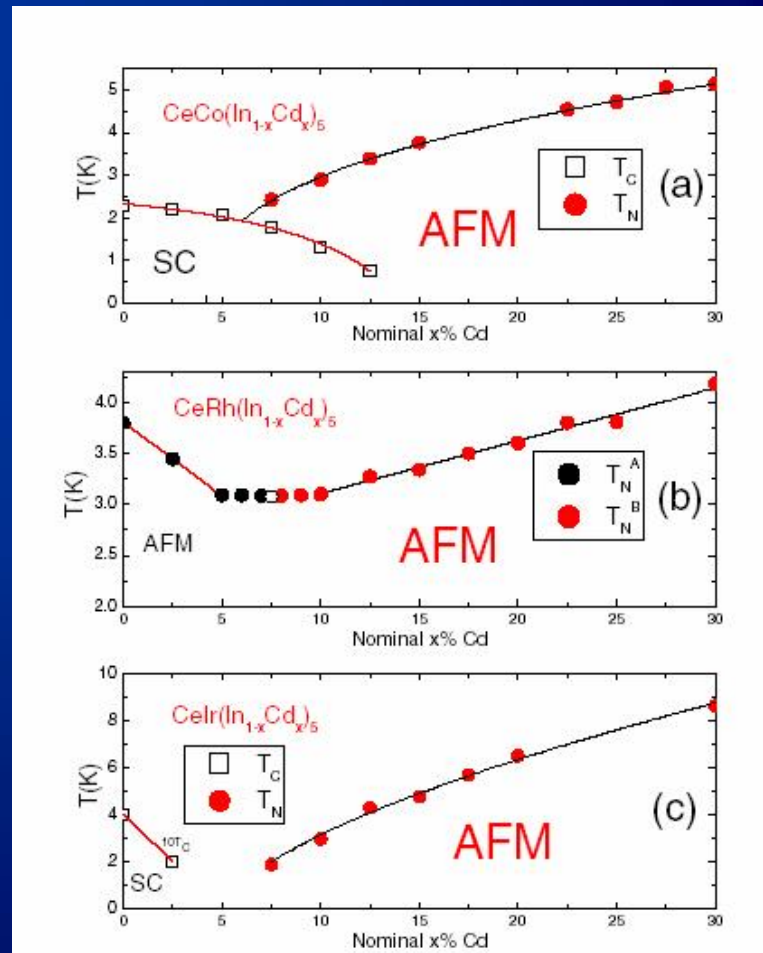
→ Disorder effects:

$T_{c\text{max}} = 1.2 \text{ K}$ for $\text{CeRhIn}4.84\text{Sn}0.16$ and $T_{c\text{max}} = 1.6 \text{ K}$ for $\text{Ce}_{0.90}\text{La}_{0.10}\text{RhIn}_5$) is roughly a factor of two smaller than that for CeRhIn_5 ($T_{c\text{max}} = 2.3 \text{ K}$).

Cd doping in CeMIn₅ – “in block” doping

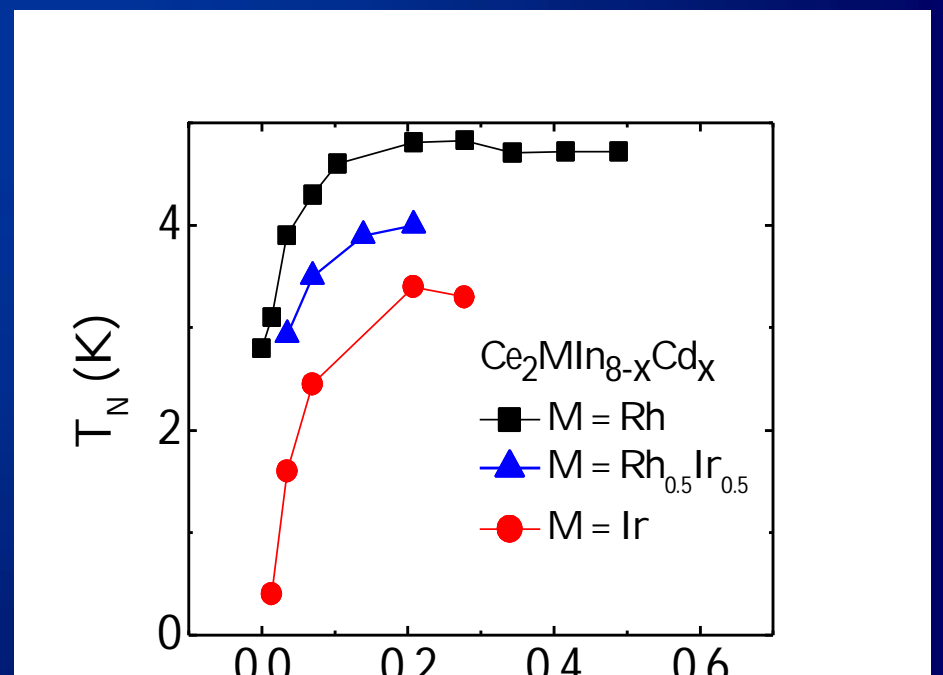
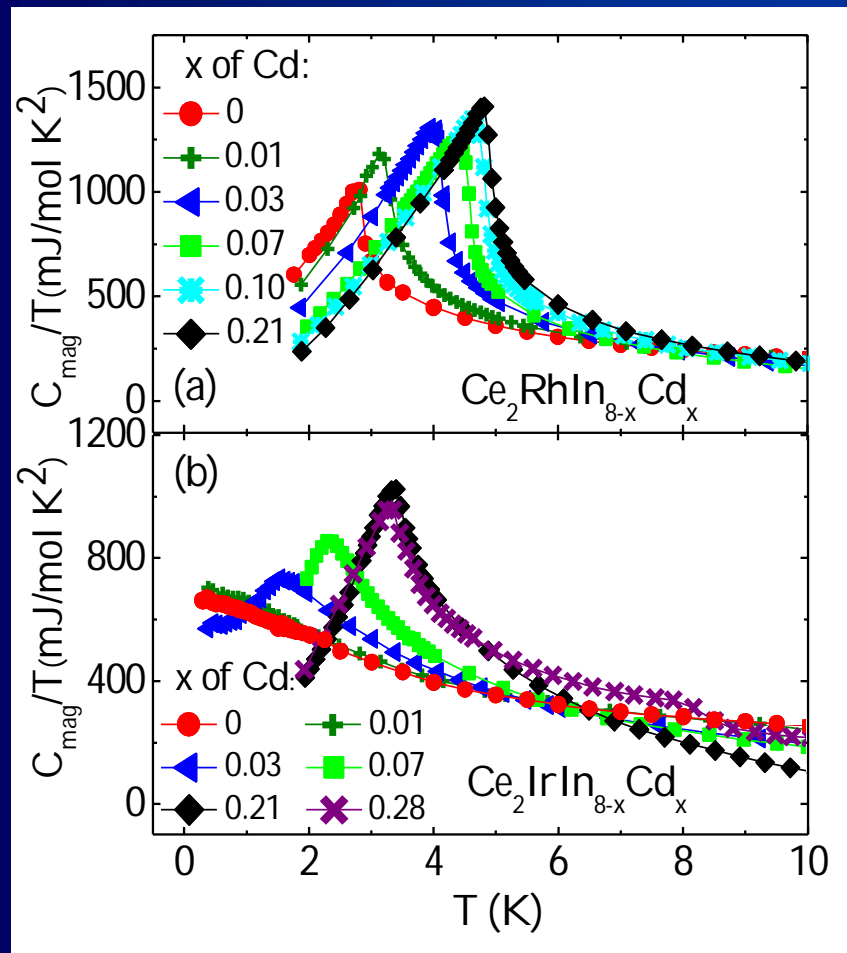


Cd has one p-electron less.
Hole doping – Fermi surface tuning



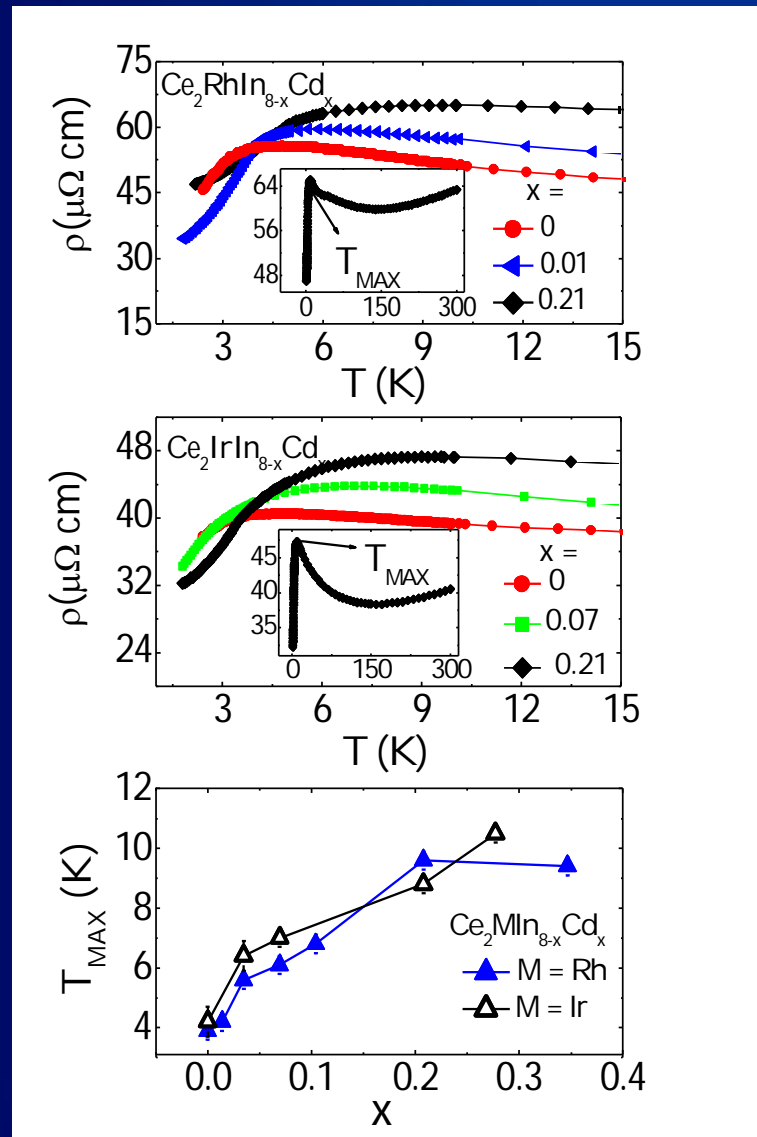
$\text{Ce}_2\text{MIn}_{8-x}\text{Cd}_x$ phase diagram

Specif-heat divided by temperature and phase diagram for Cd-doped samples



- Cd increases T_N for the compounds;
- Cd induces long range order for $M = \text{Ir}$;

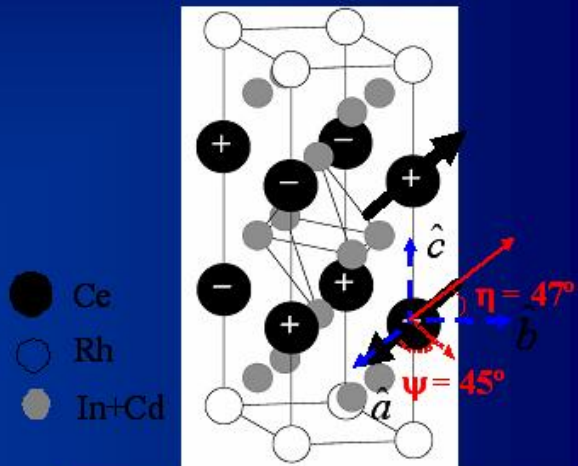
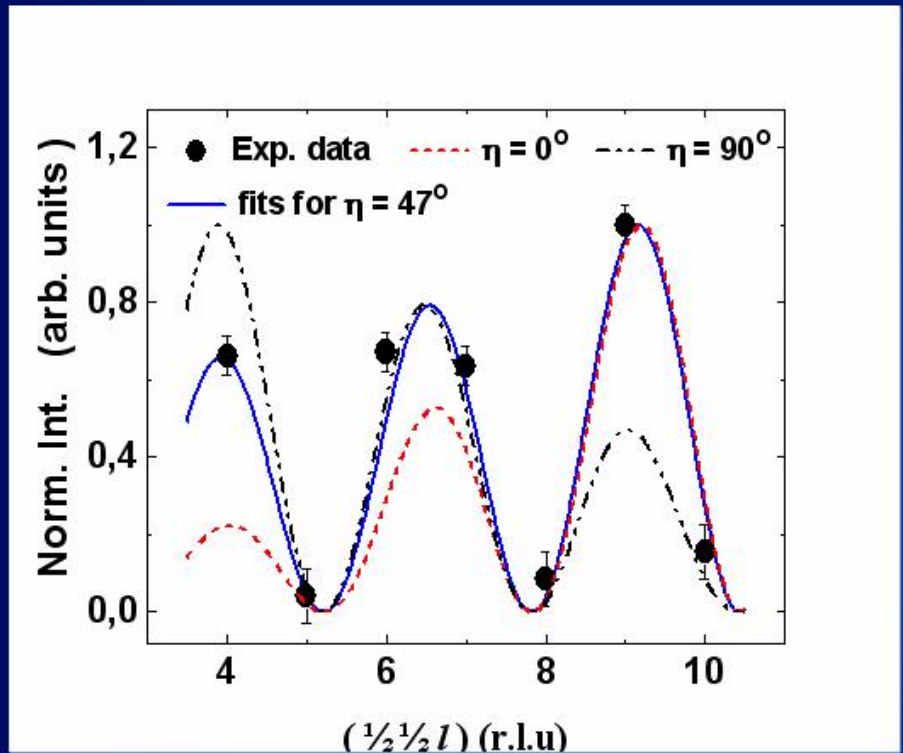
Resistivity results of $\text{Ce}_2\text{MIn}_{8-x}\text{Cd}_x$



T_N obtained from $\rho(T)$ is in good agreement with specific heat measurements;

T_{MAX} shows an increase not consistent with the decrease of the Kondo coupling.

XRMD of $\text{Ce}_2\text{RhIn}_{7.79}\text{Cd}_{0.21}$ at ESRF and NCNR



Cd-induces a small rotation of the ordered magnetic moment towards the ab-plane.

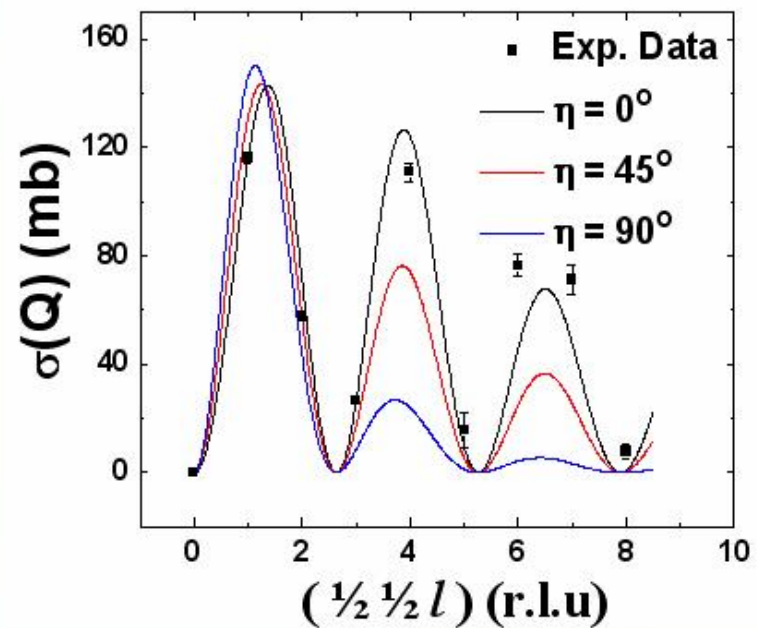
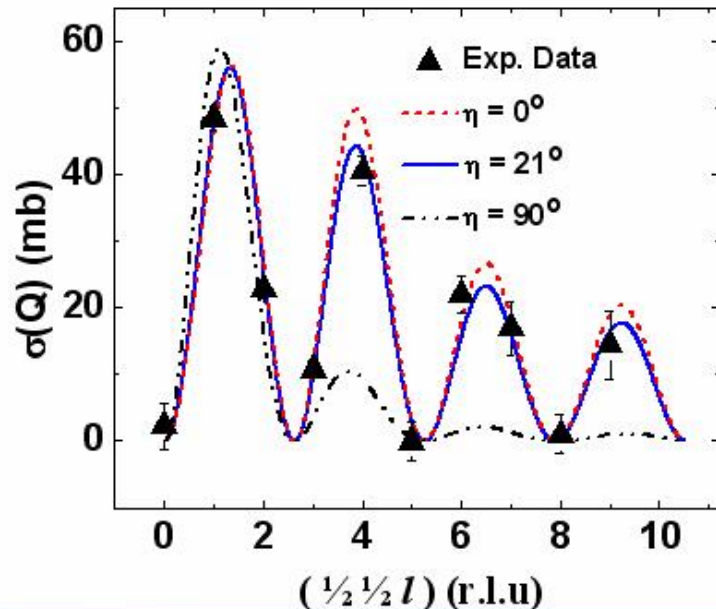
C. Adriano *et al*, PRB 81, 245115 (2010)

C. Adriano *et al*, Physica B, 404 3014 (2009).

$\text{Ce}_2(\text{Rh}_{0.5}\text{Ir}_{0.5},\text{Ir})\text{In}_{8-x}\text{Cd}_x$ at NCNR

$\text{Ce}_2\text{IrIn}_{8-x}\text{Cd}_x$

$\text{Ce}_2\text{Rh}_{0.5}\text{Ir}_{0.5}\text{In}_{8-x}\text{Cd}_x$

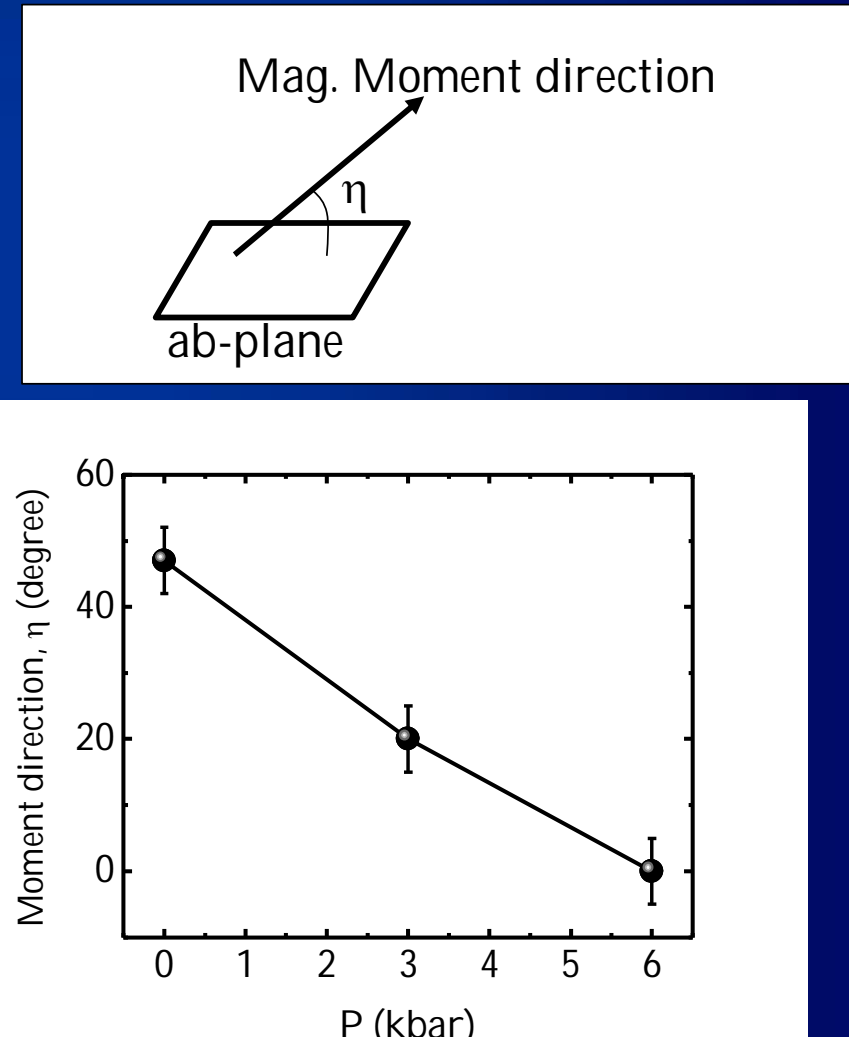
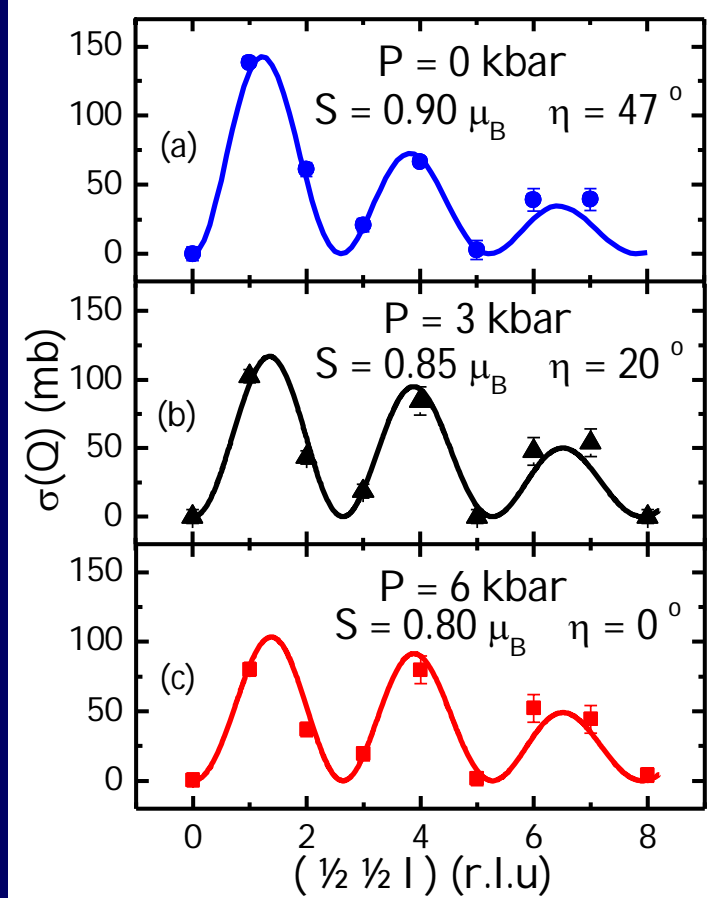


$\eta=21^\circ$ from the ab-plane;
 $M= (0.4 \pm 0.1) \mu_B$ por Ce

$\eta=0^\circ$ from the ab-plane;
 $M= (0.9 \pm 0.1) \mu_B$ por Ce

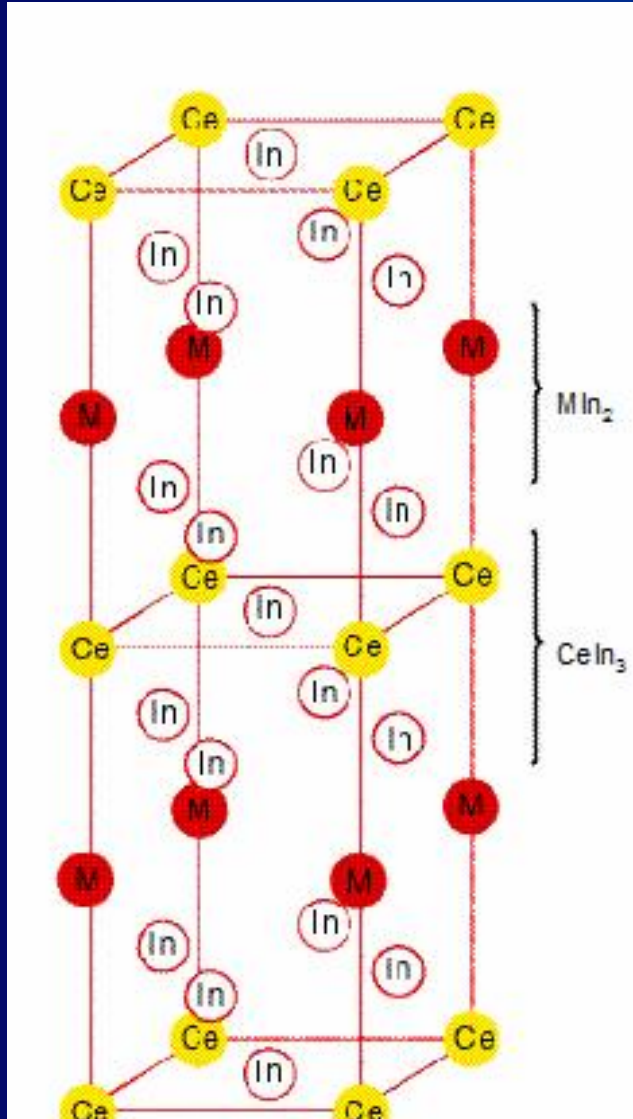
$\text{Ce}_2\text{RhIn}_{8-x}\text{Cd}_x$ under pressure

$\text{Ce}_2\text{RhIn}_{7.79}\text{Cd}_{0.21}$



No SC up to ~ 23 kbar!!

CeMIn₅ (M = Rh, Ir, Co) Family

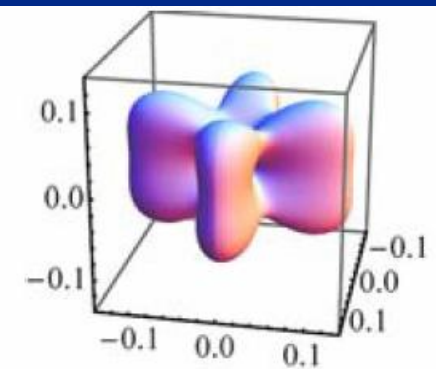


$$H_{\text{CEF}}^{\text{tetrag}} = B_2^0 O_2^0 + B_4^0 O_4^0 + B_6^0 O_6^0 + B_4^4 O_4^4 + B_6^4 O_6^4$$

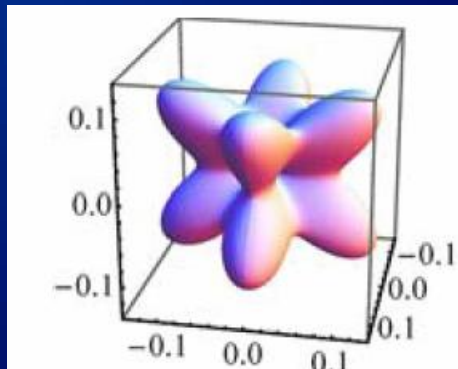
$$|2\rangle = \Gamma_6 = |\pm 1/2\rangle,$$

$$|1\rangle = \Gamma_7^1 = \beta |\pm 5/2\rangle - \alpha |\mp 3/2\rangle,$$

$$|0\rangle = \Gamma_7^2 = \alpha |\pm 5/2\rangle + \beta |\mp 3/2\rangle$$

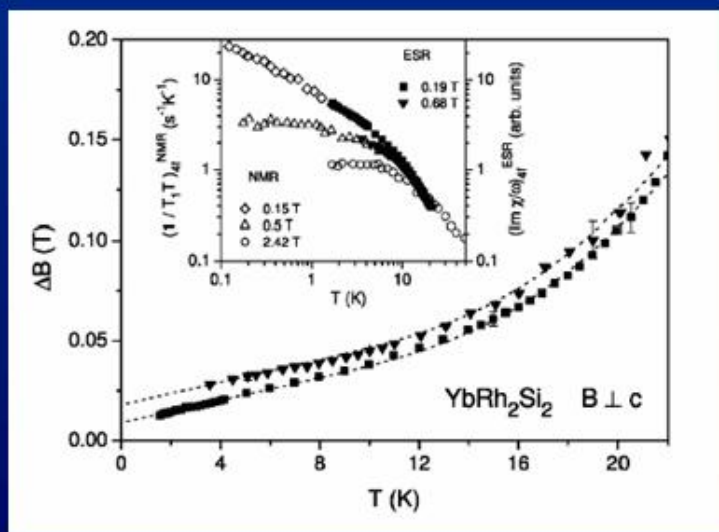
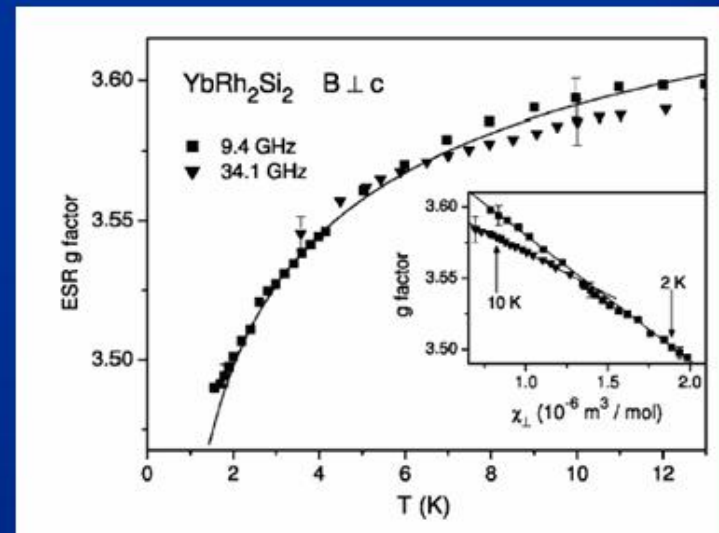
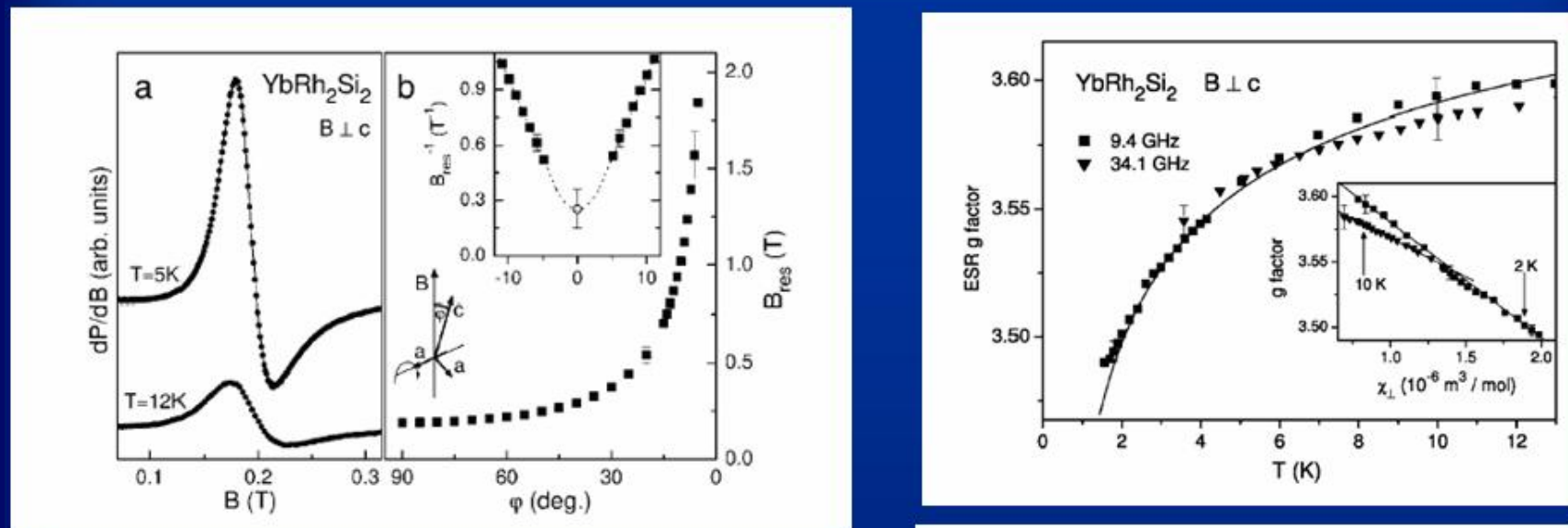


$\alpha=0.62$



$\alpha=0.36$

Probing the f-electron site: ESR in YbRh_2Si_2



- ESR signal presumably arising from localized Yb^{3+} CEF ground state.
- Spin dynamics as measured by ESR seems consistent to the formation of a Kondo Lattice seen by remained localized $4f$ electrons.

Extrapolation to α -YbAlB₄ – IV – large T_{SF}

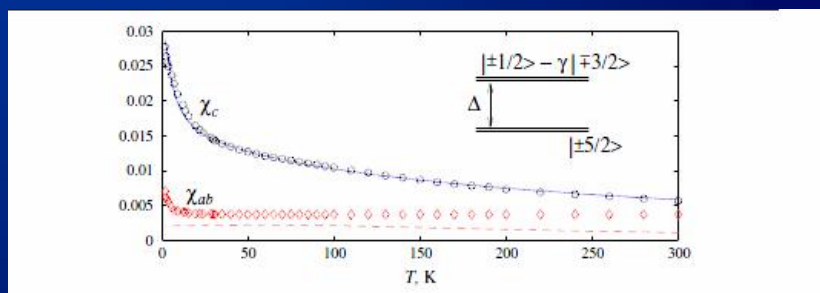
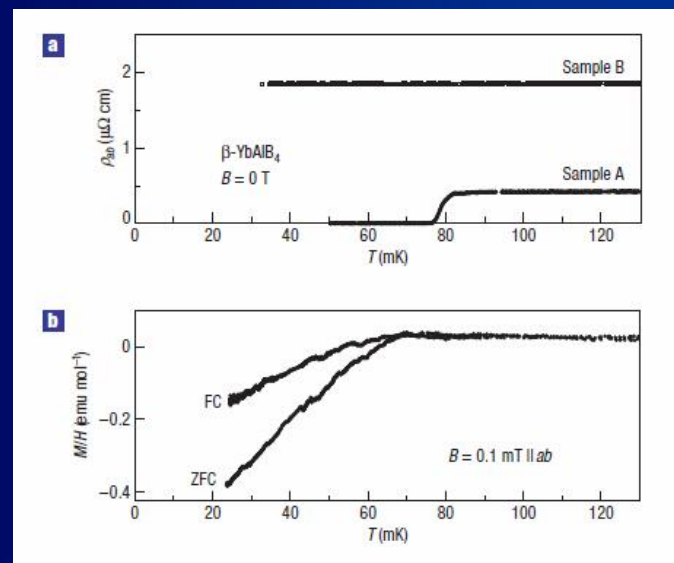
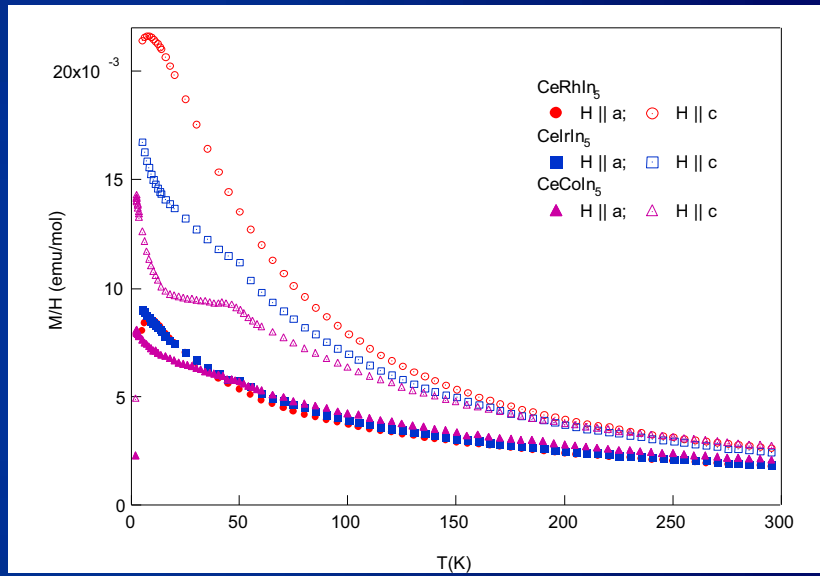
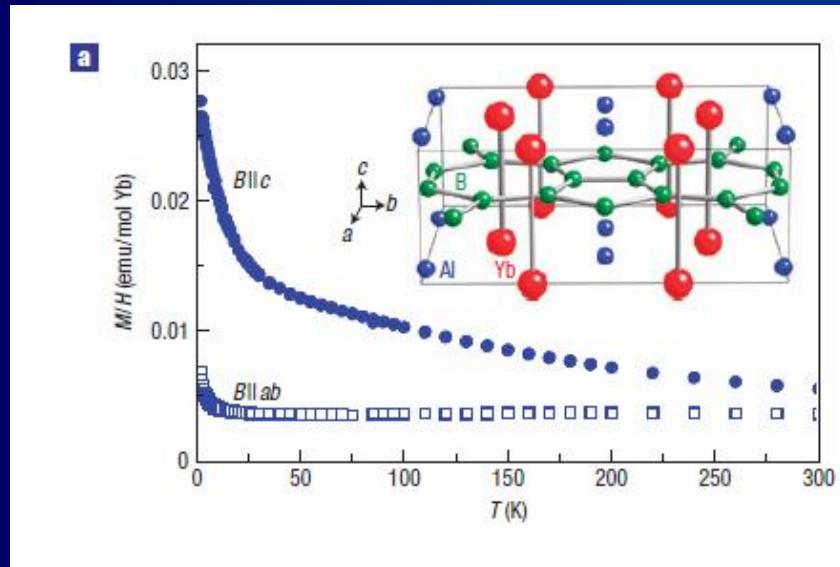
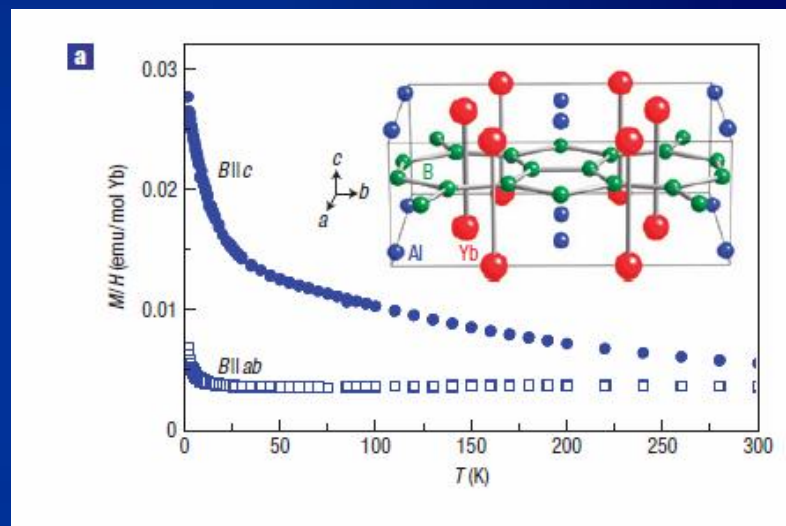
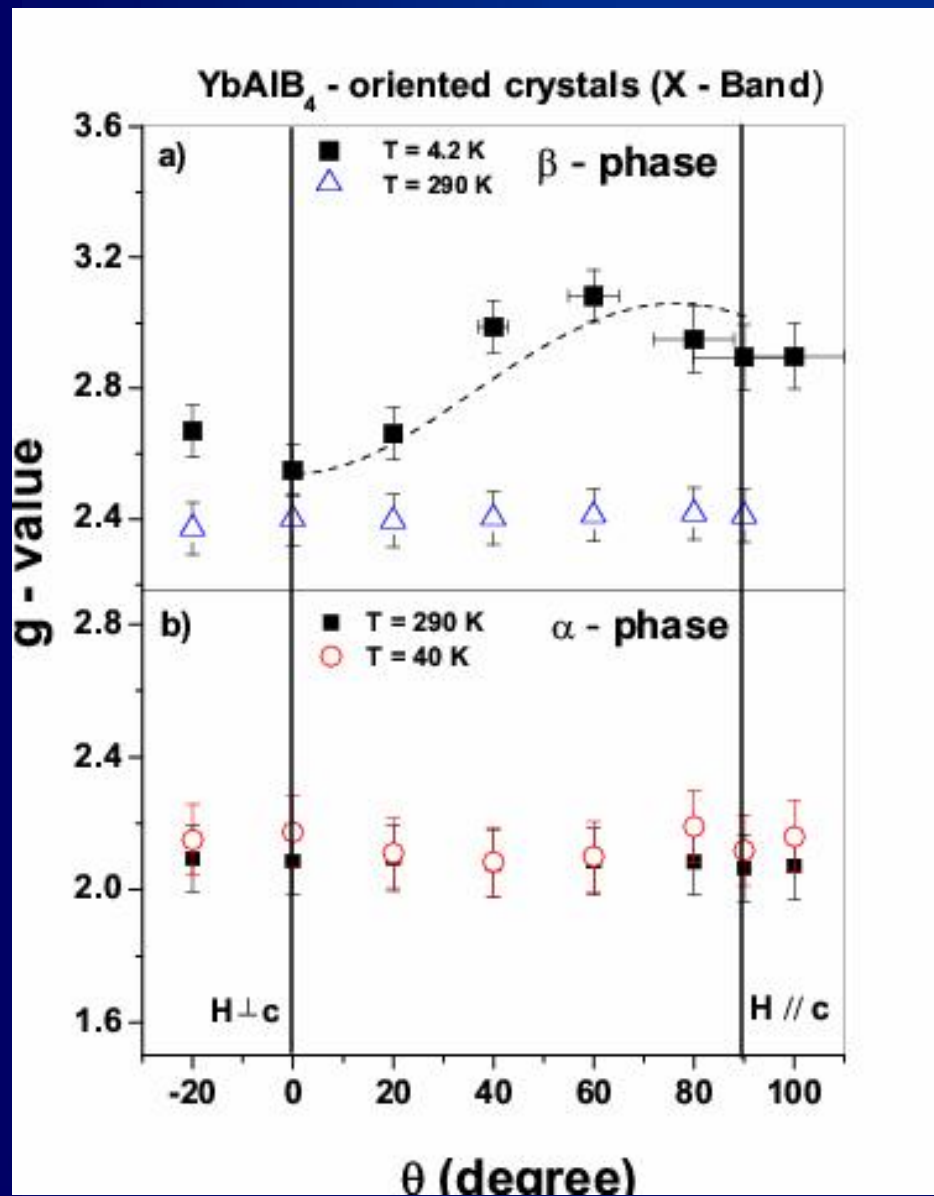


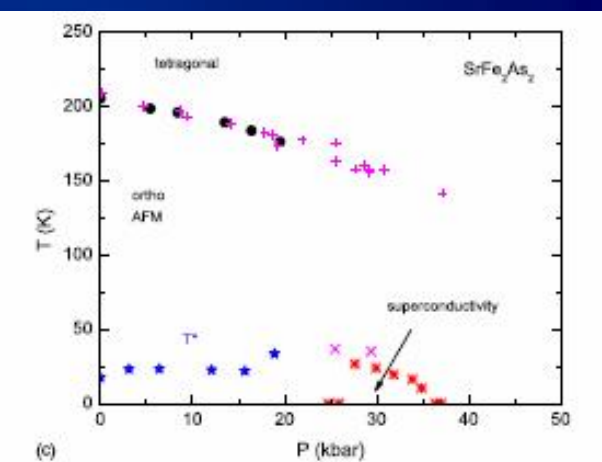
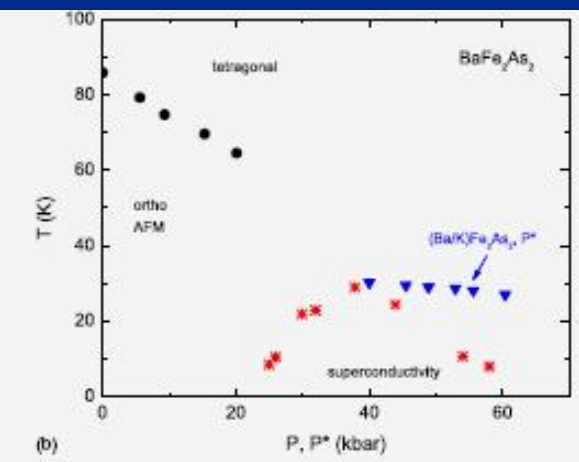
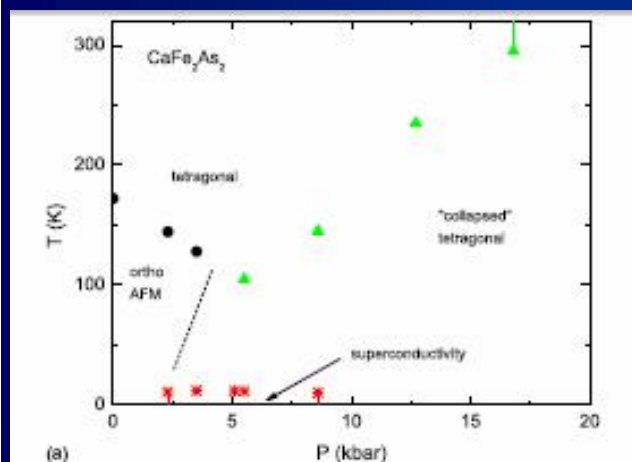
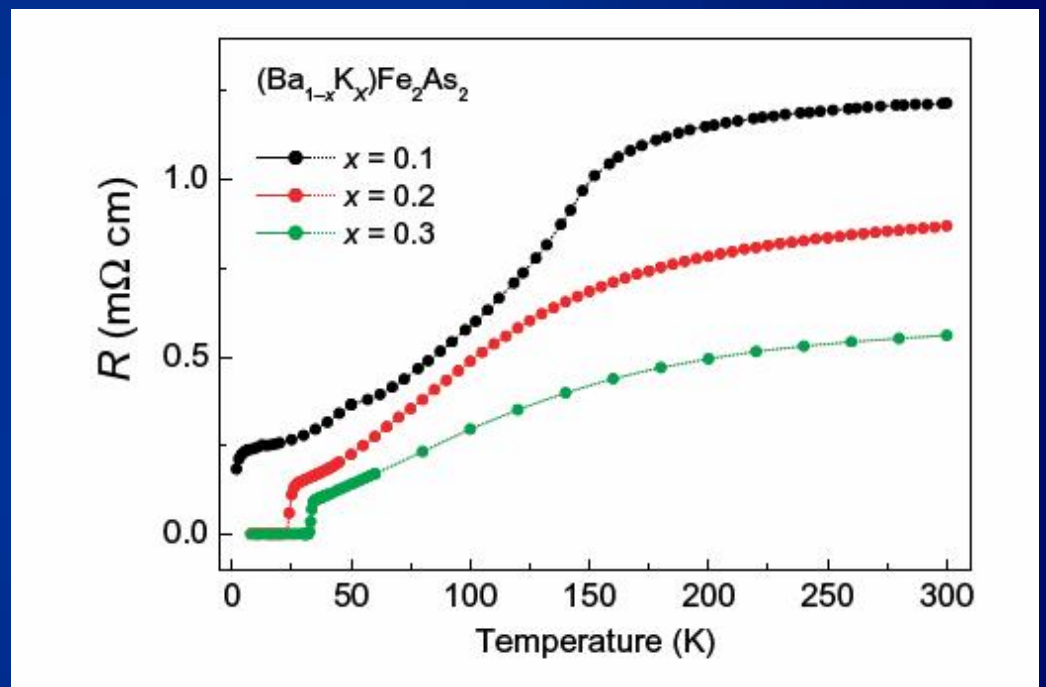
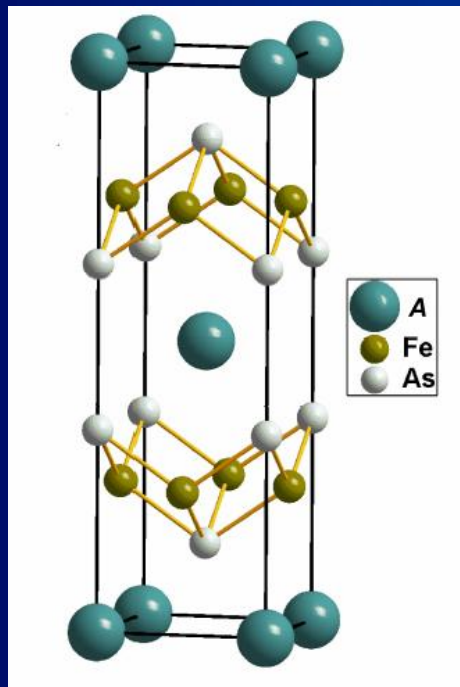
FIG. 4 (color online). (a) Theoretical fit to experimental susceptibility data [7] $\chi_c(T)$ (circles) and $\chi_{ab}(T)$ (rhombi) in the range 50–300 K using the single-ion model shown in the inset and the fitted Curie-Weiss temperature θ_{CW} . The best fit yields the lowest crystal field splitting $\Delta = 80$ K, the coefficient of admixture $\gamma \approx 0.28$ and $\theta_{\text{CW}}^{\text{th}} = -230$ K, close to the experimental value $\theta_{\text{CW}}^{\text{exp}} \sim -210$ K.

ESR g-anisotropy



This remarkable and unprecedented ESR signal found in the HFS α -YbAlB₄ behaves as a CESR at high temperatures and acquires characteristics of Yb³⁺ LM ESR at low temperature. This dual behavior in same ESR spectra strikes as an in situ unique observation of the Kondo localization of the f-electron at the quantum critical point (QCP) of α -YbAlB₄.

1-1-5 - PuCoGa₅ – FeAs-intermetallics ?

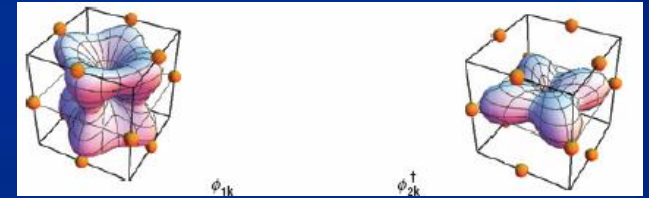


M. S. Torikachvili et al. PRB 2008.

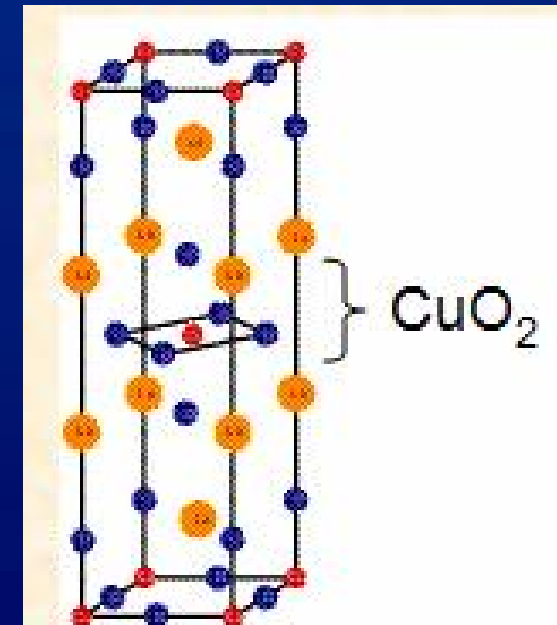
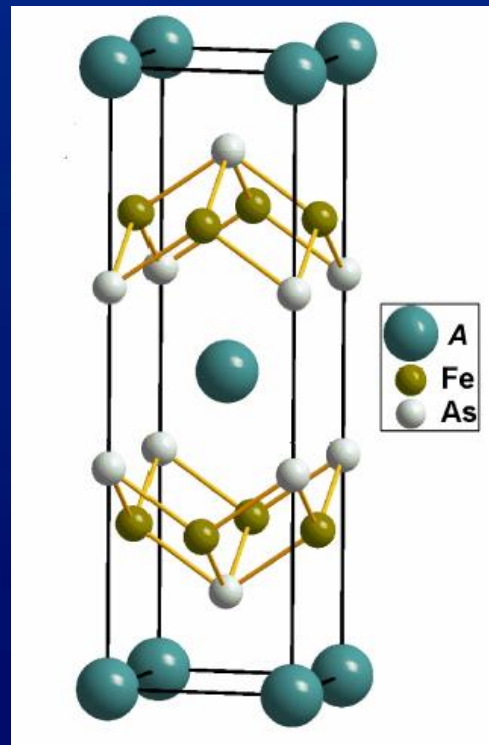
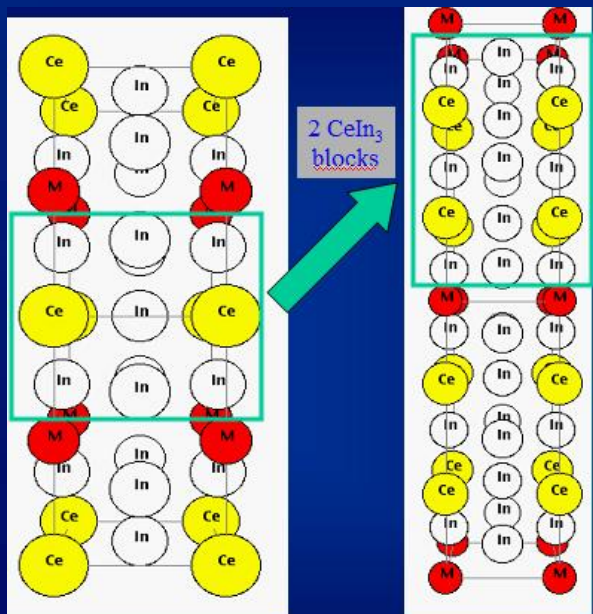
Marianne Rotter et al. New J. of Phys. (2009).

Implications for designing materials

- To increase T_c for magnetically mediated SC:
 T_{sf} , characteristic T for spin fluctuations high
Tunable carrier density



- Quasi 2-d helps a lot; maybe not much 2-d needed – increase c/a – tune CEF GS
- Need bigger bandwidths to increase T_{sf} , but keep optimized T_c/T_{sf} - 3d spins in the active layer.

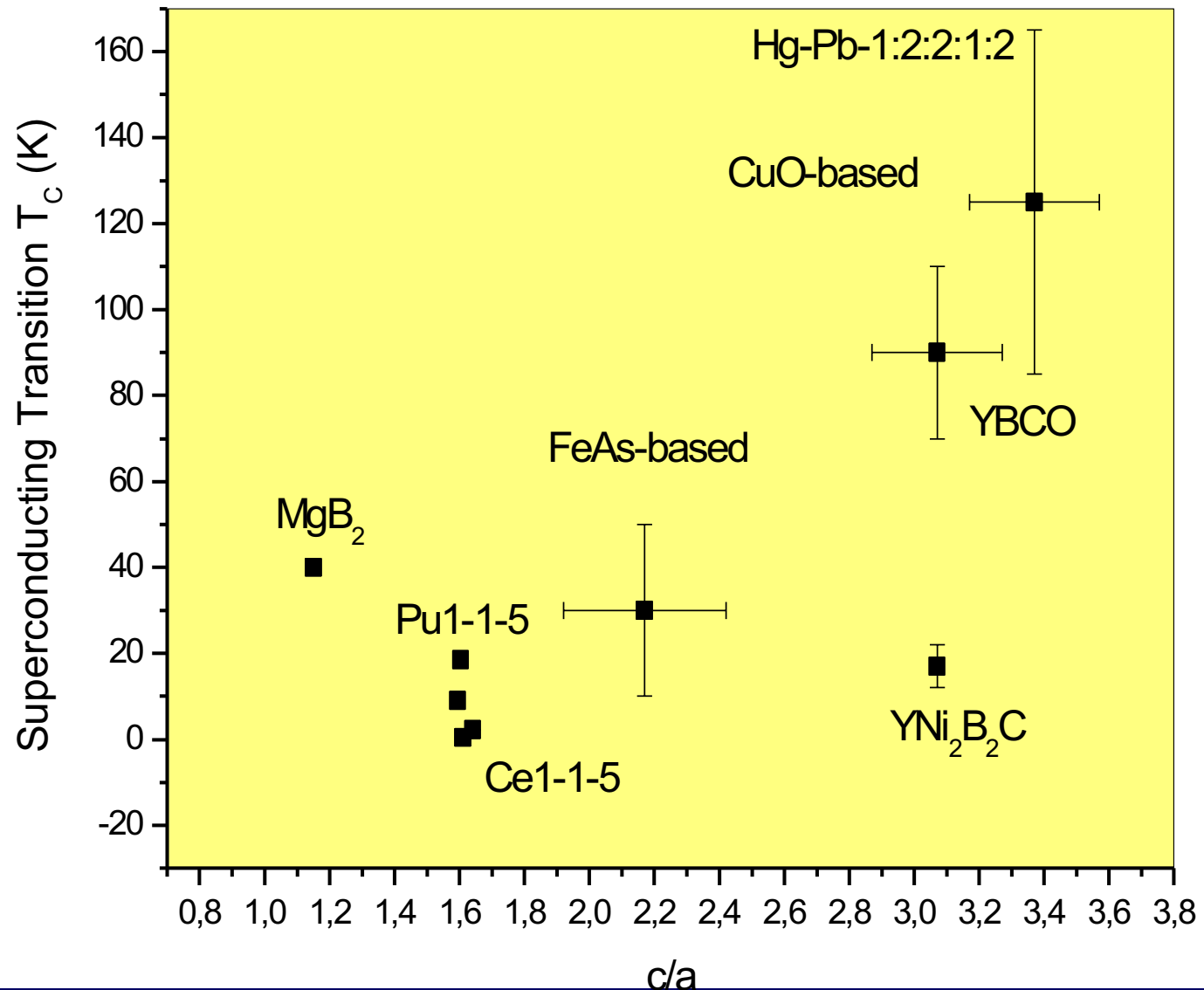


1-1-5 e 2-1-8

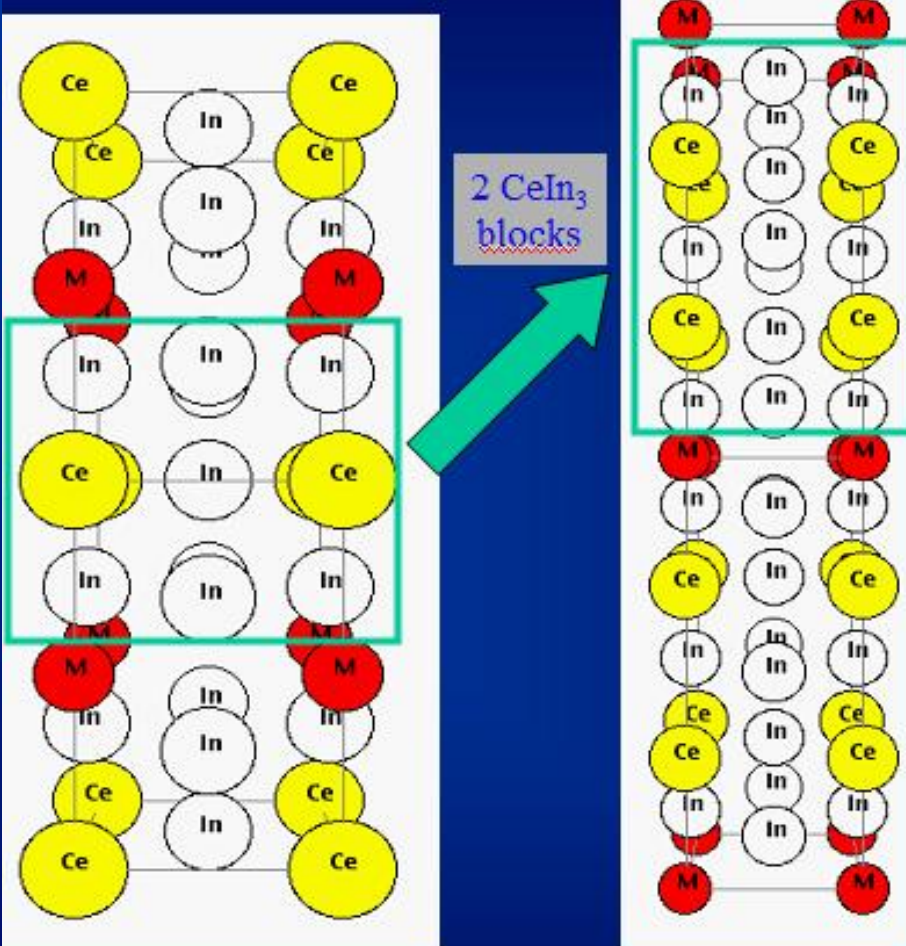
1-2-2

2-1-4, etc

Generalized c/a plot



Implications for designing materials



- 1-1-5: c/a ~ 1.6

- 2-1-8: c/a ~ 3.0 –

3d spins as the active layer.

- Examples: A₂MB₈

M = Cu, Fe, Co, Ni,
Mn, Ru, Re, Mo...

A = La, Y, Ca, Sr, Ba,
Mg, K

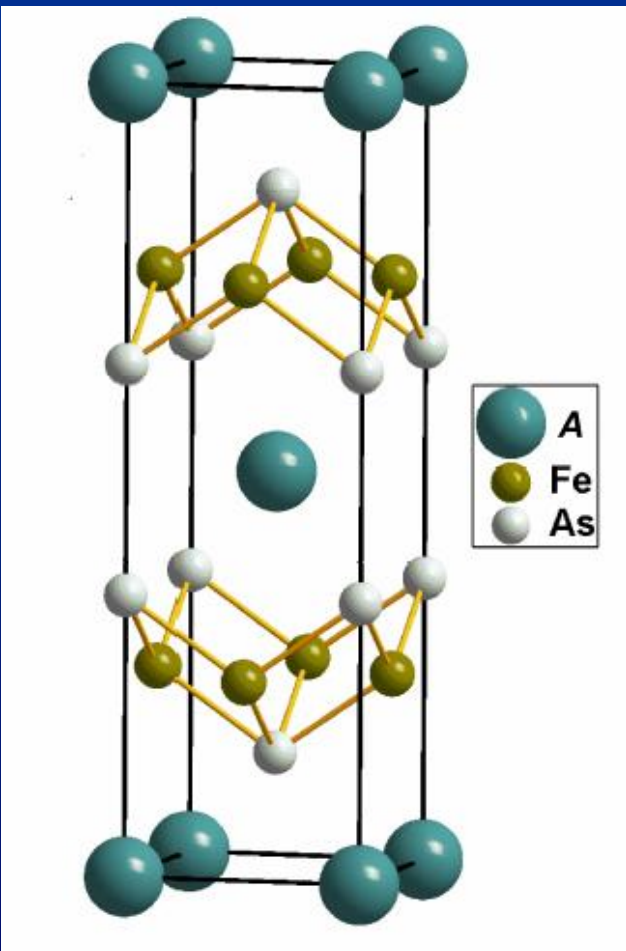
B = Bi, Sb, Ge, Sn, In,
As, etc

1-1-5 e 2-1-8

1-2-2

2-1-4, etc

Implications for designing materials



- $c/a \sim 2-3$ - 3d spins as the active layer.

- Examples: AM_2B_2

$M = Cu, Fe, Co, Ni,$
 $Mn, Ru, Re, Mo\dots$

$A = La, Y, Ca, Sr, Ba,$
 Mg, K, Li, Mg

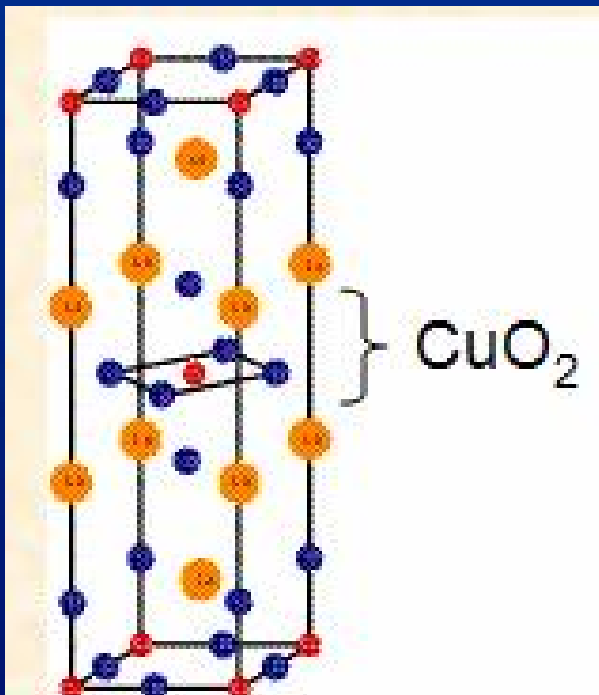
$B = Bi, Sb, Ge, Sn, In,$
etc

1-1-5 e 2-1-8

1-2-2

2-1-4, etc

Implications for designing materials



- 2-1-4: $c/a \sim 3/4$ - 3d spins as the active layer.

- Examples: A_2MB_4

- $M = Cu, Fe, Co, Ni, Mn, Ru, Re, Mo\dots$

- $A = La, Y, Ca, Sr, Ba, Mg, K$

- $B = Bi, Sb, Ge, Sn, In, Pb, etc$

1-1-5 e 2-1-8

1-2-2

2-1-4, etc

Thank you for your attention!

ESR signal in $\hat{\alpha}$ -YbAlB₄: cond-mat 0908.0044

Evidence for the existence of *Kondo coupled resonant modes* in heavy fermions

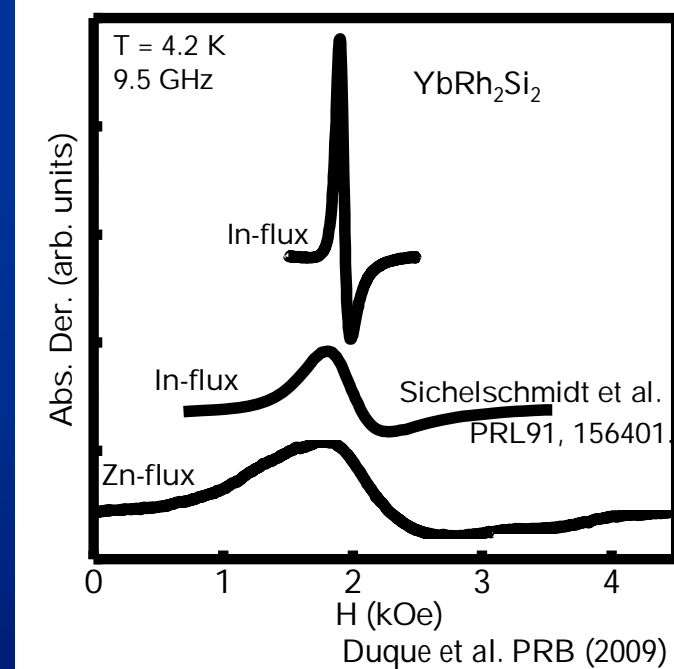
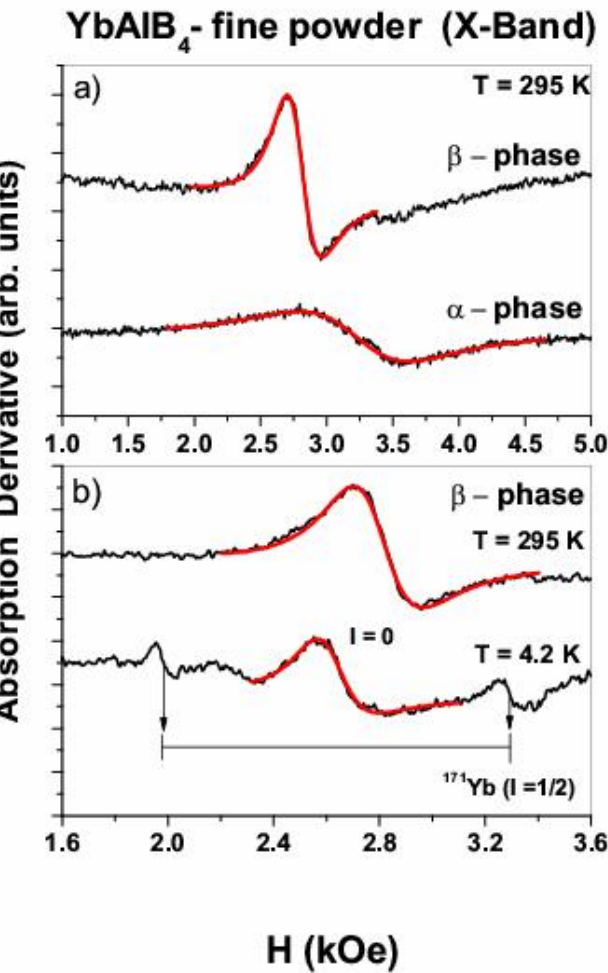
L. M. Holanda ¹, J. M. Vargas ¹, C. Rettori ¹, S. Nakatsuji ², K. Kuga ², Z. Fisk ³, S.B. Oseroff ⁴ and P. G. Pagliuso ¹

¹ Instituto de Física "Gleb Wataghin", UNICAMP, Campinas-SP, 13083-970, Brazil.

² Institute for solid State Physics (ISSP), University of Tokyo, Kashiwa 277-8581, Japan.

³ University of California, Irvine, California 92697-4573, U.S.A.

⁴ San Diego State University, San Diego, California 92182, U.S.A.



Abrahams, E.,
Wolffe, P. Phys.
Rev. B 78
104423 (2008).

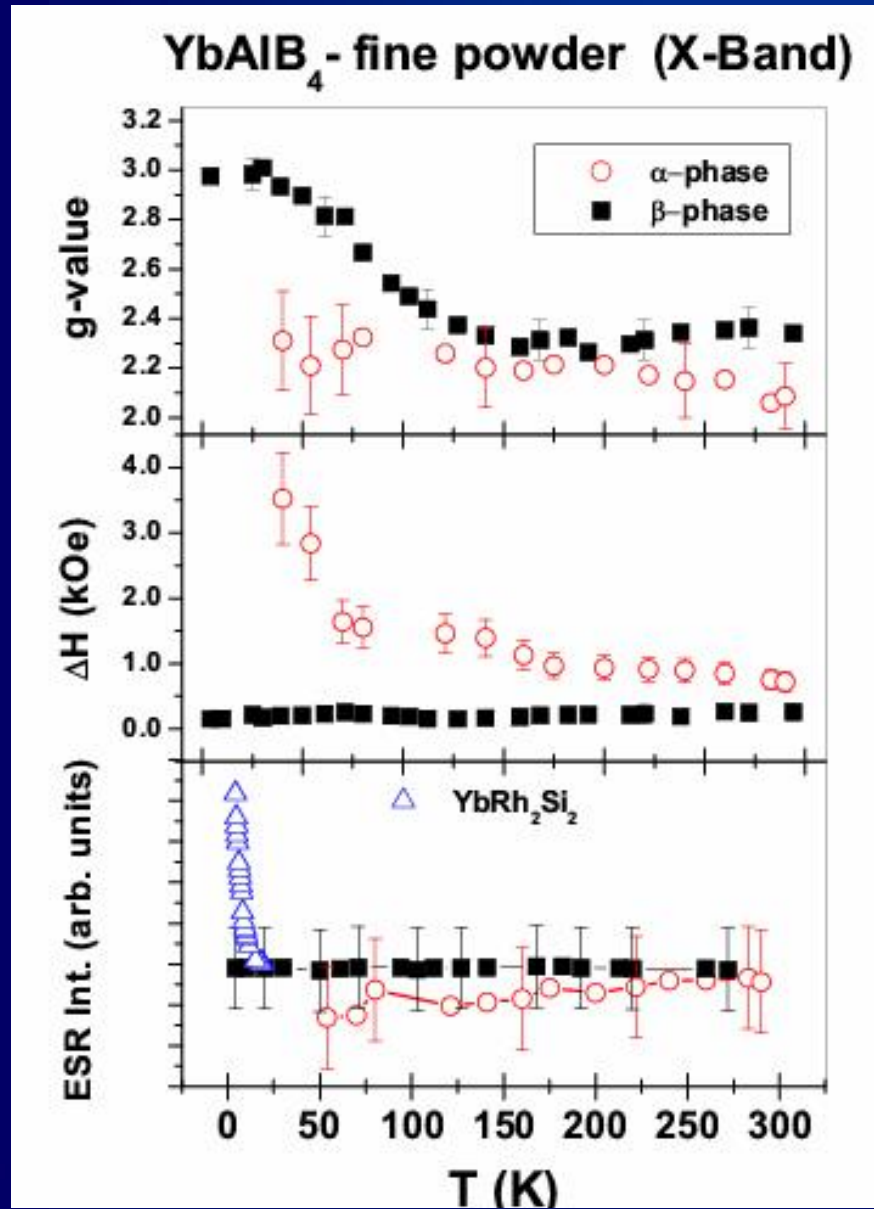
Schlottmann,
P. Phys. Rev. B
79 045104
(2009).

Kochelaev, B. I.
arXiv:0907.207
4 (2009).

$^{171}\text{A} \sim 1300 \text{ Oe}$ which is of the order of the typical values found for ^{171}Yb in low symmetry systems.

Irrefutable indication that the ESR spectra found for $\hat{\alpha}$ -YbAlB₄ acquires the characteristic of the Yb^{3+} ions at low-T.

ESR temperature dependence

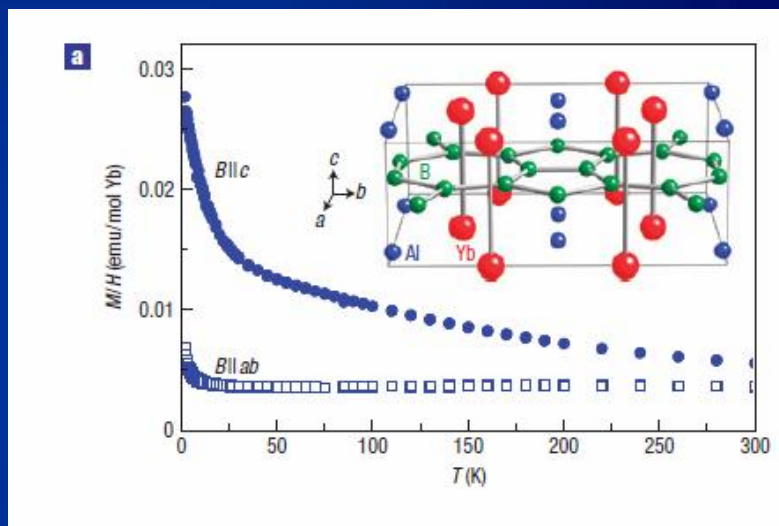
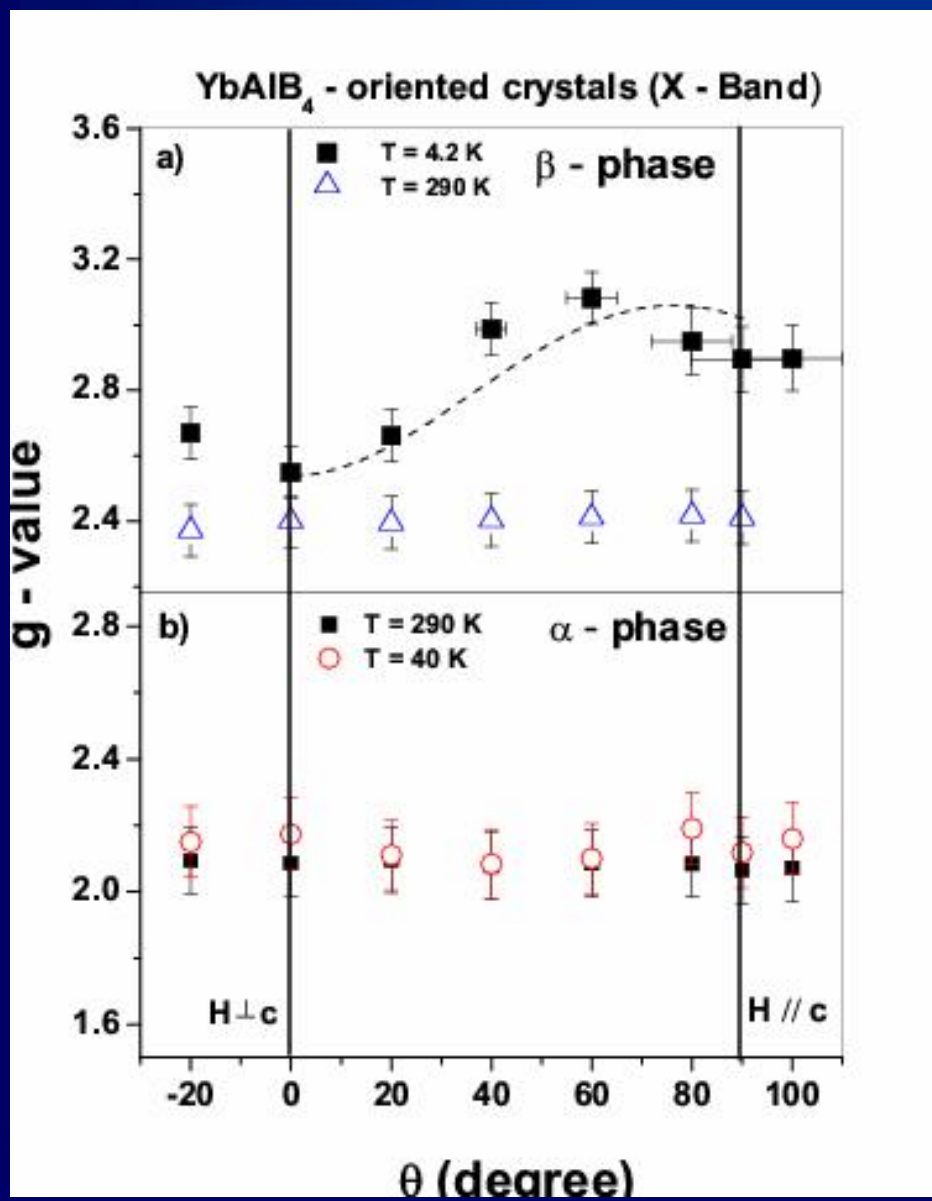


Both phases show T-independent ESR intensity – typical of CESR

g-value for the $\hat{\alpha}$ -phase shifts to larger value at low-T ($g \sim 3$): typical for Yb^{3+} Krammers doublets)

For $\hat{\alpha}$ -YbAlB₄ $\Delta H(T)$ shows a weak non-monotonic increase as a function of temperature which results in an average linewidth broadening of ~ 0.4 Oe/K in the whole temperature range. This rate is much smaller than the linear Korringa-rate found for the ESR line observed at low-T for YbRh₂Si₂. In contrast, for α -YbAlB₄ $\Delta H(T)$ increases dramatically with decreasing-T which avoid the observation of the resonance for $T < 40$ K.

g -anisotropy



This remarkable and unprecedented ESR signal found in the HFS α -YbAlB₄ behaves as a CESR at high temperatures and acquires characteristics of Yb³⁺ LM ESR at low temperature. This dual behavior in same ESR spectra strikes as an in situ unique observation of the Kondo localization of the f-electron at the quantum critical point (QCP) of α -YbAlB₄.